Real Time Monitoring of Points of Common Coupling in Distribution Systems Through State Estimation and Geometric Tests

Submitted in partial fulfillment of the requirements

of the degree of

Master of Technology

In

Power Systems Engineering

By

Nikhil Bhaskar Sardar

Roll No: 152625

Supervisor:

Prof. Maheswarapu Sydulu

Department of Electrical Engineering

NATIONAL INSTITUTE OF TECHNOLOGY WARANGAL

TELANGANA STATE-MAY-2017

DEPARTMENT OF ELECTRICAL ENGINEERING
NATIONAL INSTITUTE OF TECHNOLOGY
WARANGAL-506 004

Certificate

This is to certify that this dissertation work entitled "**Real Time Monitoring of Points of Common Coupling in Distribution Systems Through State Estimation and Geometric Tests**" is a bonafide work carried out by **Nikhil Bhaskar Sardar (152625)**, submitted to the faculty of the Electrical Engineering Department, in partial fulfillment of the requirements for the award of degree of **Master of Technology** (Electrical) with specialization in **Power Systems Engineering** from **National Institute of Technology**, **Warangal**.

Dr. SOMASEKHAR V. T.
Professor and Head
Dept. of Electrical Engineering,
National Institute of Technology,
Warangal.

Prof. Maheswarapu Sydulu
Supervisor
Dept. of Electrical Engineering,
National Institute of Technology
Warangal.

Acknowledgement

I would like to extend my sincere thanks to my guide, Prof. M Sydulu, Department of Electrical Engineering, National Institute of Technology, Warangal. He has been extremely helpful with his knowledge and enthusiasm. My project would not have been possible without the kind support he offered.

Besides my guide, I would like to thank Dr. Somasekhar V.T, Head of the Department for his excellent support directly and indirectly and also for providing us all the necessary facilities in the department.

I would like to thank the rest of the committee for their encouragement, insightful comments and feedback.

I would like to thank all the faculty members of my department who helped me by sharing their knowledge and also giving their valuable suggestions as and when needed.

I would like to express my gratitude to my parents for their kind co-operation and encouragement which helped me in completion of this project.

Nikhil Bhaskar Sardar

Roll No: 152625

Date:

Approval Sheet

This dissertation entitled **Real Time Monitoring of Points of Common Coupling in Distribution Systems Through State Estimation and Geometric Tests** by Nikhil Bhaskar Sardar is approved for the degree of Master of Technology (Power Systems Engineering).

Examiner

_____

Supervisor

_____

Prof. Maheswarapu Sydulu

Department of Electrical Engineering

NIT Warangal

Chairman

_____

Dr. SOMASEKHAR V. T.

Professor and Head

Department of Electrical Engineering

NIT Warangal

Date:

Place: NIT WARANGAL

Declaration

I declare that this written submission represents my ideas in my own words and where others' ideas or words have been included, I have adequately cited and referenced the original sources. I also declare that I have adhered to all principles of academic honesty and integrity and have not misrepresented or fabricated or falsified any idea/data/fact/source in my submission. I understand that any violation of the above will cause for disciplinary action by the Institute and can also evoke penal action from the sources which have thus not been properly cited or from whom proper permission has not been taken when needed.

_____

(Signature)

Nikhil Bhaskar Sardar

(Name of the Student)

152625

(Roll No)

Date:_____

TABLE OF CONTANTS

ABSTRACT

This thesis presents an extended state estimation method which allows the identification of unexpected power injections at multiple points of common coupling (PCCs) of power distribution grids. The developed state estimator makes use of a three-phase network modeling where active and reactive power injection levels at PCCs are estimated and checked in real time with the values expected by the system operator. The estimation algorithm applies a sparse tableau formulation or Hatchet's method in which equality constraints are employed to model power injection assumptions at PCCs. The identification of unexpected power injections is then performed using a methodology based on normalized Lagrange multipliers and geometric tests. Large weights to virtual measurements and low weights to pseudo measurements may cause the system to be ill-conditioned. In order to compare some solutions for the numerically ill conditioning problems associated with Distribution System State Estimation (DSSE), Normal equation method (NE) Hatchet's augmented matrix (AM) method for DSSE are considered. These two methods are implemented on the IEEE10-Bus network and IEEE 34 node test feeder and applicability of the proposed approach for the future of real-time monitoring on power distribution systems.

LIST OF FIGURES

LIST OF TABLES

NOMENCLATURE

List of Abbreviation

AC	**Alternating current**
DC	**Direct Current**
SCADA	**Supervisory control and data acquisition**
D-SCADA	**Distribution- Supervisory control and data acquisition**
WAMS	**Wide Area Monitoring System**
RTU	**Remote Terminal Unit**
DMS	**Distribution Management System**
NLM	**Normalized Lagrangian multiplier**
CT	**Collinearity Test**
PCC	**Points of Common Coupling**
AM	**Augmented Matrix**
NE	**Normal Equation**
SE	**State Estimation**
DSSE	**Distribution System State Estimation**
CB	**Circuit Breaker**
AGC	**Automatic Generator Control**
PS	**Power System**
DG	**Distribution Generation**
CHP	**Combine Heat and Power**
PV	**Photovoltaic Cell**

List of Symbols

X	**Reactance**
R	**Resistance**
Y	**Admittance**

σ	**Standard deviation**
λ	**Lagrangian multiplier**
λ_i^N	**Normalized Lagrangian multiplier**
$h_s(x)$	**Structural Constraint**
$h_o(x)$	**Operational Constraint**
G	**Gain matrix**
P	**Real Power**
Q	**Reactive Power**

Protective Function Used for Interconnection protection objective

81O/U	**An over/Under Frequency**
27/59	**An over/Under Voltage**
81R	**Rate of Change of Frequency Relay**
67, 21	**Phase Fault Backfeed Protection**
51V	**Restraint/Controlled Overcurrent Relay**
67N	**Grounded Direction Relay**
46	**Negative sequence Overcurrent Relay**
47	**Negative sequence voltage Relay**
32	**Direction Power Relay**

CHAPTER 1:
INTRODUCTION

1.1 INTRODUCTION

Electrical power system consist of Generators, transmission lines, Distribution networks and customers. The main purpose of electrical network is to cover the all loads in all conditions, considering all possible contingencies. The methods for analysis of electrical network have been studies even as long as is the existence of power systems. The main topics under observation have been the power flow solution and its solution with different methods (Gauss-seidel, Newton-Raphson, etc.), state estimation, optimization of power system operation, load modeling (forecasting methods, dynamic methods, etc.) over many years, most of the attention has paid to development of methods, related to transmission networks. This is because of the importance of transmission networks has always been understood and availability of initial information is extensive through different information systems (SCADA, WAMS etc.). However attention should also be paid to the analysis and development of distribution network and its problems because of importance and reliability requirements of power delivery to customers have increased noticeably. The actual security of supply and power quality from the customer's point of view is formed directly to distribution networks and also consideration of electricity market developments have cause the situation where larger understanding of distribution network operation is invisible. In last two decades the situation has been noticed and lot of attention has been given to research and solving different problems, related especially to distribution network and their operations.

The main question, when analyzing the distribution network operation is where to get the initial information. Compare to transmission network, where data and information redundancy is noticeable, but situation in distribution network is quite different. The operational information is predominantly available from larger substations when information regarding the distribution substations and low-voltage networks is modest or sometimes not available at all. When considering the analysis of distribution networks, one must also consider the characteristics of network. Although a lot of methods have been developed for transmission network, but it is not possible to use them directly in distribution network analysis. The problem is that, in general, the distribution networks are usually unbalanced three phase networks or even one phase network, their configuration is radial or sometimes weakly mesh and the branches have usually low X/R

ratios. For example, direct application of Newton-Raphson or other well –known methods for distribution networks power flow studies is complicated and in many cases lead to divergence and they are ineffective. Therefore, the main question is to development of appropriate analysis methods for distribution network and how to incorporate those distribution network characteristics in order to compose an efficient, reliable robust algorithm and methodology.

1.2 POWER SYSTEM STATE ESTIMATION

Power system state estimation has gained an important role for understanding and operating the system. Almost every power system control Centre has possession of state estimator. Methods and development of state estimation have remarkably matured over four decades. The main purpose of the state estimation is to filter the defective information data, eliminate incorrect measurements and produced reliable state estimates. With proper redundancy of measurement, it is possible to eliminate the effect of bad data and allowed the temporary loss of measurements without significantly affecting the quality of estimated value. The measurement used for network analysis are obtained through monitoring system

E.g. SCADA and they may include large error or may be insufficient due to error in transducer or communication channel etc. In addition, state estimation enables, to a certain extent, to determine the power flows in part of network that are not directly metered. The reliable information obtain from the state estimation is used for power system contingency analysis, optimal power flow, security study etc. (Fig.1.1)

There are two main possibilities of state estimation i.e. static and dynamic state estimation. The static state estimation is based on the data corresponding to certain time moment, i.e. information on one certain moment is used and no earlier data or results from previous estimations are utilized. But in case of dynamic state estimation, previously collected data is additionally used. But *the experience shows that the static state estimator makes less and smaller error, therefore static state estimators are more frequently used.*

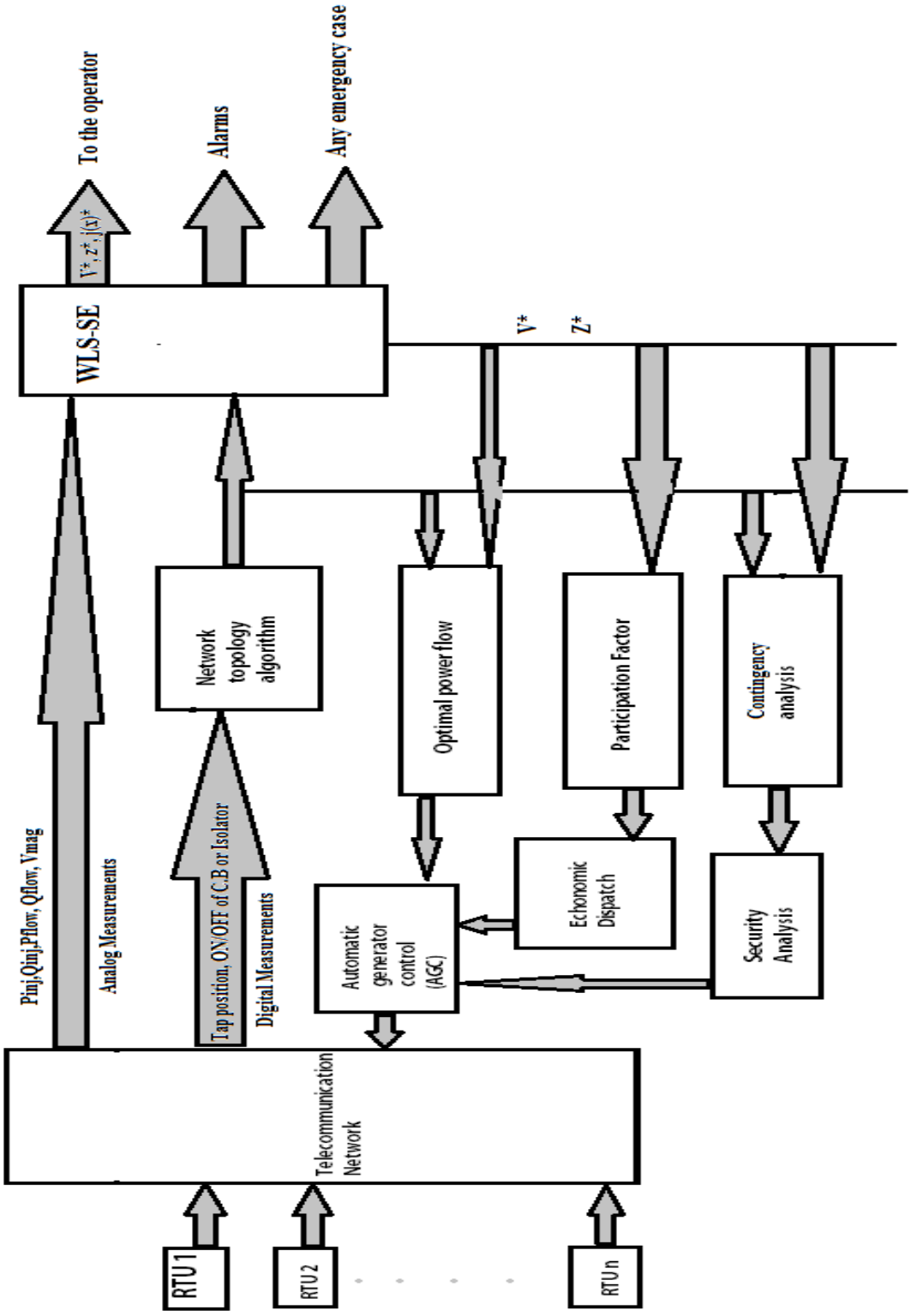

Fig. 1.1 Application of State estimation [31]

State estimator may be basically considered as a filters between raw measurements obtained from the network and the application functions that requires the reliable data on current state of system. (Fig 1.2) State estimators include the following functions:

- Topology processor
- Observability analysis
- State estimation solution
- Bad data processing.
- Parameter and structural error processing.

The topology processor gather and status data about different communication equipment e.g. circuit breaker etc., and configures the diagram of the system. As a results it generates a bus/ branch model of power system. Usually the model includes all buses within the observable area as well as it may include selected buses from neighboring system in order to build up and update the external system model.

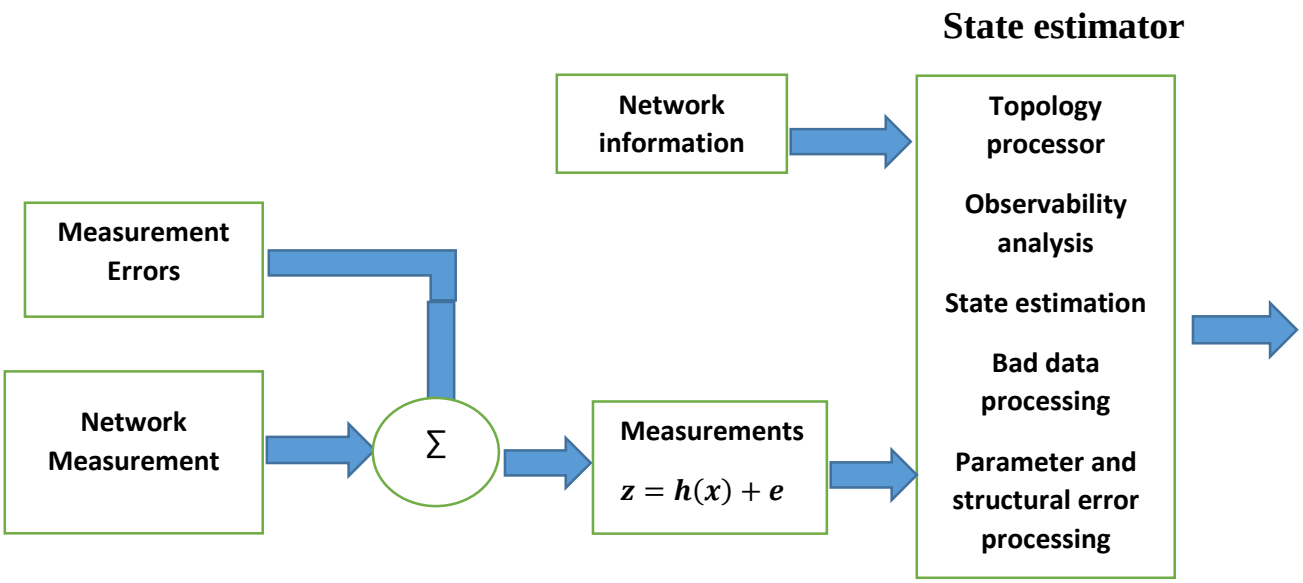

Fig. 1.2 Principal scheme of state estimator [24]

The objective of state estimation is to determine the best estimate for the system state, which includes complex bus voltage in entire power system, is based on the system model and on the gathered measurements from the system. Best estimates for all the line flows, load and generator outputs are also provided as a result of state estimation.

1.3 DISTRIBUTION SYSTEM STATE ESTIMATION

1.3.1 INTRODUCTION TO DISTRIBUTION SYSTEM STATE ESTIMATION (DSSE)

In Electrical system, purpose of distribution network/system is to distribute electrical energy from transmission substations to loads (customers). Distribution network consists of:

- Different types of lines (overhead lines and underground cables).
- Different voltage levels (medium and low-voltage).
- Different network configuration (radial and meshed)

All the above factors influence the distribution network security of supply, economical efficiency and quality of power. Distribution and transmission systems are very different from each other.

Transmission System	Distribution system
• High X/R ratio • Highly mesh connected. • Highly stable • Well condition system • Highly balanced network	• Low X/R ratio • Highly Radial network. • Less Stable • Ill condition system • Unbalanced network

Table 1.1 Difference between transmission system and distribution system

Initial research into DSSE began in the 1990's. DSSE presents a number of new challenges, since the characteristics of distribution networks differ fundamentally from transmission networks in the following ways:

- Construction: Most distribution networks have a radial construction (whereas transmission systems are more meshed), often with low X/R ratios. Distribution networks are defined by medium/low voltage levels. For this reason, and due to the physical characteristics of the lines, X/R ratios equal to few units or even equal to unity are possible. This leads to the impossibility of adopting simplifications commonly used in the estimators developed for transmission systems, as for example, neglecting resistances because of dominant inductive terms. As a further consequence, decoupled versions of the estimators are not so easily obtained.

- Redundancy : For technical and economic reasons the number of measurement points in distribution networks is much lower than in transmission networks i.e. Distribution network has low redundancy level as compare to transmission system. Because of the lack of redundancy, the available measurements are critical for the estimator uncertainty and robustness (with respect to measurement loss or degradation), and for the implementation of auxiliary functions such as bad data detection, topology error identification and parameter check. Because of *Low number of measurement devices,* the biggest problem for the evaluation of the state of the network. The observability of the network can only be obtained by exploiting the so-called pseudo-measurements.

- Measurement types: Most of the available input data at the distribution level are measurements (or pseudo measurements) of power or current injections. Direct measurements of voltages and power flows are rare.

- Scale and complexity: Distribution networks in rural areas are very different from those in urban areas and have very large numbers of components. This means that the methods developed for DSSE need to be scalable, have a relatively low computational burden, and be applicable across a range of different network types.

- Phase imbalances: Conventional SE techniques assume that the network is a balanced system. However, distribution systems, can have significant phase imbalances, requiring the use of full three-phase system models.

- Network model uncertainty. In the SE framework, line impedances of the network are generally assumed to be known. Actually, the knowledge of network model parameters has large uncertainty due to network aging and lack of accurate measurement campaigns. This can lead to a degradation of SE performance.

- *High number of nodes:* As mentioned before, the distribution networks are typically very large networks, with a high number of nodes. This (along with the need of developing three-phase estimators) leads to very large systems, resulting in the explosion of execution times of the algorithms and in demanding requirements for large data acquisition and storage within the calculation center of the network.

As a consequences, traditional State Estimation methods frequently suffer from convergence and/or numerical difficulties when applied to distribution system.

1.3.2 DISTRIBUTION-MANAGEMENT SYSTEM (DMS)

A DMS is a collection of applications that can monitor and control the entire distribution network efficiently and reliably. It acts as a decision support system to assist the control room and field operating personnel with the monitoring and control of the electric distribution system. Improving the reliability and quality of service in terms of reducing outages, minimizing outage time, maintaining acceptable frequency and voltage levels are the key deliverables of a DMS.

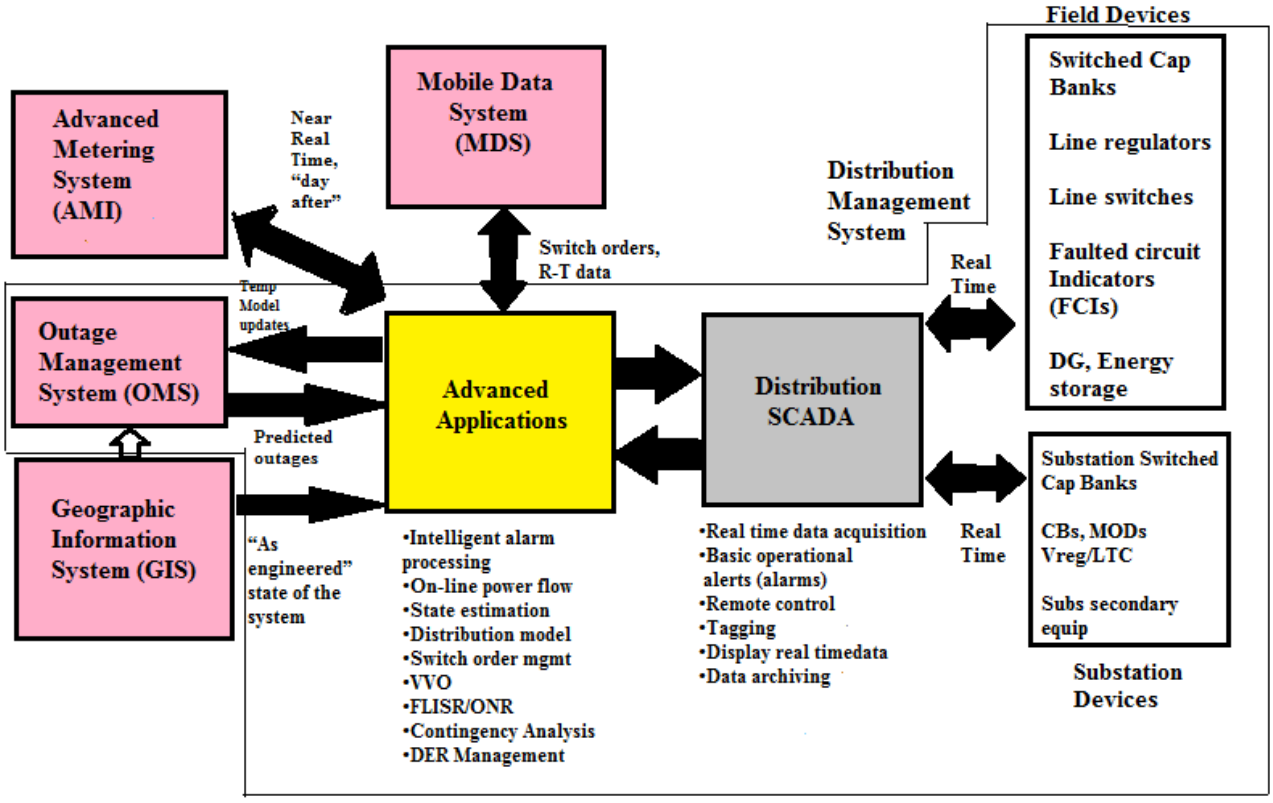

Fig. 1.3 Distribution Management System Components Interactions with Operational Support Systems [25]

A DMS solution creates the context to tightly integrate tools and systems addressing different aspects of the distribution operator's and/or dispatcher's work tasks, including but not restricted to:

- **Outage management system (OMS)** – provides the ability to view the current connectivity of the distribution feeders and safely manage day-to-day and emergency restoration work.
- **Mobile date system (MDS)**– provides the ability for work crews to communicate electronically with the OMS directly from the field, reducing delays in performing tasks and improving safety.
- **Distribution supervisory control and data acquisition (D-SCADA)**

  As communication and distribution automation technology is being deployed, a scalable and flexible SCADA provides real-time telemetry information to keep the operating model as close as possible to the real conditions in the field, as well as remote fast switching to improve reliability and reduce operational costs (fuel, labor, etc.).

Typical Distribution Control Center a Few Years Ago

Fig. 1.4 Typical Distribution Control Center a Few Years Ago

- Distribution System was operated manually with wall- mounted switching diagrams.
- Mostly paper driven processes.

Electronic Map Visualization

Fig 1.5 Current Trend in Control Center Design

- Static map boards replaced by large screen, video displays
- Operator workstations include large number of computer monitors (side-by side)

In modern distribution-management system (DMS), **DSSE** plays a critical role to estimate the **real-time system states** that are unable to be obtained *from the limited measuring instruments* at the distribution system level. With DSSE, the operators can calculate the theoretical power loss, guide network reconfiguration, and prevent distribution lines from overloading, etc. Therefore, they can improve the capability of monitoring, controlling and economically dispatching distribution systems, and finally improve the power quality and reliability of distribution systems. DSE is a fundamental function in DMS.

1.4 DISTRIBUTION GENERATION (DG)

The Distributed Generation (DG) concept basically advocates the connection of small to medium size generating units at the sub-transmission and distribution levels. Distributed generation is considered as an electrical source connected to the power system, in a point very close to/or at consumer´s site, which is small enough compared with the centralized power plants. Some part of the energy-demand is supplied by the centralized generation and another part is produced by distributed generation. The electricity is going to be produced closer to the customers.

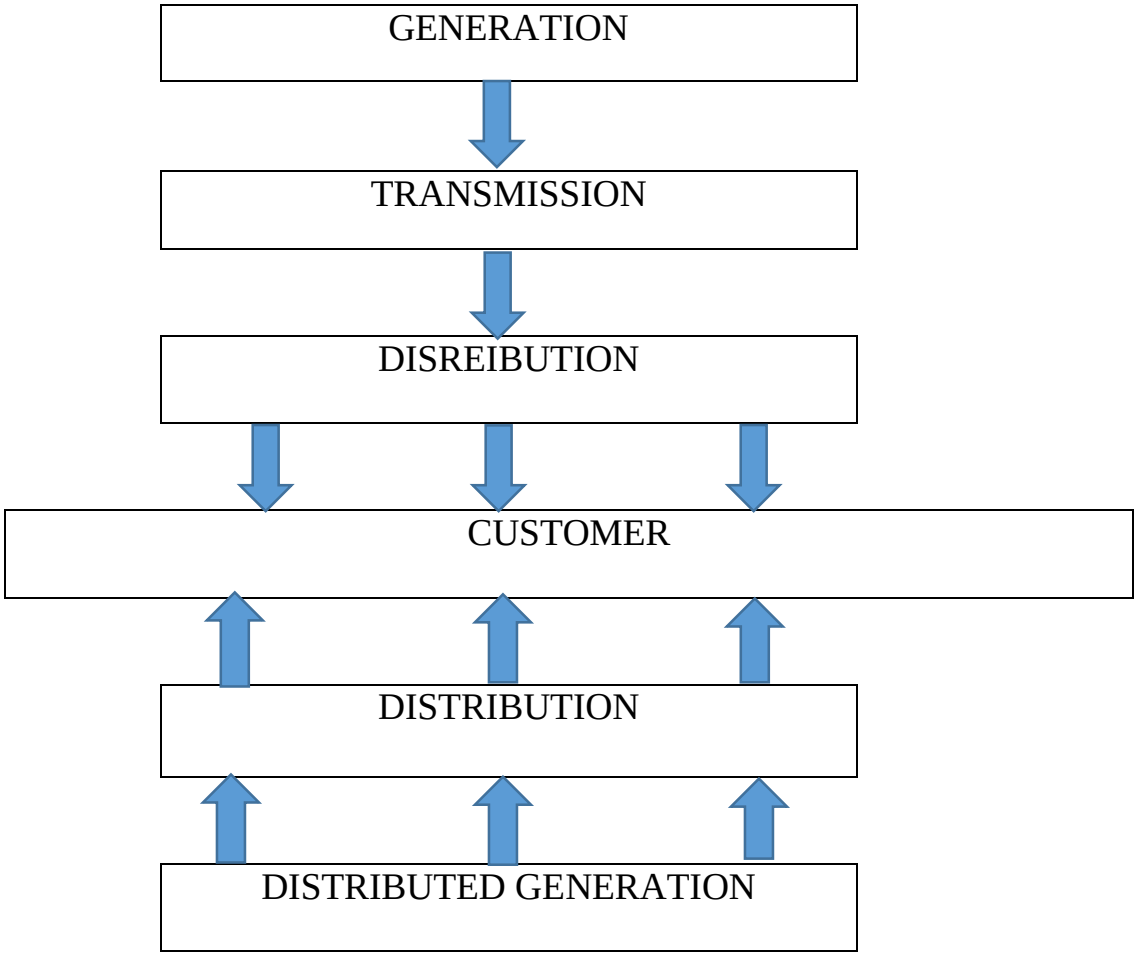

Fig.1.6 New industrial conception of the electrical energy supply [24]

To clarify about the DG concept, some categories that define the size of the **generation unit** are presented in Table 1.2 [24].

Type	Size
Micro distributed generation	**1Watt < 5Kw**
Small distributed generation	**5kW < 5 MW**
Medium distributed generation	**5 MW < 50MW**
Large distributed generation	**50MW < 300MW**

Table 1.2 Size of the DG [24]

1.4.1 TYPES OF DISTRIBUTED GENERATION

DG can be classified into two major groups,

- Inverter based DG
- Rotating machine DG.

Normally, inverters are used in DG systems after the generation process, as the generated voltage may be in DC or AC form, but it is required to be changed to the nominal voltage and frequency. Therefore, it has to be converted first to DC and then back to AC with the nominal parameters through the rectifier. The DG technologies, which are available at the present:

- Photovoltaic systems
- Wind turbines
- Fuel cells
- Micro turbines
- Synchronous and induction generators.

1.4.1.1 PHOTOVOLTAIC SYSTEMS (PV)

A photovoltaic system, converts the light received from the sun into electric energy. In this system, semi conductive materials are used in the construction of solar cells, which transform the self-contained energy of photons into electricity, when they are exposed to sun light. The cells are placed in an array that is either fixed or moving to keep tracking the sun in order to generate the maximum power.

Advantages:

1. Environmental friendly without any kind of emission.
2. Easy to use.
3. With simple designs and it does not require any other fuel than solar light.

Disadvantages:

1. Need large space.
2. High initial cost.

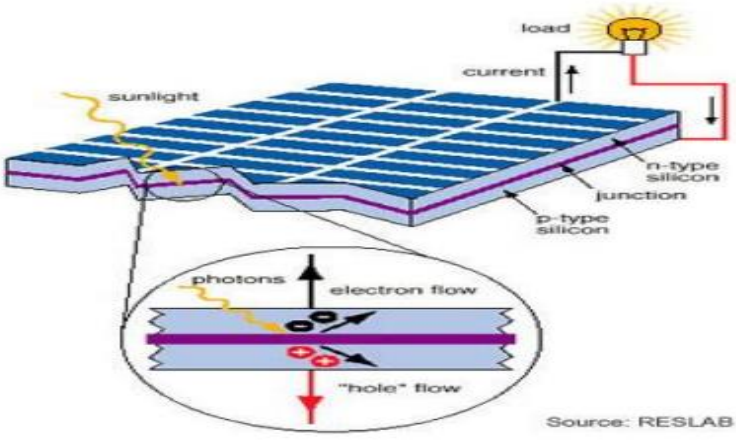

Fig. 1.7 Schematic diagram of a photovoltaic system [26]

PV systems generate DC voltage then transferred to AC with the aid of inverters. There are two general designs that are typically used: with and without battery storages.

1.4.1.2 Wind Turbines

Wind turbines transform wind energy into electricity. The wind is a highly variable source, which cannot be stored, thus, it must be handled according to this characteristic. A general scheme of a wind turbine is shown in Fig. 1.8, where its main components are presented.

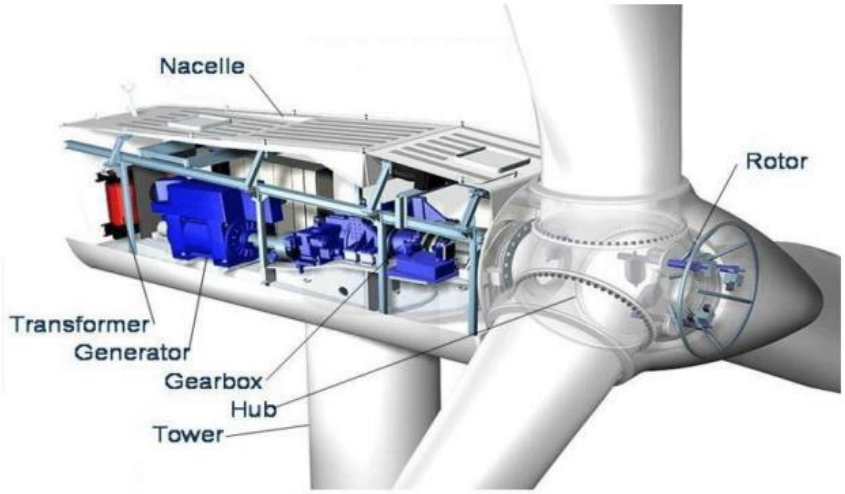

Fig.1.8 Schematic operation diagram of a wind turbine [26]

In the most common system, the generator system gives an AC output voltage that is dependent on the wind speed. As wind speed is variable, the voltage generated has to be transferred to DC and back again to AC with the aid of inverters. However, fixed speed wind turbines are directly connected to grid.

Advantages:

1. Low Maintenance
2. Low pollution

Disadvantages

1. *High Installation Cost:* The cost depends on the following things, turbine size, installation contracts, and kind of turbine, location, freight, utility system upgrades, metering equipment, maintenance, and warranty. The commercial wind turbine cost is about $1- $2 million a MW nameplate capacity installed and if you buy the same turbine in 2 MW, its cost would be about $2.8 million. The 10 KW wind turbine price is about $28,000and 100 KW price is about $ 48,000.

1.4.1.3 Fuel Cells

Fuel cells operation is similar to a battery that is continuously charged with a fuel gas with high hydrogen content; this is the charge of the fuel cell together with air, which supplies the required oxygen for the chemical reaction.

The fuel cell utilizes the reaction of hydrogen and oxygen with the aid of an ion conducting electrolyte to produce an induced DC voltage. The DC voltage is converted into AC voltage using inverters and then is delivered to the grid.

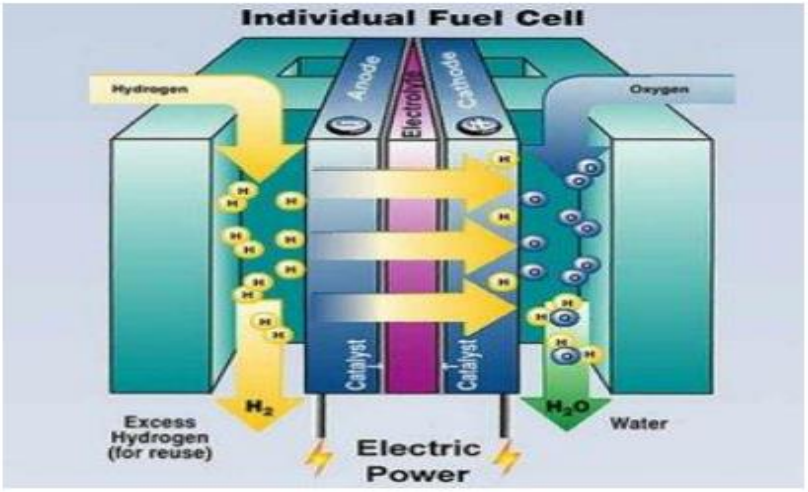

Fig. 1.9 Schematic diagram of a fuel cell [26]

Advantages:

1. High reliability due to absence of moving part.
2. No generation of Noise.
3. Operated with a width spectrum of fossil fuels with higher efficiency than any other generation device.

Disadvantages:

1. High Running cost.

1.4.1.4 Micro-Turbines

A micro-turbine is a mechanism that uses the flow of a gas, to covert thermal energy into mechanical energy. The combustible (usually gas) is mixed in the combustor chamber with air, which is pumped by the compressor. This product makes the turbine to rotate, which at the same time, impulses the generator and the compressor. In the most commonly used design the compressor and turbine are mounted above the same shaft as the electric generator. This is shown in Fig. 1.10

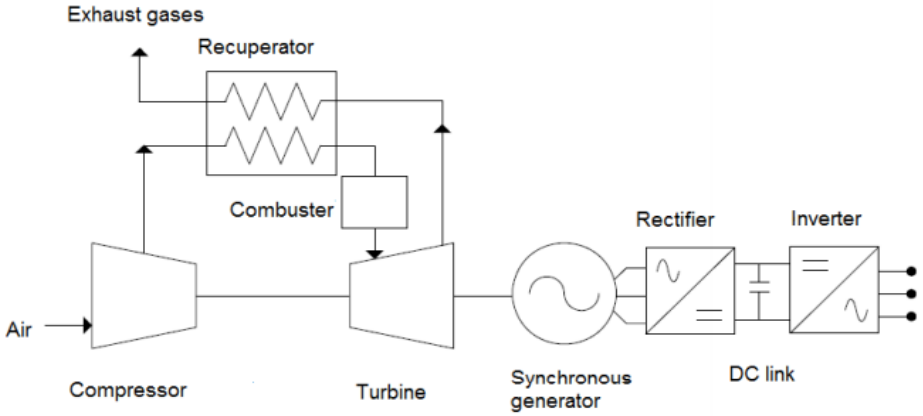

Fig 1.10 Schematic diagram of a micro-turbine [26]

The output voltage from micro-turbines cannot be connected directly to the power grid or utility, it has to be transferred to DC and then converted back to AC in order to have the nominal voltage and frequency of the utility.

Advantages:

1. Clean operation with low emissions.
2. Good efficiency.

Disadvantages:

1. High maintenance cost
2. The lack of experience in this field.

1.4.1.5 Induction and Synchronous Generators

Induction and synchronous generators are electrical machines which convert mechanic energy into electric energy then dispatched to the network or loads. Induction generators produce electrical power when their shaft is rotated faster than the synchronous frequency driven by a certain prime mover (turbine, engine). The flux direction in the rotor is changed as well as the direction of the active currents, allowing the machine to provide power to the load or network to which it is connected. The power factor of the induction generator is load dependent and with an electronic controller its speed can be allowed to vary with the speed of the wind. The cost and performance of such a system is generally more attractive than the alternative systems using a synchronous generator.

The induction generator needs reactive power to build up the magnetic field, taking it from the mains. Therefore, the operation of the asynchronous machine is normally not possible without the corresponding three-phase mains. In that case, reactive sources such as capacitor banks would be required, making the reactive power for the generator and the load accessible at the respective locations. Hence, induction generators cannot be easily used as a backup generation unit, for instance during islanded operation.

The synchronous generator operates at a specific synchronous speed and hence is a constant-speed generator. In contrast with the induction generator, whose operation involves a lagging power factor, the synchronous generator has variable power factor characteristic and therefore is suitable for power factor correction applications. A generator connected to a very large (infinite bus) electrical system will have little or no effect on its frequency and voltage, as well as, its rotor speed and terminal voltage will be governed by the grid. Normally, a change in the field excitation will cause a change in the operating power factor, whilst a change in mechanical power input will change the corresponding electrical power output. Thus, when a synchronous generator operates on infinite bus bars, over-excitation will cause the generator to provide power at lagging power factor and during under-excitation the generator will deliver power at leading power factor. Thus, synchronous generator is a source or sink of reactive power. Nowadays, synchronous generators are also employed in distribution generator systems, in thermal, hydro, or wind power plants. Normally, they do not take part in the system frequency control as they are operated as constant power sources when they are connected in low voltage level. These generators can be of different ratings starting from kW range up to few MW ratings.

1.4.2 BENEFITS OF DISTRIBUTED GENERATION (DG)

- Connection of DG is intended to increase the reliability of power supply provided to the customers, using local sources, and if possible, reduce the losses of the transmission and distribution systems. One of the major impacts of Distributed generation is on the losses in a feeder. Locating the DG units is an important criterion that has to be analyzed to be able to achieve a better reliability of the system with reduced losses. Locating DG units to minimize losses is similar to locating capacitor banks to reduce losses. The main difference between both situations is that DG may contribute with active power and reactive power (P and Q). On the other hand, capacitor banks only contribute with reactive power flow (Q). Mainly, generators in the system operate with a power factor range between 0.85 lagging and unity, but the presence of inverters and synchronous generators provides a contribution to reactive power compensation (leading current).

- The connection of DG to the power system could improve the voltage profile, power quality and support voltage stability. Therefore, the system can withstand higher loading situations.

- The installation of DG takes less time and payback period. Many countries are subsidizing the development of renewable energy projects through a portfolio obligation and green power certificates. This incentives investment in small generation plants.

- Some DG technologies have low pollution and good overall efficiencies like combined heat and power (CHP) and micro-turbines. Besides, renewable energy based DG like photovoltaic and wind turbines contribute to the reduction of greenhouse gases.

1.4.3 DISADVANTSGES OF DISTRIBUTED GENERATION (DG)

- Many DG are connected to the grid via power converters, which injects harmonics into the system. DG can be a source of harmonics to the network. Harmonics produced can be either from the generation unit itself (synchronous generator) or from the power electronics equipment such as inverters. Rotating generators are another source of harmonics, that depends on the design of the generators winding (pitch of the coils), core non-linearity's, grounding and other factors that may result in significant harmonics propagation.

- The connection of DG might cause over-voltage, fluctuation and unbalance of the system voltage if coordination with the utility supply is not properly achieved.

- Depending on the network configuration, the penetration level and the nature of the DG technology, the power injection of DG may increase the power losses in the distribution system.

- The presence of DG in a network affects the short circuit levels of the network. It creates an increase in the fault currents when compared to normal conditions at which no DG is installed in the network. The fault contribution from a single small DG is not large, but even so, it will be an increase in the fault current. In the case of many small units, or few large units, the short circuits levels can be altered enough to cause miss coordination between protective devices, like fuses or relays. The influence of DG to faults depends on some factors such as the generating size of the DG, the distance of the DG from the fault location and the type of DG. This could affect the reliability and safety of the distribution system. In the case of one small DG embedded in the system, it will have little effect on the increase of the level of short circuit currents. On the other hand, if many small units or a few large units are installed in the system, they can alter the short circuit levels sufficient to cause fuse-breaker miss-coordination. This could affect the reliability and safety of the distribution system.

1.5 POINTS OF COMMON COUPLING (PCC)

A PCC is generically defined as a point where a local power system is connected to an area power system. It can thus be seen as an umbrella concept which covers the interconnection point of the distribution network with DG installations, aggregated loads, and even micro grids.

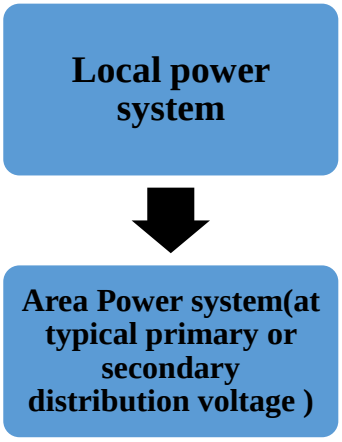

Fig. 1.11 Points of common coupling

PCCs are expected to exhibit large power injection uncertainties when compared to regular load connection points. This behavior is particularly expected of PCCs that interconnect renewable energy resources such as wind and photovoltaic (PV) generation to distribution systems, due to their intrinsic variability.

1.5.1 NEED FOR REAL TIME MONITORING OF PCC

The progressive interconnection of distributed generation (DG) have brought about several challenges to the operation of distribution systems. As a result, the task of maintaining secure and reliable operation conditions in distribution networks has become increasingly complex. In fact, due to the interconnection of wind and solar energy sources, **DG power outputs** are subject to significant variability during unfavorable periods.

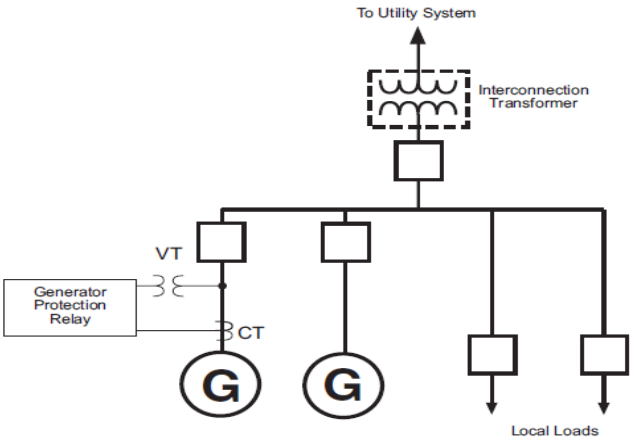

Fig. 1.12 Typical Generator Protection [25]

Generator protection provides detection of:

1. Generator internal short circuits;
2. Abnormal operating conditions i.e. loss of field, reverse power, over excitation and unbalanced currents.

Conventional technologies might be subjected to forced outages or unscheduled maintenances without prior warning to system operators.

1.5.1.1 PROTECTION COORDINATION

The PCC has to be properly protected to avoid any damage to both sides, the DG equipment and the utility equipment, during fault conditions. In the interconnection of the DG to the distribution utility grid, there are some protection requirements that are established by the utility. Interconnection protection is usually dependent on size, type of generator, interconnection point and interconnecting transformer connection.

The protection is based on the following factors:

- Protection should respond to the failure of parallel operation of the DG and the utility.
- Protecting the system from fault currents and transient over voltages generated by the DG during fault conditions in the system.

- Protecting the DG from hazards it may face during any disturbance occurring in the system such as automatic reclosing of re-closers as this can cause damage depending on the type of the generator used by the DG.
- Network characteristics at the point of DG interconnection. Considering the capability of power transfer at this point and the type of interconnection.

The generator protection is one of the most important devices, typically located at the generator´s terminals. Its function is to detect internal short circuits and abnormal operating conditions of the generator itself, for instance: reverse power flow, over excitation of the generator and unbalanced currents.

.

1.5.1.2 ISLANDING DETECTION

The techniques used in detecting islanding situations are based on measuring the output parameters of the DG and a decision is taken to decide whether these parameters define an islanding situation or not.

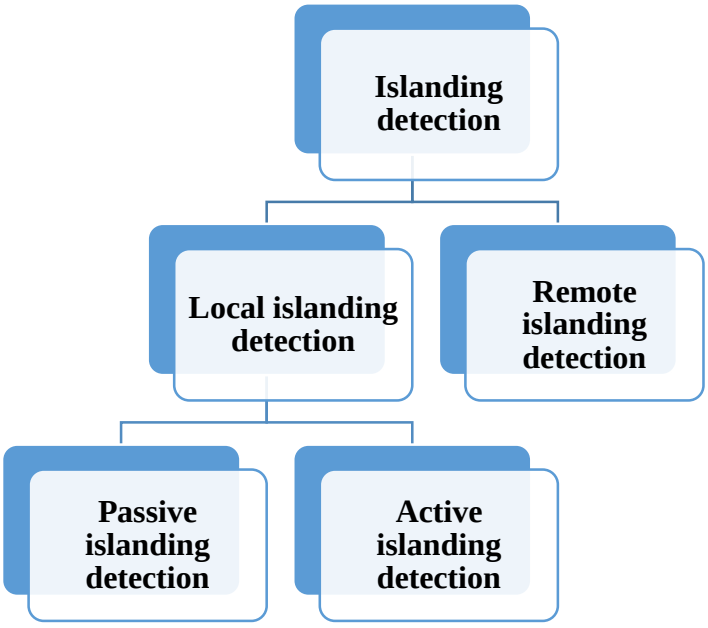

Fig.1.13 Islanding detections techniques

- *Remote islanding detection technique:* It is based on communication between utilities and DGs. Remote detection techniques have higher reliability than local detection techniques, but they are expensive to implement in many distribution system.

- *Local islanding detection technique:* This are based on the measurement of the system parameters at the DG location, like voltage, frequency, etc.

- *Passive islanding detection technique:* This technique monitor the variations occurring in the power system parameters such as the short circuit levels, phase displacement and the rate of output power as in most cases of utility disconnection the nominal network voltage, current and frequency are affected.

One of the direct and efficient islanding detection methods is by **monitoring the trip status** of the main utility circuit breaker and as soon as the main circuit breaker trips, an instantaneous signal is sent to the circuit breaker at the interconnection between the DG and the utility system to trip the interconnection circuit breaker preventing the occurrence of islanding. Even though this method seems to be easy and direct, its implementation is difficult due the distribution of DGs in a large geographic range that will require special comprehensive monitoring techniques with committed systems.

1.5.1.3 DG INTERCONNECTION PROTECTION

Properly designed interconnection protection should address the concerns of both the DG owner, as well as the utility, at the lowest possible cost. The major functions of interconnect protection is to prevent system islanding by detecting asynchronous DG operation. This detection and tripping must be rapid enough to allow automatic reclosing by the utility.

DG interconnection protection methods:

- Detection of loss of parallel operation with utility
- Fault backfeed detection
- Detection of damaging system conditions

- **Abnormal power flow**
- Restoration

Interconnect protection provides the protection that allows the dispersed generators to operate in parallel with the utility grid. Typically, protection requirements to connect a dispersed generator to the utility grid are established by each individual utility.

The functional levels of interconnection protection vary widely depending on factors such as:

- generator size,
- point of interconnection to the utility system (distribution or sub-transmission)
- type of generator (induction, synchronous, asynchronous)
- interconnection transformer configuration

Interconnection protection objective	**Protection function used**
Detection of loss of parallel operation with utility system	81O/U, 81R*, 27/59, 59I, TT**
Fault backfeed detection	Phase Faults: 51V, 67, 21 Ground Faults: 51N, 67N, 59N, 27N
Detection of damaging system conditions	47, 46
Abnormal power flow detection	32
Restoration	25

Table 1.3 Specific objectives of an interconnection protection system**.**

1.5.1.3.1 DETECTION OF LOSS OF PARALLEL OPERATION WITH THE UTILITY SYSTEM

The most basic and universal means of detecting loss of parallel operation with the utility is to establish **an over/ underfrequency (81O/U) and over/undervoltage (27/59)** "window" within which the DG is allowed to operate. When the DG is islanded from the utility system, either due to a fault or other abnormal condition, the frequency and voltage will quickly move outside the operating window if there is a significant difference between load and dispersed generator levels.

In some cogeneration applications such as within the petrochemical and pulp and paper industries, **rate of change of frequency relays (81R)** are used to more rapidly detect the loss of utility supply. The 81R function separates the plant facility from the utility.
When the loss of parallel operation is detected, the dispersed generator must be separated from the utility system quickly enough to allow the utility breaker at the substation to automatically reclose.

1.5.1.3.2 FAULT BACKFEED DETECTION

For small DG, no specific fault backfeed detection is generally provided. For these small generators, the detection of loss of parallel operation via 81O/U and 27/59 relays is all the interconnection protection necessary. *The larger the DG*, the greater is the chance that it will contribute significant current to a utility system fault. For this situation, fault backfeed detection in addition to loss of parallel operation protection is provided. In developing backfeed removal protection, the decay of current for external faults needs to be addressed. Typically, relay functions such as the **67, 21 or 51V are used to provide phase fault backfeed detection**. When developing settings for the 67 and 21 relays, the relay pickup setting must be set above the level of generation current being supplied by the DG to the utility system. Some utilities supervise a voltage restraint/controlled overcurrent relay (51V) with the 67 function to increase pickup sensitivity. Ground fault backfeed removal depends on the primary winding connection of the interconnection transformer. For grounded primary transformer winding, a 51N neutral overcurrent relay or, in some cases, a 67N ground direction relay is used.

1.5.1.3.3 DETECTION OF DAMAGING SYSTEM CONDITIONS

Unbalanced current conditions caused by open conductors or phase reversals on the utility supply circuit can subject the DG to a high level of negative sequence current. This high negative sequence current results in rapid rotor heating causing IPP generator damage. Many utilities provide the protection against these unbalanced currents as part of the interconnection protection package using **a negative sequence overcurrent relay 46**, as shown in fig.1.14. To provide protection for phase reversals caused by inadvertent “phase swapping” after power restoration, **a negative sequence voltage relay 47** is also used.

1.5.1.3.4 ABNORMAL POWER FLOW

Some interconnection contracts between cogenerating DG and the utility prohibit the DG from providing power to the utility. The cogenerating DG provides power solely to the local load at the DG facility and reduces utility demand charges by "peak shaving." It is the frequent practice of utilities to install **a directional power relay (32)** to trip the DG if power inadvertently flows into the utility system for a predetermined time in violation of the interconnection contract.

Due to the complexity in establishing settings for protective functions, unexpected trips might occur without previous warnings to system operators. All these issues highlight the importance to follow PCC power injections in real time.

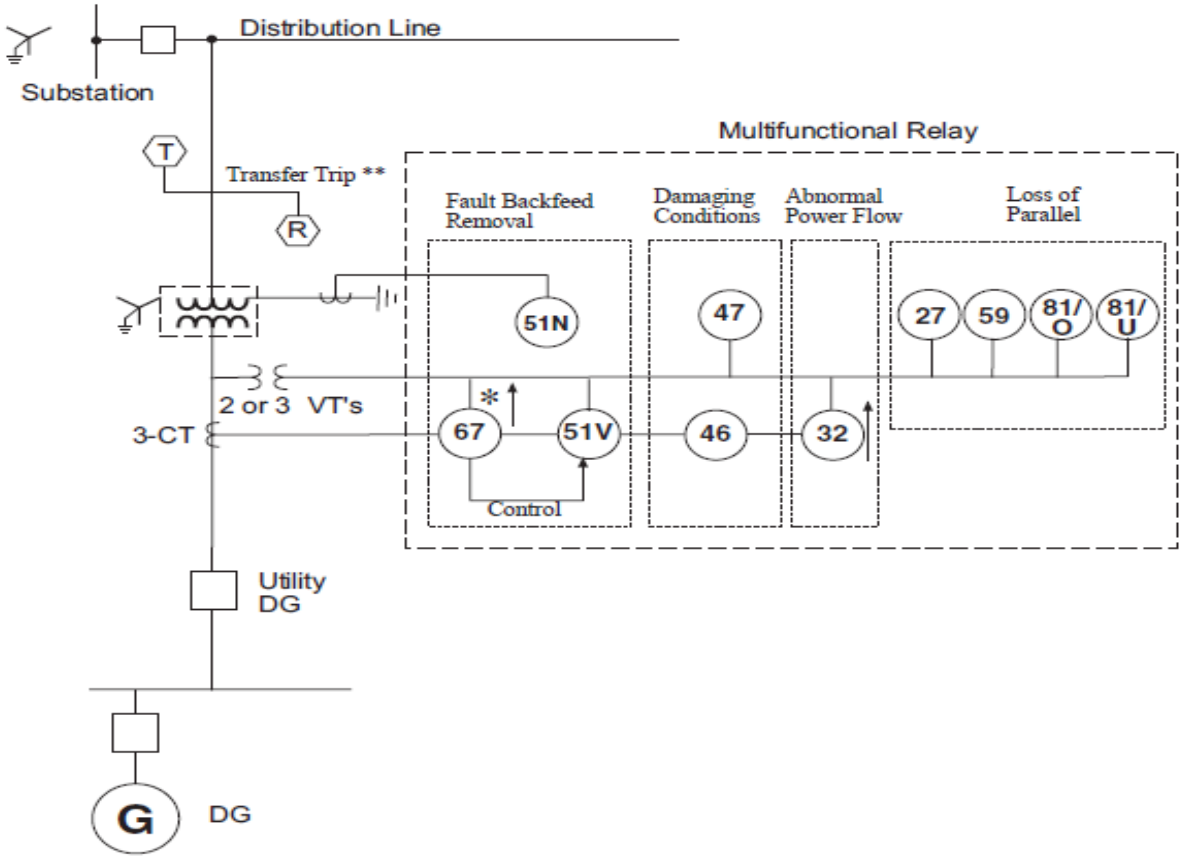

Fig. 1.14 Typical Protection for Moderately-Sized DG with Wye-Grounded (Pri) Interconnection Transformer. [26]

1.6 MODELING OF DISTRIUBUTION NETWORK VOLTAGE REGULATOR

1.6.1 INTRODUCTION

A voltage regulator is a device that keeps a predetermined voltage in a distribution line in despite of the load variations within its rated power. It consists of an autotransformer able to increase or reduce its output voltage by means of automatic tap changing. The command of the commutation mechanism can be done automatically or by manual operation. A voltage regulator is equipped with controls and accessories for its tap to be adjusted automatically under load conditions. These accessories are sensitive to voltage variations as to keep the output voltage within a determined range. The most common device is a mono-phase regulator that can be used in mono-phase systems. For three-phase distribution systems, three mono-phase regulators can be connected in grounded wye or closed delta conforming a three-phase regulator bank. Alternatively, two regulators can be connected in open delta, in such a case, only two of the three voltages are controlled. A voltage regulator is able to control the voltage of the bus where it is located, or to control the voltage of a distant bus.

1.6.2 MATHEMATICAL MODEL OF VOLTAGE REGULATORS

Voltage regulators are autotransformers with automatic or manual tap changing .Voltage variation is obtained by the changing of the autotransformer winding taps. The tap position is determined by a control circuit. Commonly, a voltage regulator can modify 10% of the nominal voltage, usually in 32 steps

There are two ways of connecting voltage regulators:

1. TYPE A
2. TYPE B

Tha main differences between connections TYPE A and TYPE B are the service and utilization voltages and their internal connections. These connections can be raising or lowering

1.6.2.1 TYPE A STEP-VOLTAGE REGULATOR

In a TYPE A connected voltage regulator, the primary circuit of the system is connected directly to the shunt winding; the series winding is connected to the shunt winding and to the regulated circuit via taps. Since the shunt winding is connected to the primary circuit the core excitation is variable.

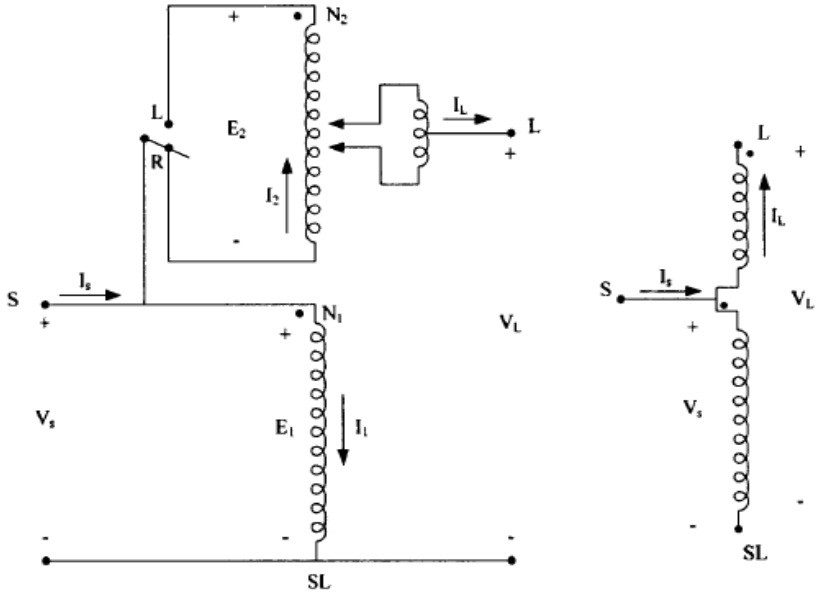

Fig.1.15 Voltage regulator of step to step TYPE A in position raise.

	Service Voltage		Utilization Voltage	
	Minimum	Maximum	Minimum	Maximum
TYPE A	114(-5%)	126(+5%)	110(-8.30/0)	125(+4.2%)
TYPE B	110(-8.30/0)	127(+5.8%)	106(-11.70/0)	127(+5.80/0)

Table 1.4 Voltages ranges of TYPE A and TYPE B regulators for 120v

Service Voltage: is the voltage at the beginning of the feeder or at the substation.

Utilization Voltage: is the voltage at the line terminals, or the voltage used by the equipment.

1.6.2.2 TYPE B STEP-VOLTAGE REGULATOR

The most common connection for voltage regulators is type B

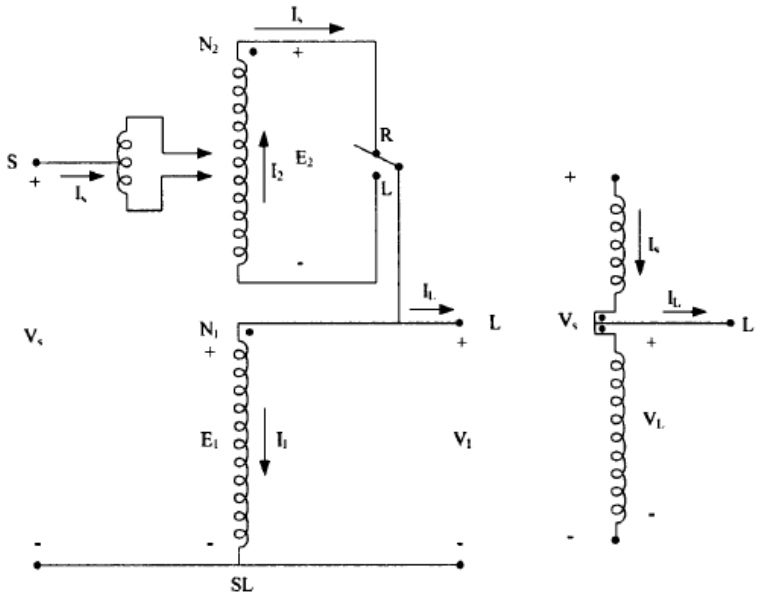

Fig.1.16 Type B voltage regulator in the raise position.

Current and voltage equations for the type B regulator in raise position are as follow:

- Voltage equation:

$$\frac{n2}{n1} = \frac{E2}{E1} \ldots\ldots\ldots \text{ Winding ratio}$$

VS=E1-E2 ……Source voltage

VL=E1……..Load voltage

$$E2 = \left(\frac{n2}{n1}\right) * E1 = \left(\frac{n2}{n1}\right) * VL$$

$$VS = \left(1 - \frac{n2}{n1}\right) * VL$$

$$VS = a_R * VL \ldots\ldots\ldots\ldots\ldots\ldots\ldots\ldots\ldots\ldots\ldots\ldots (1.1)$$

Where, $a_R = \left(1 - \frac{n2}{n1}\right)$

- Current equation

$$\frac{n2}{n1} = \frac{I1}{I2} \ldots\ldots\ldots \text{ Winding ratio}$$

IL=IS-I1……. Load current

& I2=Is

$$I1 = \left(\frac{n2}{n1}\right) * I2 = \left(\frac{n2}{n1}\right) * IS$$

$$IL = \left(1 - \frac{n2}{n1}\right) * IS$$

IL= a_R * IS……..… (1.2)

Where, $a_R = \left(1 - \frac{n2}{n1}\right)$

Voltage and current equations for the type B regulator in lower position are as follow:

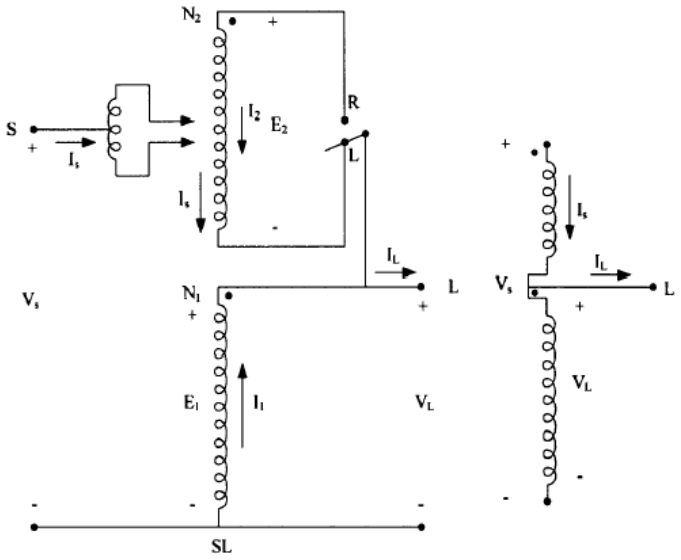

Fig.1.17 Type B voltage regulator in the lower position.

- Voltage equation:

$$\frac{n2}{n1} = \frac{E2}{E1} \ldots\ldots\ldots \text{Winding ratio}$$

VS=E1+E2 ……Source voltage

VL=E1……...Load voltage

$$E2 = \left(\frac{n2}{n1}\right) * E1 = \left(\frac{n2}{n1}\right) * VL$$

$$VS = \left(1 + \frac{n2}{n1}\right) * VL$$

VS=a_R *VL……. (1.3)

Where, a_R=$\left(1 + \frac{n2}{n1}\right)$

- Current equation

$$\frac{n2}{n1} = \frac{I1}{I2} \ldots\ldots\ldots \text{ Winding ratio}$$

IL=IS+I1……. Load current

& I2=Is

$$I1 = \left(\frac{n2}{n1}\right) * I2 = \left(\frac{n2}{n1}\right) * IS$$

$$IL = \left(1 + \frac{n2}{n1}\right) * IS$$

IL= a_R * IS……..…… (1.4)

Where, a_R=$\left(1 + \frac{n2}{n1}\right)$

The difference between the voltage and current equations of the type B regulator in the raise or lower position is the sign of the winding ratio $\left(\frac{n2}{n1}\right)$, the actual winding ratio in each winding is unknown, and the tap position is known.

The equations of the effective winding ratio $\mathbf{a_R}$ can be modified in function of the tap position. Each tap can change the voltage 0.00625 in p.u, then the effective ratio is given by:

$$\mathbf{a_R = 1 \pm 0.00625 * Tap} \ldots\ldots\ldots\ldots\ldots\ldots\ldots \text{ (1.5)}$$

In (1.5) the negative sign refers to the raise position, and the positive refers to the lower position.

In type A and type B regulators the ratios of source voltage and current with respect to the load voltage and current are given by:

TYPE A : $\boldsymbol{VS = \left(\frac{1}{a_R}\right) * VL}$ $\boldsymbol{IS = a_R * IL}$

TYPE B : $\boldsymbol{VS = a_R * VL}$ $\boldsymbol{IS = \left(\frac{1}{a_R}\right) * IL}$

Sign for equation (1.5)

	Type A	Type B
Raise	+	-
Lower	-	+

A single-phase step by step voltage regulator can be externally connected to form a three-phase regulator bank. In a single-phase regulator connection each regulator has a compensating circuit, then, the regulator taps can be modified separately.

1.6.3 CONNECTION METHODS OF VOLTAGE REGULATORS

Typically three-phase voltage regulators can be connected in the following ways:

1. Three regulators connected in grounded wye
2. Two regulators connected in open delta
3. Three regulators connected in closed delta

1.6.3.1 WYE-CONNECTED REGULATOR

Three single-phase type B regulators can be connected in wye as shown in Fig. 1.18 In this case, the polarity of the winding is in the raise position. When the regulator is at the lower position a reversing switch is reconnected to the series windings and is associated to the output terminal

The following voltage and current equations are used regardless of the regulator position:

$$\begin{bmatrix} Van \\ Vbn \\ Vcn \end{bmatrix} = \begin{bmatrix} \frac{1}{a_{Ra}} & 0 & 0 \\ 0 & \frac{1}{a_{Rb}} & 0 \\ 0 & 0 & \frac{1}{a_{Rc}} \end{bmatrix} * \begin{bmatrix} VAn \\ VBn \\ VCn \end{bmatrix} \quad \text{..... (1.6)}$$

$$\begin{bmatrix} Ia \\ Ib \\ Ic \end{bmatrix} = \begin{bmatrix} a_{Ra} & 0 & 0 \\ 0 & a_{Rb} & 0 \\ 0 & 0 & a_{Rc} \end{bmatrix} * \begin{bmatrix} IA \\ IB \\ IC \end{bmatrix} \quad \text{..... (1.7)}$$

Where, a_{Ra}, a_{Rb} & a_{Rc} are the effective transformation ratios of phases A, Band C.

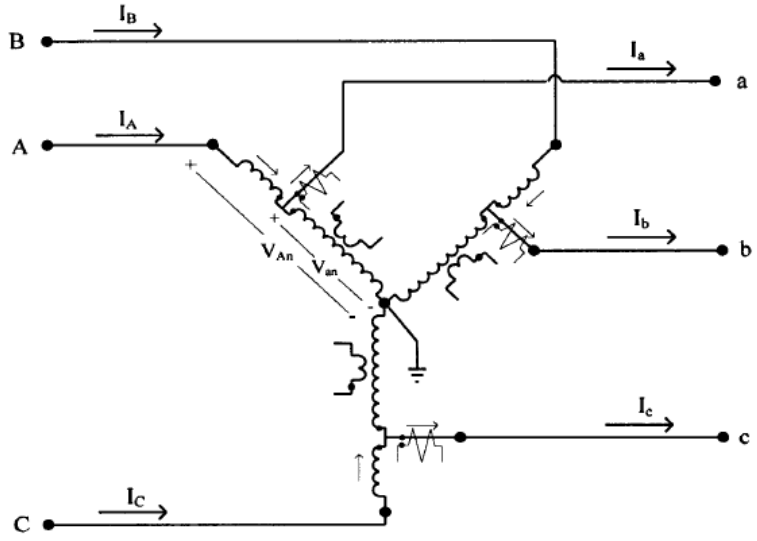

Fig.1.18 Wye connected regulator.

1.6.3.2 OPEN DELTA CONNECTED REGULATOR

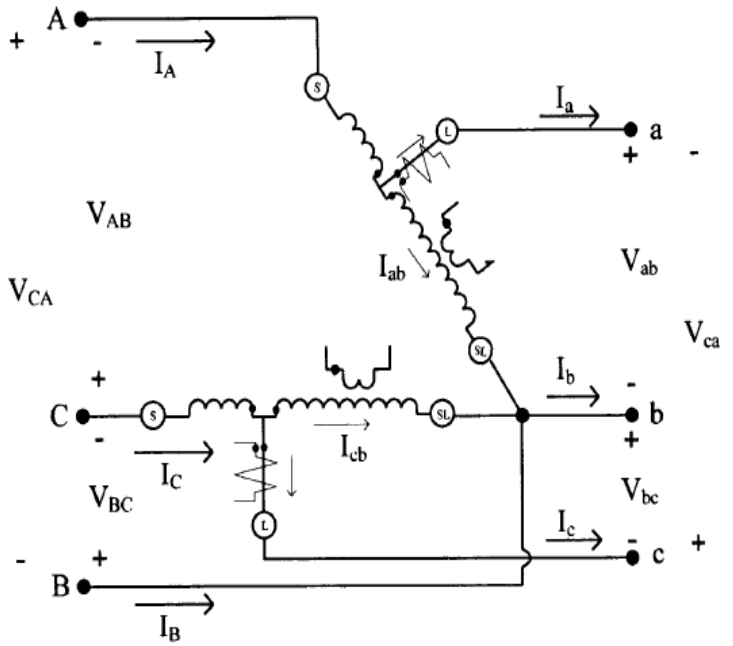

Fig.1.19 Open delta connected regulator.

There are three ways of connecting both regulators:

1. Two regulators connected between phases AB & CB
2. Two regulators connected between phases BC & AC
3. Three regulators connected between phases CA & BA

The following voltage and current equations are used.

$$\begin{bmatrix} Vab \\ Vbc \\ Vca \end{bmatrix} = \begin{bmatrix} \frac{1}{a_{Rab}} & 0 & 0 \\ 0 & \frac{1}{a_{Rcb}} & 0 \\ -\frac{1}{aRab} & -\frac{1}{a_{Rcb}} & 0 \end{bmatrix} * \begin{bmatrix} VAB \\ VBC \\ VCA \end{bmatrix} \ldots\ldots\ldots\ldots\ldots\ldots\ldots\ldots\ldots \text{(1.8)}$$

$$\begin{bmatrix} Ia \\ Ib \\ Ic \end{bmatrix} = \begin{bmatrix} a_{Rab} & 0 & 0 \\ -a_{Rab} & 0 & -a_{Rcb} \\ 0 & 0 & a_{Rcb} \end{bmatrix} * \begin{bmatrix} IA \\ IB \\ IC \end{bmatrix} \ldots\ldots\ldots\ldots \text{(1.9)}$$

In (1.8) & (1.9) $a_{R}ab$ & $a_{R}cb$ are effective transformation ratios of phases AB, CB

1.6.3.3 CLOSE DELTA CONNECTED REGULATON

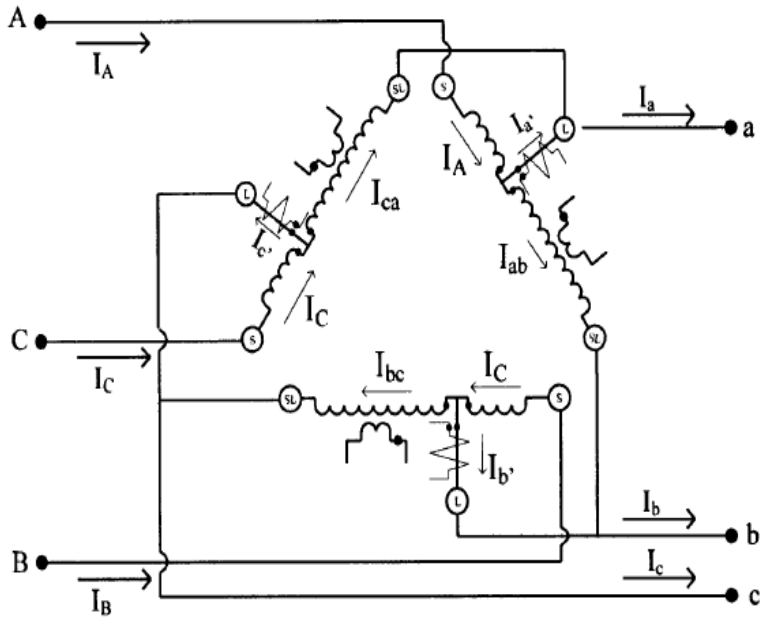

Fig.1.20 Closed delta-connected regulator.

The following voltage and current equations are used

$$\begin{bmatrix} Vab \\ Vbc \\ Vca \end{bmatrix} = \text{inv} \begin{bmatrix} a_{R}ab & 1 - a_{R}bc & 0 \\ 0 & a_{R}bc & 1 - a_{R}ca \\ 1 - a_{R}ab & 0 & a_{R}ca \end{bmatrix} * \begin{bmatrix} VAB \\ VBC \\ VCA \end{bmatrix} \quad \text{..... (1.10)}$$

$$\begin{bmatrix} Ia \\ Ib \\ Ic \end{bmatrix} = \begin{bmatrix} a_{R}ab & 0 & 1 - a_{R}ca \\ 1 - a_{R}ab & a_{R}bc & 0 \\ 0 & 1 - a_{R}bc & a_{R}ca \end{bmatrix} * \begin{bmatrix} IA \\ IB \\ IC \end{bmatrix} \quad \text{..... (1.11)}$$

In(1.10) & (1.11) a_{Rab}, a_{Rbc} & a_{Rca} are the effective transformation ratios among phases AB, BC and CA of the regulator.

1.7 LITERATURE REVIEW

M. E. Baran et al 1994 [10] presents state estimation for real time monitoring of distribution system aiming at contributing to grid situation awareness. Proposed method is based on Weighted Least Square method. Proposed method indicates that state estimation can improve the forecasted load data by using real time measurements.

Catalina Gómez-Quiles *et et,2013, [11]* ,This paper generalizes the recently introduced bilinear formulation of the WLS state estimation problem to those cases in which equality constraints must be explicitly considered. The proposed formulation prevents the ill-conditioning typically arising when exact-injection constraints are handled as virtual measurements with huge weights, while the excellent convergence speed of the bilinear scheme, which for practical purposes reaches the optimal solution in a single iteration, is fully preserved.

A. Simões Costa et al, 2007 [13], presents an application of State Estimation to the problem of monitoring Distributed Generation in distribution systems. The proposed method provides a tool to check whether the current levels of distributed generation installed on a distribution feeder is consistent with the values expected by the system operator. If not, statistical hypothesis tests are performed to identify the generating units whose outputs are inconsistent with the measurements taken along the feeder.

E. M. Lourenço at et 2006 [15], in their study of method for topology error identification in generalized state estimation based on collinearity tests involving Lagrange multipliers and the columns of the corresponding covariance matrix is presented. The method is conceptually simple, therefore being suitable for real-time applications.

Felix f. wu at et,1988 [18] presents the triangular-factorization-based observability analysis and the normalized-midual-based bad data processing are extended to *state* estimation using Hachtel's augmented matrix method. The Hachtel's method is numerically robust, computationally efficient, and reasonable in extra storage requirement. Paper shows that the observability analysis can be carried out in the process of triangular factorization of the augmented coefficient matrix used in

the Hachtel's method. The Hachtel's approach to state estimation provides an attractive alternative to the standard normal equations approach

A.K Mishra et al 2012 [23] in their study of load flow method for distribution system with distributed generations, the proposed method is basically from modified from Forward/Backward sweep method of radial distribution system to take account of DG. Proposed methods takes advantages of simplicity of radial distribution network as well as consideration of DG. And proposed methodology found fast, accurate and reliable.

Young-Hyun Moon and Byoung-Kon et al,[25] proposes fast and reliable distribution systems load flow algorithm based on Ybus formation by adopting the rectangular coordinate which requires a neglect of only second order term in linearization procedure and witch gives better convergences characteristics compare to Newton Raphson or Fast decoupled load flow method.

Kevin A. Clements at et 1998 [27], introduces a method for topology error identification based on the use of normalized Lagrange multiplier. The proposed methodology models circuit breakers as network switching branches whose statuses are treated *as* operational constraints in the state estimation problem. The corresponding Lagrange multipliers are then normalized and used as a tool for topology error identification. The method of normalized Lagrange multipliers can detection of errors in both analog measurements and constraints. The proposed algorithm has been able to identify the topology error in a limited number of steps and recover the correct circuit breaker statuses.

K.A. Clements at et,1986[30] proposes method for detecting and identifying multiple bad data in electric power networks is developed by providing a geometric interpretation of the familiar normalized residuals test for single bad data. This generalized multiple bad data test amounts to determining whether the residual vector lies in a subspace determined by the suspect measurements and whether any portions of that subspace are orthogonal to the residual vector. Efficient computational algorithms exploiting the sparsity structures of the matrices and vectors used in the multiple bad data tests will be the subject of a forthcoming paper.

1.8 OBJECTIVE OF THESIS

Nowadays, smart grid initiatives promotes at different extents the integration of renewable and distributed energy resources. The PCC where, local power system is connected to an area power system are expected to exhibit large power injection uncertainties when compared to regular load connection points. This behavior is particularly expected of PCCs that interconnect renewable energy resources to distribution network, due to their intrinsic variability, which lead to sudden and unexpected changes of power injections at PCCs. This uncertainties of power injections will cause the malfunctioning of protective devices and unexpected trip might occur without prior warning to system operators. This issue highlight the importance of developing means to observe and follow PCCs power injections variations in real time.

The objective of thesis is to monitor PCCs in real time by taking help of State estimation method. The proposed approach aims at exploring the filtering properties of state estimation to detect inconsistencies in PCC power injections.

The developed state estimator relies on a three phase network model, in which power injections at PCCs are estimated and checked in real time with value expected by system operation. But the proposed approach utilizes equality constraints to model the power injection assumptions at PCC. Normalized Lagrangian multipliers and geometric tests are then performed to identify unexpected deviations from the assumed power injection levels.

Because of limited numbers of real time measurements in distribution network, distribution networks are often classified as unobservable. Large number of zero node injections of higher weighting factors need to add in order to make system observable. This cause an ill condition of system. This thesis presents normalized Lagrangian multiplier method to handle virtual measurements. The estimation algorithm applies a sparse tableau formulation or Hatchet's method in which equality constraints are employed to model power injection assumptions at PCCs. The identification of unexpected power injections is then performed using a methodology based on normalized Lagrange multipliers and geometric tests. State Estimation (SE) methods are implemented on the IEEE10-Bus network and IEEE 34 node test feeder and applicability of the proposed approach for the future of real-time monitoring on power distribution systems.

1.9 THESIS ORGANIZATION

The thesis is divided into 5 chapters. Chapter 1 to 2 give the background information, required to understand the characteristics of transmission and distribution network and their operation. Chapter 3 to 5 discuss the distribution network Load Flow methods, State Estimation methods, used for real time monitoring of points of common coupling (PCC) in distribution network operation and conclusions.

Chapter 1 covers brief introduction about power system and distribution system state estimation, difference between transmission network and distribution network, followed by introduction and information about distribution management system. Further, it represents the introduction about new industrial conception of the electrical energy supply and different types of distribution generation used in distribution network and followed by their advantages and disadvantages in distribution network, concept of points of common coupling (PCC) in distribution network and need of monitoring of PCC in real time. It also includes the different types of voltage regulators the modeling of voltage regulator used in distribution network.

Chapter 2 covers the concept of observability and its relevance in electrical system. Followed by Rootvector based technique employed no IEEE 34-node test feeder.

Chapter 3 of thesis covers, different load flow methods of distribution network, each method's advantages and disadvantages, followed by Forward backward sweep method implementation algorithm with considering and without regulator. Forward backward sweep algorithm is implemented on 10 bus radial distribution network and IEEE 34-node test feeder.

Chapter 4 represents Traditional State estimation method description of Weighted Least Square based State Estimation (WLS-SE). It also coves the mathematic formulation and structure of Jacobian matrix and types of measurements used in WLS-SE, flowchart for WLS- State estimation Algorithm and conventional bad data detection method used in WLS-SE.

Chapter 5 covers the most important part of thesis. It describes the principle of proposed *Extended State Estimation method* for distribution network for real time monitoring of Point of Common Coupling and developed algorithm for distribution network state estimation. It also describes the problem formulation and equality constraints solution method. Distribution system modeling for equality constraints is also discussed. The modeling of power injection, assumptions and method used and detailed implementation algorithm for identification of unexpected power injection at PCCs are discussed in detail, Proposed algorithms are implemented on IEEE 10-Bus radial distribution network and IEEE 34-node test feeder. Test system data and results of case studies. Case studies, been made using proposed algorithms on IEEE 10-Bus ad IEEE 34-node test feeder. The test results are analyzed to draw major conclusions.

In addition to the conclusions, future work and references are reported.

CHAPTER 2

OBSEVABILITY ANALYSIS

2.1 INTRODUCTION TO OBSERVABILITY ANALYSIS IN DISTRIBUTION NETWORK

Observability analysis is a very important tool in State Estimation. An Observability analysis is done before attempting the state estimation. An electrical network is said to be observable if the available measurements are sufficient to estimate all the state variables uniquely within that network. The insufficiency of measurements leads to the unobservability of the system that makes it a serious problem of DSSE.

There are two types of measurements that can be added to improve the system Observability:

- **Pseudomeasurements**: historical load data used to improve the observability in the DSSE problem.
- **Virtual measurements**: are kind of information that does not require metering, such as zero injection buses. The information of a zero injection may be used in DSSE as a very accurate measurement. Virtual measurements are zero voltage drops in closed switching devices, zero power flows in open switching devices, and zero bus injections that can be found at the nodes such as a switching station.

Only a limited number of' real-time measurements are available in distribution network, as discussed in section (1.3.1). As a result, distribution networks are often classified as unobservable. In order to obtain an SE under this condition, Pseudo measurements with large margins of error can be added and they increase the **data** redundancy of SE.

Hence, if a large number of pseudo-measurements are used in the state estimation, the estimated state can contain a significant amount of uncertainty even if the network is classified as observable. If the zero-injection measurements are taken out of the measurement sets, the system may not be observable. To avoid this problem, zero injection measurements should be placed in both the real time measurement set and pseudo measurement set.

2.2 TESTS FOR OBSERVABILITY

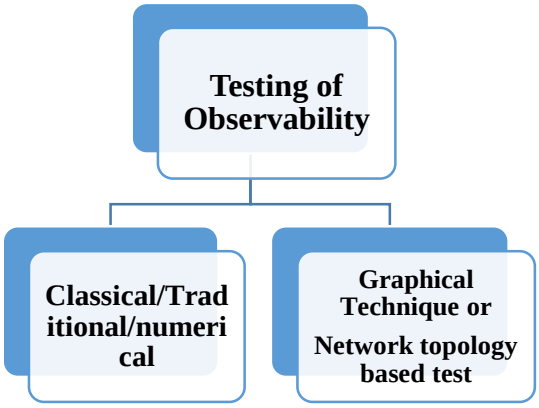

Fig 2.1 Observability analysis methods

The numerical method is based on the analysis of the rank of the Jacobian matrix. If the number of linear independent measurements is equal to or greater than the number of state variables, the column rank of the network is full. In this case, the network is found to be observable. If the rank is not full, the network is classified as unobservable.

The topological method determines the network observability by forming a tree. A tree is a set of connected and loop-free branches of the network. The network is found to be observable if a tree can be formed using given set of measurements.

2.3 IEEE 34-NODE TEST FEEDER

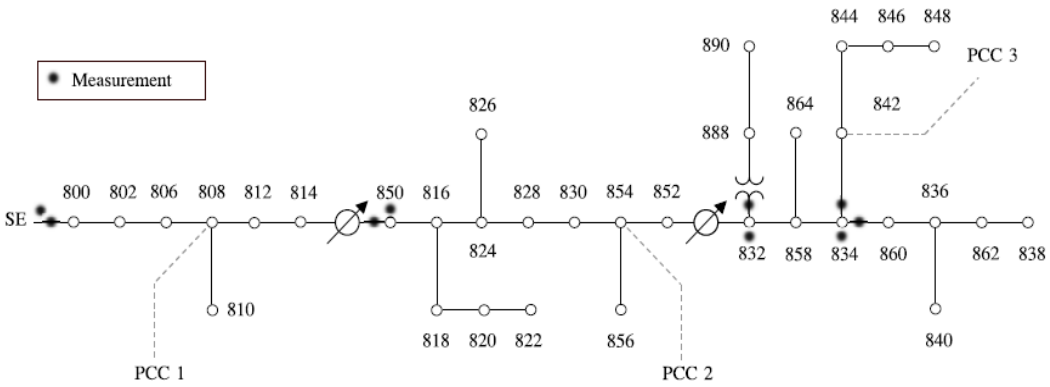

Fig. 2.2 IEEE 34-node test feeder [9]

2.4 RENAMED IEEE-34 NODE-TEST FEEDER

Criterion is used for node and line numbering:

- The nodes are numbered sequentially in ascending order proceeding from layer to layer, in such a way that any path is from the root node to a terminal node, encounters nodes numbered in the ascending order.
- Each branch starts from the sending bus (at the root side) and is identified by the number of its (unique) receiving bus.

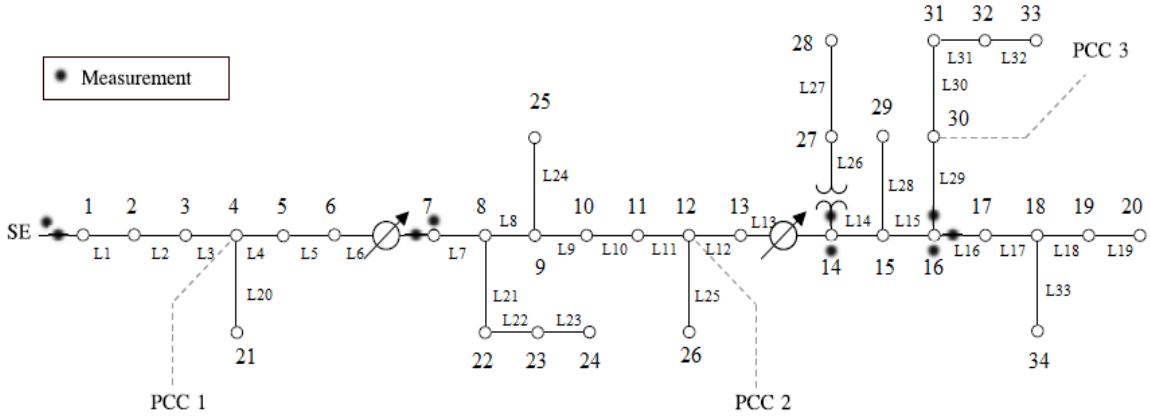

Fig. 2.3 Renamed IEEE 34-node test feeder [9]

2.5 ROOTVECTOR TECHNIQUE.

For explanation of Rootvector technique we have taken IEEE 34-node test feeder.

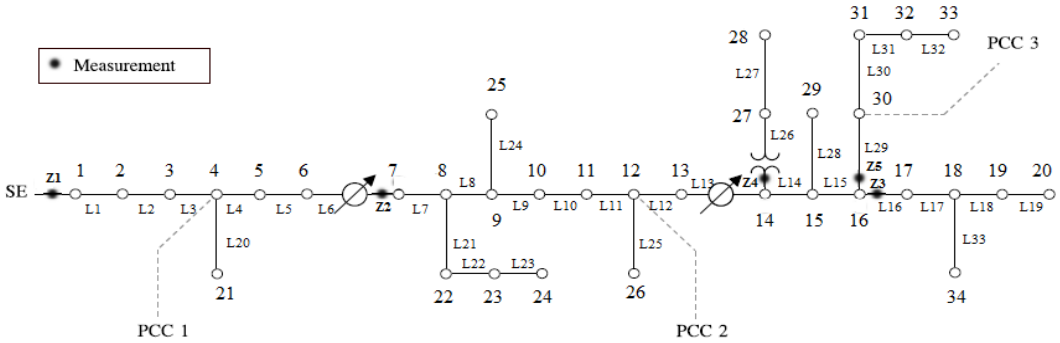

Fig. 2.4 IEEE 34-node test feeder with real time measurement set [9]

Above diagram shows IEEE 34-node test feeder with 33 lines and has *5 measurements* in network. The types of measurements are: power flow and current flow. Line data of IEEE 34-

node test feeder is shown in appendix-B. The measurements are given the nomenclature as Z1, Z2,……,Z5

The detailed procedure for Rootvector technique is as follows:

1. *Initialized the Rootvector of size (n*1) to 0., where n is a number of buses , n=34*

Bus no	1	2	3	4	5	6	7	8	9	10	11	12
Rootvector	0	0	0	0	0	0	0	0	0	0	0	0

Bus no	13	14	15	16	17	18	19	20	21	22	23	24
Rootvector	0	0	0	0	0	0	0	0	0	0	0	0

Bus no	25	26	27	28	29	30	31	32	33	34
Rootvector	0	0	0	0	0	0	0	0	0	0

2 *Pick up the 1st measurement i.e. Z1*

p=LP (1) =1,
q=LQ (1) =2

Set Rootvector (p) =p, Rootvector (q) =q, if Rootvector (p) =0, Rootvector (q) =0
Here Z1 is acting as branch of tree, Therefore root of Rootvector (2) is Rootvector (1)

Bus no	1	2	3	4	5	6	7	8	9	10	11	12
Rootvector	1	1	0	0	0	0	0	0	0	0	0	0

Bus no	13	14	15	16	17	18	19	20	21	22	23	24
Rootvector	0	0	0	0	0	0	0	0	0	0	0	0

Bus no	25	26	27	28	29	30	31	32	33	34
Rootvector	0	0	0	0	0	0	0	0	0	0

At this stage Rootvector clearly indicate that, bus 1 & 2 are already visited & having same common root as bus 1. Zero elements in other than bus 1& 2 indicate that these buses are not yet visited.

3. *Pick up the 2st measurement i.e. Z2*

p=LP(1)=6,
q=LQ(1)=7
set Rootvector (p)=p, Rootvector(q)=q, if Rootvector(p)=0, Rootvector(q)=0
Here Z1 is acting as branch of tree, Therefore root of Rootvector (7) is Rootvector (6)

Bus no	1	2	3	4	5	6	7	8	9	10	11	12
Rootvector	1	1	0	0	0	6	6	0	0	0	0	0

Bus no	13	14	15	16	17	18	19	20	21	22	23	24
Rootvector	0	0	0	0	0	0	0	0	0	0	0	0

Bus no	25	26	27	28	29	30	31	32	33	34
Rootvector	0	0	0	0	0	0	0	0	0	0

4 *Pick up the 3rd measurement i.e. Z3*

p=LP(1)=16,
q=LQ(1)=17,
Set Rootvector (p)=p, Rootvector(q)=q, if Rootvector(p)=0, Rootvector(q)=0
Here Z3 is acting as branch of tree, Therefore root of Rootvector (17) is Rootvector (16)

Bus no	1	2	3	4	5	6	7	8	9	10	11	12
Rootvector	1	1	0	0	0	6	6	0	0	0	0	0

Bus no	13	14	15	16	17	18	19	20	21	22	23	24
Rootvector	0	0	0	16	16	0	0	0	0	0	0	0

Bus no	25	26	27	28	29	30	31	32	33	34
Rootvector	0	0	0	0	0	0	0	0	0	0

5 *Pick up the 4th measurement i.e. Z4*

p=LP(1)=14,
q=LQ(1)=27,
set Rootvector (p)=p, Rootvector(q)=q, if Rootvector(p)=0, Rootvector(q)=0
Here Z1 is acting as branch of tree, Therefore root of Rootvector (27) is Rootvector (14)

Bus no	1	2	3	4	5	6	7	8	9	10	11	12
Rootvector	1	1	0	0	0	6	6	0	0	0	0	0

Bus no	13	14	15	16	17	18	19	20	21	22	23	24
Rootvector	0	14	0	16	17	0	0	0	0	0	0	0

Bus no	25	26	27	28	29	30	31	32	33	34
Rootvector	0	0	14	0	0	0	0	0	0	0

6 *Pick up the 5th measurement i.e. Z5*

p=LP(1)=16,
q=LQ(1)=30,
set Rootvector (p)=p, Rootvector(q)=q, if Rootvector(p)=0, Rootvector(q)=0
Here Z1 is acting as branch of tree, Therefore root of Rootvector (30) is Rootvector (16)

Bus no	1	2	3	4	5	6	7	8	9	10	11	12
Rootvector	1	1	0	0	0	6	6	0	0	0	0	0

Bus no	13	14	15	16	17	18	19	20	21	22	23	24
Rootvector	0	14	0	16	17	0	0	0	0	0	0	0

Bus no	25	26	27	28	29	30	31	32	33	34
Rootvector	0	0	14	0	0	16	0	0	0	0

Observation:
Because of limited number of' real-time measurements, IEEE 34-node test feeder distribution network is unobservable. In order to make it observable, large number of Virtual and Pseudo measurements need to be added.

2.6 TEST SYSTEMS

Observability test is carried out on two test system. A brief description of these systems as follows:

2.6.1 IEEE 10 bus network

- **The first test system is IEEE 10-Bus radial network**

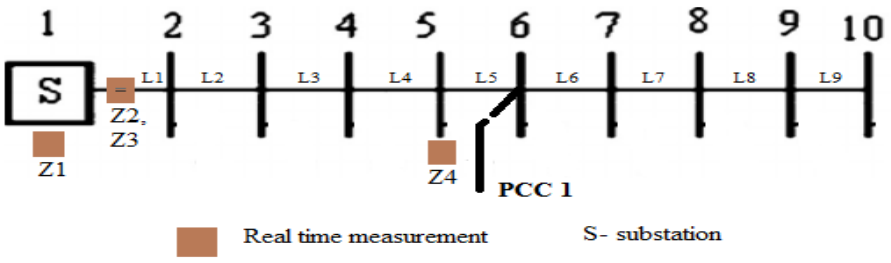

Fig. 2.5 IEEE 10-Bus radial network.

Total no of buses (n) =10

Total no of lines (nline) =9

Total number of Number of PCCs= 1

Total number of real time measurements (m) =4

2.6.1.1 TEST RESULTS

Observability analysis and Rootvector technique is implemented on IEEE 10 –Bus radial network, results are as follow:

Number of measurements			**Total Number**		**Redundancy Level**
Regular	Virtual	Pseudo	States	Measurements	
4	16	7	20	27	1.35
Regular Measurements					
|V1|, P1-2, Q1-2, |V5|					

Table 2.1 Addition of virtual and Pseudo measurements in IEEE 10-Bus system.

Measurements/ Z(i)	Zcode (i)	Zlocation(i)	Sigma(i)
Real Time measurements			
1	5	1	0.00159
0.55	3	1	0.03
0.219	3	1	0.03
0.9541	5	5	0.00159
Virtual Measurements			
0	1	2	0.00001
0	2	2	0.00001
0	1	3	0.00001
0	2	3	0.00001
0	1	4	0.00001
0	2	4	0.00001
0	1	5	0.00001
0	2	5	0.00001
0	1	7	0.00001
0	2	7	0.00001
0	1	8	0.00001
0	2	8	0.00001
0	1	9	0.00001
0	2	9	0.00001
0	1	10	0.00001
0	2	10	0.00001
Pseudo Measurements			
0.24256	6	-2	0.20
0.20109	3	5	0.20
0.27475	3	8	0.20
0.1972	6	-9	0.20
0.36	6	-3	0.20
0.01245	**1**	**6**	**0.20**
0.0112	**2**	**6**	**0.20**

Table 2.2 Virtual and Pseudo measurement data for IEEE 10-Bus System.

2.6.1.2 DISCUSSIONS

Because of limited numbers of real time measurements (4 real time measurements) in IEEE 10-Bus radial system and (17 real time measurements) in IEEE 34-node test feeder network initially this systems ware unobservable. And measurements redundancy was very low. In order to make systems observable, 16 zero node injection as virtual measurements and 7 pseudo measurements are added in IEEE 10-Bus network. After addition of virtual and pseudo measurements, redundancy became 1.35 as shown in Table 2.1 and Table 2.2

2.6.2 IEEE 34-node test feeder

- Another test system is IEEE 34-node test feeder as shown below:

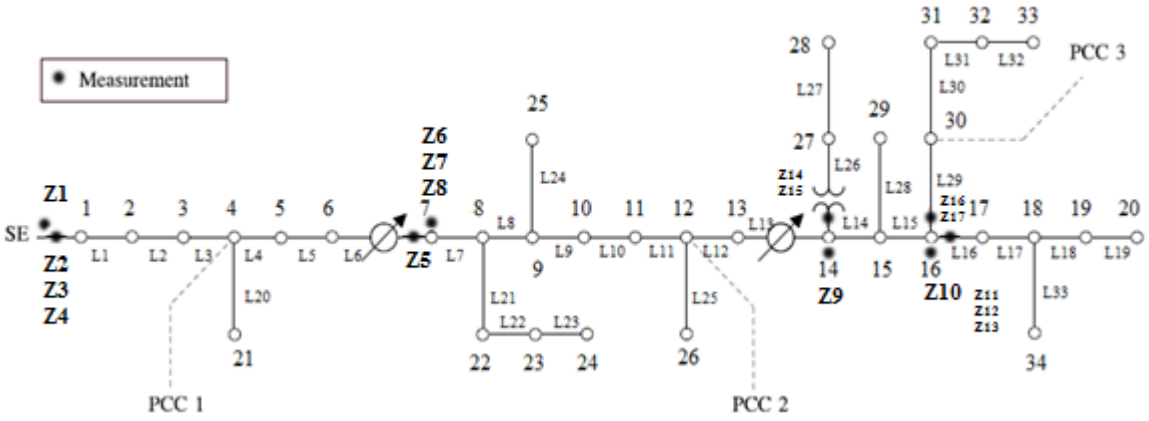

Fig. 2.6 IEEE 34-node test feeder with real time measurements

Total no of buses (n) =34

Total no of lines (nline) =33

Total number of Number of PCCs= 3

Total number of real time measurements (m) =17

Line and load data and measurement data of IEEE 34-node test feeder System is given in Appendix B.

2.6.2.1 TEST RESULTS

Observability analysis is conducted on IEEE 34-node test feeder radial network, results are as follow:

Number of measurements			**Total Number**		**Redundancy Level**
Regular	Virtual	Pseudo	States	Measurements	
17	45	32	68	94	1.38
Regular Measurements					
|V1|, P1-2, Q1-2, P6-7 ,Q6-7, |I6-7| , |V7|, |V14|, P16-17, Q16-17, |I16-17|, |V16|, P14-27, Q14-27, |I14-27|, P16-30, Q16-30 , |I16-30|,					

Table 2.3 Addition of virtual and Pseudo measurements in IEEE 34-node test feeder network.

Measurements/ Z(i)	Zcode (i)	Zlocation(i)	Sigma(i)
Real Time measurements			
0.9998	5	1	0.00159
0.120	3	1	0.03
0.2150	4	1	0.03
0.2928	3	6	0.03
0.09108	4	6	0.03
0.9925	5	7	0.00159
0.5283	6	-6	0.03
0.9897	5	14	0.00159
0.9784	5	16	0.00159
0.15093	3	16	0.03
0.07910	4	16	0.03
0.1183	6	-16	0.03
0.101093	3	26	0.003
0.0183	6	-26	0.03
0.1079	3	29	0.03
0.12572	6	-29	0.03
0.6910	4	29	0.03
Virtual measurements			
0	1	2	0.00001
0	2	2	0.00001
0	1	3	0.00001
0	2	3	0.00001
0	1	5	0.00001
0	2	5	0.00001
0	1	8	0.00001
0	2	8	0.00001
0	1	9	0.00001
0	2	9	0.00001
0	1	10	0.00001
0	2	10	0.00001
0	1	11	0.00001
0	2	11	0.00001
0	1	13	0.00001
0	2	13	0.00001
0	1	15	0.00001
0	2	15	0.00001
0	1	17	0.00001
0	2	17	0.00001
0	1	18	0.00001
0	2	18	0.00001
0	1	19	0.00001
0	2	19	0.00001
0	1	20	0.00001

0	2	20	0.00001
0	1	21	0.00001
0	2	21	0.00001
0	1	22	0.00001
0	2	22	0.00001
0	1	23	0.00001
0	2	23	0.00001
0	1	24	0.00001
0	2	24	0.00001
0	1	25	0.00001
0	2	25	0.00001
0	1	27	0.00001
0	2	27	0.00001
0	1	28	0.00001
0	2	28	0.00001
0	1	31	0.00001
0	2	31	0.00001
0	1	32	0.00001
0	1	33	0.00001
0	2	33	0.00001
Pseudo Measurements			
0.7472	3	2	0.20
1.02578	4	2	0.20
0.2028	3	3	0.20
0.0959	4	3	0.20
0.215	6	-3	0.20
0.20109	3	5	0.20
0.2557	4	5	0.20
0.2622	6	-5	0.20
0.1117	4	8	0.20
0.1679	3	9	0.20
0.1214	4	9	0.20
0.1997	6	-9	0.20
0.001109	3	15	0.20
0.10	4	15	0.20
0.1526	6	-15	0.20
0.1214	3	18	0.20
0.107	4	18	0.20
0.126	6	-18	0.20
1.19	4	22	0.20
0.30856	6	-22	0.20
0.42015	4	24	0.20
0.8308	6	-24	0.20
0.09475	4	6	0.20

0.5247	6	-6	0.20
0.5195	4	32	0.20
0.015	**1**	**4**	**0.20**
0.01125	**2**	**4**	**0.20**
0.850	**1**	**12**	**0.20**
0.0256	**2**	**12**	**0.20**
0.094	**1**	**30**	**0.20**
0.1012	**2**	**30**	**0.20**

Table 2.4 Virtual and Pseudo measurement data for IEEE 34-node test feeder.

6.2.2.2 Discussions

Because of limited numbers of real time measurements (17 real time measurements) in IEEE 34-node test feeder network initially this systems ware unobservable. And measurements redundancy was very low. In order to make systems observable, 45 zero node injection as virtual measurements and 32 pseudo measurements are added in IEEE34-node test feeder.

After addition of virtual and pseudo measurements, redundancy became 1.38.

CHAPTER 3

LOAD FLOW METHODS OF RADIAL DISTRIBUTION SYSTEM

3.1 INTRODUCTION

The optimal distribution system planning is very important for the growth of distribution system (DS) network and plays an important role for effective usage of the distribution system. With the continuing increase in load demand, the future expansion of the network depends on the load flow study of the distribution system network and thus is one of the most important system studies for electrical engineering. In case of loss minimization, voltage control, Var. planning, sizing and location of shunt capacitors, state estimation, security analysis, it is very important to solve the power flow algorithm as efficient as possible. The traditional load flow algorithms are not suitable for DS because of Special characteristics of DS, such as unbalanced three phase loads, radial structure and high branch R/X ratios.

Load flow algorithm/methods can be put in three category:

1. Direct methods :

It is based on direct matrix multiplication, where loop impedance matrix are being formulated by using special topology of distributed networks that requires tremendous computation work for the formation of loop matrix inversion and renumbering of nodes.

2. Newton–Raphson and FDLF methods :

It requires the formulation of Jacobian matrix as well as its lower and upper triangular (LU) factorization that demands more time for calculations and it also requires special treatment for ill-conditioned system.

3. Forward/backward sweep based methods.

The Forward-Backward Sweep Method (FBSM) is easy to program and runs quickly.

3.2 FORWARD/BACKWARD SWEEP METHOD

The backward/forward sweep method for the load-flow computation is an iterative method in which, at each iteration two computational stages are performed: The load flow of a single source network can be solved iteratively from two sets of recursive equations. The first set of equations for calculation of the current or power flow through the branches starting from the last branch and proceeding in the backward direction towards the root node. The other set of equations are for calculating the voltage magnitude and angle of each node starting from the root node and proceeding in the forward direction towards the last node.

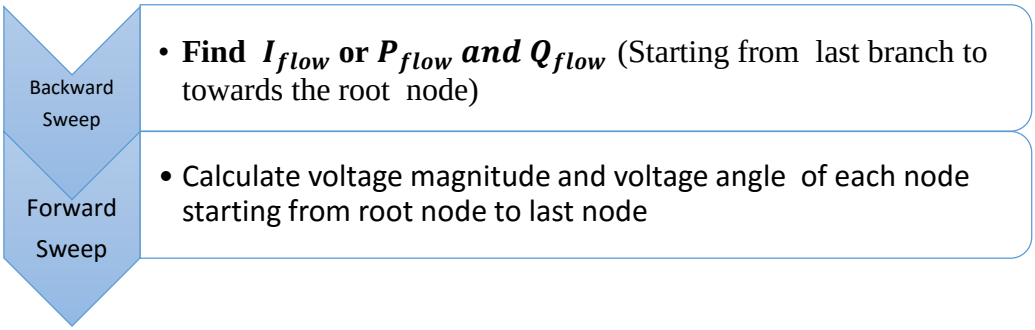

Fig. 3.1 steps of Forward/Backward sweep Load Flow method.

3.2.1 IMPLEMENTATION LEVEL ALGORITHUM FOR FORWARD/BACKWARD SWEEP METHOD WITHOUT REGULATOR

- Step 1: // Start //
- Step 2: // a) Read system size *n*, number of lines *nline*, epsilon & itermax //
  // b) Read line data LP(k), LQ(k) ,r(k), x(k) & tap *for k=1 to nline* //
  // c) Read Load data Pload (i) & Qload (i), *for i=1 to n //*
- Step 3: // Form the sparsity vectors ITAGF, ITAGTO, and ADJQ. //
- Step 4: // Initialize the bus voltages as V(i) = 1.0 , & vold(i)=v(i); *for i =1 to n //*
- Step 5: // Calculate load currents IL (i), *for i = 2 to n //*

```
for i=1:n
        IL(i)=conj((Pload_pu(i),Qload_pu(i)))/conj(v(i));
end

// end of i loop //
```

- Step 6:// Calculate branch currents IB(k) in Backward direction. *K=1 to nline*

```
for i=n:-1:2
   sum=0;
        if(nlcont(i)>1)
                jstart=itagf(i);
                jstop=itagto(i);
 for j=jstart+1:jstop
                  q=adjl(j);
                 Sum=sum+IB (q);
 end

// end of j loop //

          IB (i-1)=sum+IL(i);
else
           IB (i-1)=IL(i);
end
end

// end of i loop //
```

- Step 7:// Calculate the voltage drops as $\Delta V(i)=Z(i)*IB(i)$ & Find receiving end voltages in the forward direction as $V(re(i)) = V(se(i)) - \Delta V(i)$, *for i = 1 to n //*

```
 for k=1:nline
       deltaV(k)=z(k)*IB(k); % volt drop in each branch
           p=lp(k);
           q=lq(k);
        v(q)=v(p)-deltaV(k); % Calculation of Receiving end volt
end

// end of i loop //
```

- Step 8:// : Find delV and Update the voltages , delv=V-Vold , delVmax=max(delV)

```
for  i=1:n
 delv(i)=v(i)-vold(i);
          if  (abs(delv(i))>delvmax)
          delvmax=abs(delv(i));
          end
         vold(i)=v(i),
```

```
    end
// end of i loop //
```

- Step 9: // Find error in voltage i.e. delVmax. If it is less than 0.00001 then load flow is converged otherwise go to step 5. //

- Step 10:// Once load flow is converged bus voltages and branch currents are known then find power flow of each branch.
- Step 11:// Stop

3.2.2 IMPLEMENTATION LEVEL ALGORITHUM FOR FORWARD/BACKWARD SWEEP METHOD WITH REGULATOR

- Step 1: // Start //

- Step 2: // a) Read system size *n*, number of lines *nline*, epsilon & itermax //
  // b) Read line data LP(k), LQ(k) ,r(k), x(k) & tap *for k=1 to nline* //
  // c) Read Load data Pload (i) & Qload (i) for *i=1 to n //*
  d) Read bus number where voltage regulator has been placed,
  i.e. reg_1, reg_2,… reg_n
- Step 3: // Form the sparsity vectors ITAGF, ITAGTO, and ADJQ. //
- Step 4: // Initialize the bus voltages as V(i) = 1.0 , & vold(i)=v(i); *for i =1 to n //*
- Step 5: // Calculate load currents IL (i), *for i = 2 to n //*

```
for i=1:n
        IL(i)=conj((Pload_pu(i),Qload_pu(i)))/conj(v(i));
end
```

// end of i loop //

- Step 6:// Calculate branch currents IB(k) in Backward direction. *K=1 to nline*

```
for i=n:-1:2
   sum=0;
        if(nlcont(i)>1)
                jstart=itagf(i);
                jstop=itagto(i);
```

```
for j=jstart+1:jstop
                    q=adjl(j);
                   sum=sum+IB(q);
end
// end of j loop //

          IB(i-1)=sum+IL(i);
else
           IB(i-1)=IL(i);
end
end

// end of i loop //
```

- Step 7:// Calculate the voltage drops as $\Delta V(i)=Z(i)*IB(i)$ & Find receiving end voltages in the forward direction as $V(re(i)) = V(se(i)) - \Delta V(i)$, *for i = 1 to n //*

```
for k=1:nline
      deltaV(k)=z(k)*IB(k); % volt drop in each branch
          p=lp(k);
          q=lq(k);
       v(q)=v(p)-deltaV(k); % Calculation of Receiving end volt
end

// end of i loop //
```

- Step 8:// find a number of taps requires to rise the voltage in voltage regulator//

```
diff_1=1-abs(v(reg_1));
tap_1=abs((diff_1./0.00625));
tap_1=round(tap_1);   // number of taps requires to rise the voltage //
aR_1=(1-0.00625*tap_1);
v(reg_1)=v(reg_1)./aR_1;
```

- Step 9:// : Find delV and Update the voltages , delv=V-Vold , delVmax=max(delV)

```
 for  i=1:n
delv(i)=v(i)-vold(i);
          if  (abs(delv(i))>delvmax)
                   delvmax=abs(delv(i));
          end
         vold(i)=v(i),
 end
 // end of i loop //
```

- Step 10: // Find error in voltage i.e. delVmax. If it is less than 0.0001 then load flow is converged otherwise go to step 5. //

- Step 11:// Once load flow is converged bus voltages and branch currents are known then find power flow of each branch.

- Step 12:// Stop

3.3 CASE STUDIES AND CASE RESULTS

3.3.1 IEEE 10-Bus network

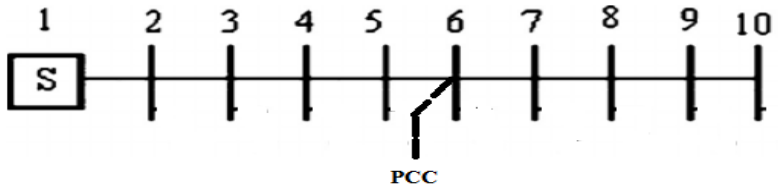

Line data and lod data of IEEE 10-Bus network are given in *APPENDIX A*

Forward/backward sweep load flow algorithm has implemented on IEEE 10 radial distribution networks. And results is as follow:

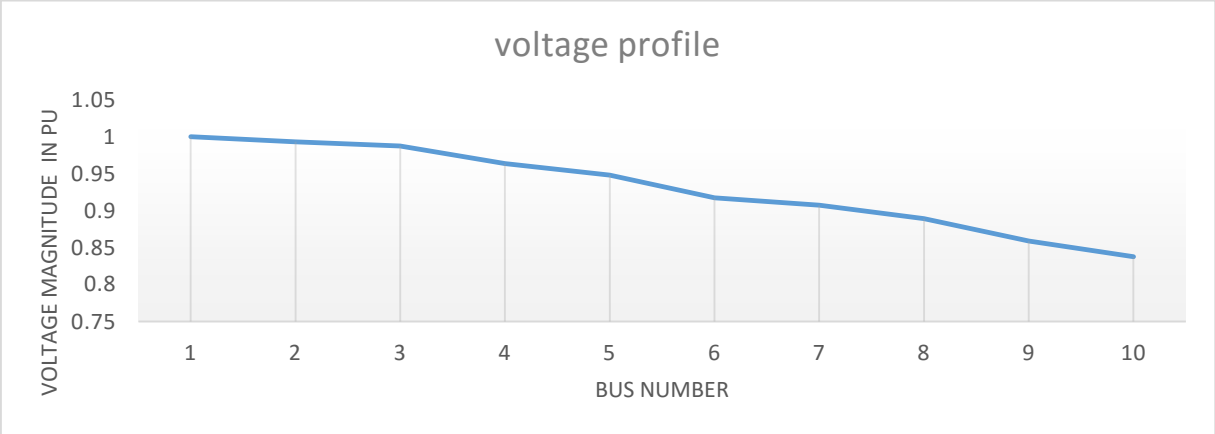

Fig. 3.2 IEEE 10 bus voltage profile

3.3.2 IEEE 34-Node test feeder

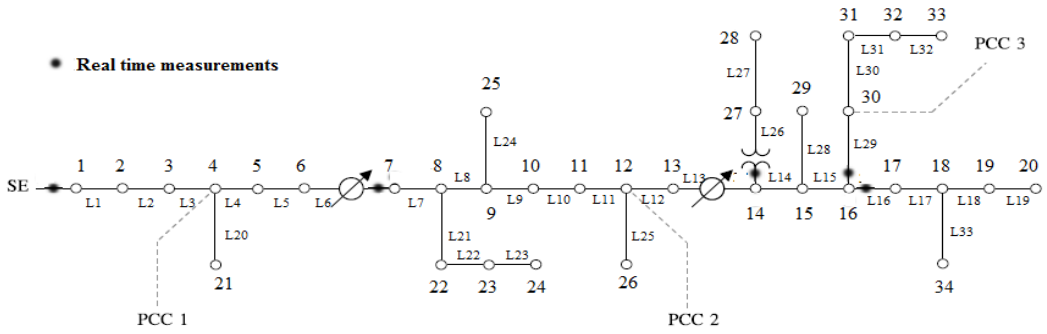

Line data and load data of IEEE 34-Node test feeder are given in *APPENDIX B*

Forward/backward sweep load flow algorithm *with and without regulator* case has performed on IEEE 34-node test feeder radial distribution networks. Result is as follow:

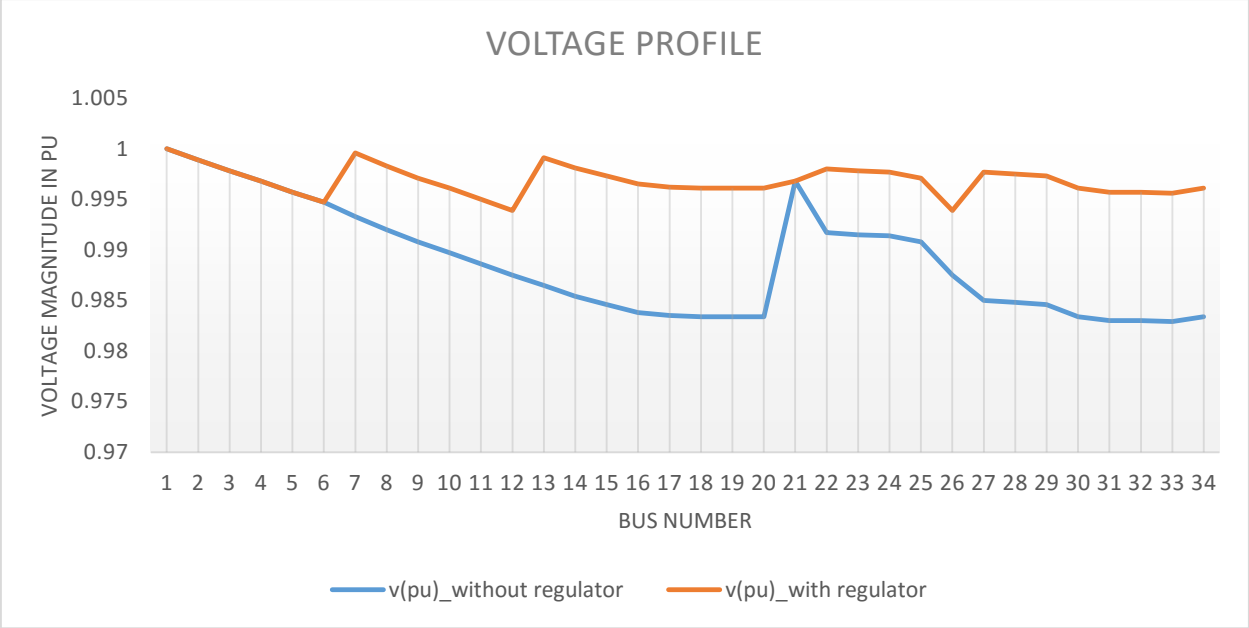

Fig. 3.3 voltage profile of IEEE 34-node test feeder with and without regulator.

3.4 DISCUSSIONS

In IEEE 34-node test feeder, two regulators has placed at bus no.7 and at bus no.13. A voltage regulator is able to control the voltage of the bus where it is located, or to control the voltage of a distant buses. As shown in fig.3.3, the voltage magnitude of bus no.7 and bus no.13 got improved.

CHAPTER 4

STATE ESTIMATION

4.1 INTRODUCTION

State estimation techniques have been developed and applied at the generation and transmission levels for more than 30 years. The most commonly used approach is the Weighted-Least-Square (WLS) method. Weighted Least Square (WLS) estimators are the most popular and considerable efforts have been devoted to reduce the computational requirements. SE is used to improve system observability, check for and detect errors in both system measurements and network parameters, and to mitigate against measurement and communication system noise. It also called as *Normal Equation (NE) method for DSSE.*

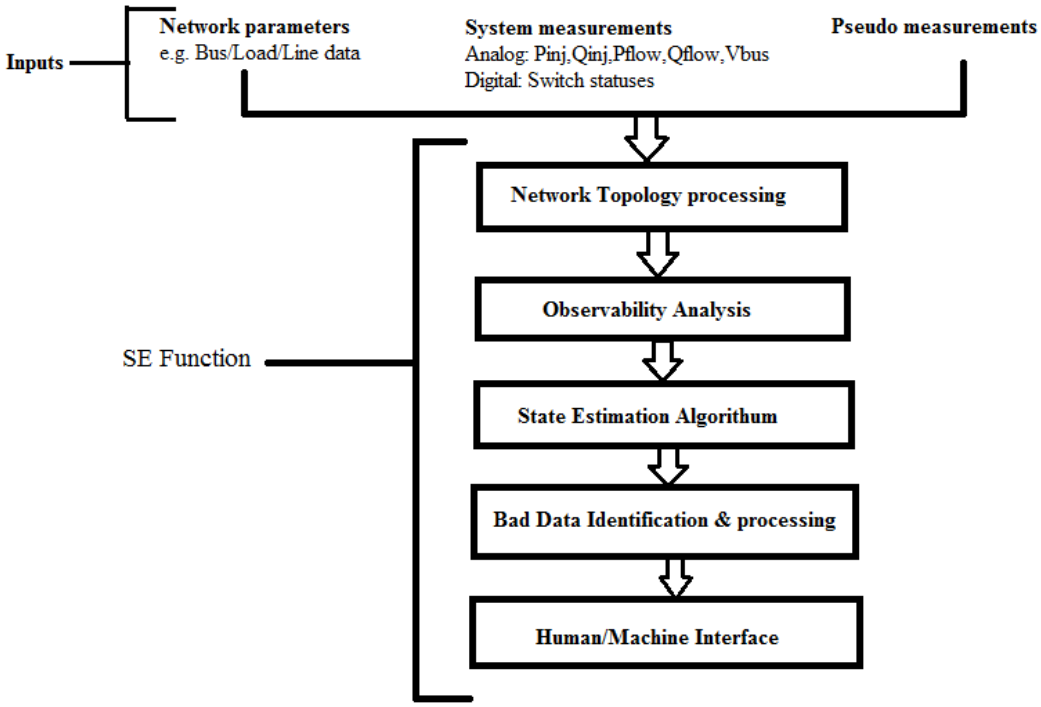

Fig. 4.1 the main functions provided by power system state estimation. [7]

Normal Equation (NE) methods is nothing but Conventional WLS State estimation method. In which, highly weighted zero power injection measurements are considered as virtual measurements and real & reactive power injections assumptions at PCC are considered as pseudo measurements.

Structure of error covariance matrix in NE method is given by

$$R = \begin{bmatrix} R_m & 0 & 0 \\ 0 & R_v & 0 \\ 0 & 0 & R_p \end{bmatrix} \quad \text{..... (4.1)}$$

In (4.1) weighting factors of real time, virtual and pseudo measurements are considered as Rm, Rv and Rp respectively.

4.2 PROBLEM FORMULATION FOR CONVENTIONAL STATE ESTIMATION

The network state is expressed as the vector x, containing the voltage magnitudes and phase angles at each node in the system. To estimate x, the set of measurements from the network, z, is applied. The values in z can comprise of measurements of power injections or voltage magnitudes at system buses, measurements of active and reactive power and current flows in system branches, pseudo-measurements (i.e. estimates) & virtual measurements (zero power injections) of network quantities, or any combination of the above. This forms a set of over-determined, non-linear equations:

$$\boldsymbol{Z = h(x) + \eta}$$

Where,

Z= Measurement vector, $\eta = \boldsymbol{meter\ error}$

$\boldsymbol{h(x) = vector\ of\ non\ linear\ function\ relating\ measurements\ and\ state}$.

And diagonal covariance matrix R,

$$\mathbf{R} = \{ \eta^{\boldsymbol{T}} * \eta \},$$

$$\mathbf{R} = \begin{bmatrix} \eta_1^2 & \mathbf{0} & \mathbf{0} \\ \mathbf{0} & \eta_2^2 & \mathbf{0} \\ \mathbf{0} & \mathbf{0} & \eta_3^2 \end{bmatrix}$$

And state variable vector will be composed by voltage magnitude and phase angle of each node is given by,

$[x]=[\delta 1, \delta 2, \delta 3 \ldots \delta n, v_1, v_2, v_3 \ldots .. v_n]$ Where, *n* is a number of buses

The state estimation can be found minimizing the scalar function $\boldsymbol{j(x)}$, sum of the weighted error,

$$\boldsymbol{j(x)} = \eta^{\boldsymbol{T}} * \boldsymbol{R} * \eta$$

$$\boldsymbol{j(x)} = (\boldsymbol{Z} - \boldsymbol{h(x)})^{\boldsymbol{T}} * \boldsymbol{R} * (\boldsymbol{Z} - \boldsymbol{h(x)})$$

$$\frac{\boldsymbol{\partial h(h)}}{\boldsymbol{\partial x}} = -\mathbf{2}[\boldsymbol{H}]^{\boldsymbol{T}} * [\boldsymbol{R}]^{-\mathbf{1}} * [\boldsymbol{Z} - \boldsymbol{h(x)}]$$

Applying Newton's method and equating above equation to zero:

$$[\boldsymbol{H}]^{\boldsymbol{T}} * [\boldsymbol{R}]^{-\mathbf{1}} * \boldsymbol{Z} = [\boldsymbol{H}]^{\boldsymbol{T}} * [\boldsymbol{R}]^{-\mathbf{1}} * \boldsymbol{h(x)}$$

Linearizing by Taylors series expansion:

$$[\boldsymbol{H^T} * \boldsymbol{R^{-1}} * \boldsymbol{H}]*[\Delta \mathbf{x}] = \boldsymbol{H^T} * \boldsymbol{R^{-1}} * (\boldsymbol{Z} - \boldsymbol{h(x_0)})$$

$$[\boldsymbol{H^T R^{-1} H}] = \boldsymbol{H_{eff}} \quad \& \quad \boldsymbol{H^T R^{-1}(Z - h(x_0))} = \Delta \boldsymbol{Z_{eff}}$$

$$\boldsymbol{Therefore}, \ [\boldsymbol{H_{eff}}][\Delta \mathbf{x}] = \Delta \boldsymbol{Z_{eff}}$$

And Jacobian matrix [H] is given by,

$$[\boldsymbol{H}] = \begin{bmatrix} \boldsymbol{\partial h1/\partial x_1} & \boldsymbol{\partial h1/\partial x_2} & \ldots \\ \boldsymbol{\partial h2/\partial x_1} & \boldsymbol{\partial h2/\partial x_1} & \ldots \\ \ldots & \ldots & \ldots \end{bmatrix}$$

Residual vector *r* i.e. ΔZ is equal to term $[\boldsymbol{Z - h(x)}]$

The state estimate *x* can be found by numerical solution i.e. iterative solution of following equation:

$$\Delta \boldsymbol{x} = (\boldsymbol{H^T R^{-1} H})^{-1} \boldsymbol{H^T R^{-1}} \Delta \boldsymbol{Z}$$

4.3 TYPES OF MEASUREMENTS

Types of Measurements	Measurement code	Location
Active power injection (Pp)	**1**	Bus number =p
Reactive power injection Qp	**2**	Bus number = p
Active line power flow on k^{th} line Ppq	**3**	If at sending end :+k If at receiving end :-k
Reactive power flow on k^{th} line Qpq	**4**	If at sending end :+k If at receiving end :-k
Voltage magnitude Vp	**5**	Bus number = p
Square of current flow on k^{th} line	**6**	If at sending end :+k If at receiving end :-k

Table 4.1 Types of measurements used in state estimation

4.4 STRUCTURE OF JACOBIAN MATRIX

[H] is a Jacobian matrix for measurement function matrix *h(x).* The equations are derived using polar natation and as below:

$$\text{Ip}= \sum_{q=1}^{n} Y_{pq}E_q$$

$$S_p = P_p + jQ_p = E_p * I_p^*$$

$$E_p = V_p \angle \delta p = e_p + jf_p$$

$$E_q = V_q \angle \delta q = e_q + jf_q$$

$$\text{Ypq} = |\text{Ypq}|\angle \theta pq = Gpq + jBpq$$

$$P_p = \sum_{q=1}^{n}\left(V_pV_q\left|Y_{pq}\right|\cos(\delta pq - \theta pq)\right)$$

$$\boldsymbol{P_p = V_p^2\, G_{pp} + G_{pq}\left(e_pe_q + f_pf_q\right) + B_{pp}(f_pe_q - e_pf_q)} \quad \ldots\ldots\ldots\ldots\ldots\ldots \quad (4.2)$$

And

$$Q_p = \sum_{q=1}^{n}\left(V_pV_q\left|Y_{pq}\right|\sin(\delta pq - \theta pq)\right)$$

$$\boldsymbol{Q_p = -V_p^2\, B_{pp} - B_{pq}(e_p e_q + f_p f_q) + G_{pp}(f_p e_q - e_p f_q)}\ldots\ldots\ldots\ldots\ldots\ldots\ (4.3)$$

Equivalent model of distribution system is shown in figure 4.2 is used to calculate the line power and current flows:

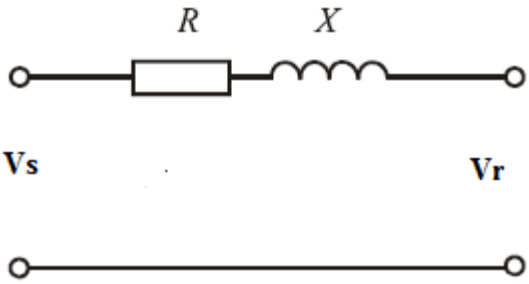

Fig. 4.2 Model of distribution network

$Z_{line} = R + jX$ & $y_{line}(k) = g_{line} + jb_{line} = |y_{line}| \angle \theta_k$

In distribution network *ycp(k)=ycq(k)=0*;

$$\boldsymbol{S_{pq} = P_{pq} + jQ_{pq} = (E_p) * (I_{pq}^*)}$$

$$\boldsymbol{P_{pq}} = V_p^2 |y_{line}(k)| \cos(\theta_k) - V_p V_q |y_{line}(k)| \cos(\delta_{pq} - \theta_k)$$

$$\boldsymbol{P_{pq} = V_q^2\, g_{line}(k) - g_{line}(k)(e_p e_q + f_p f_q) - b_{line}(k)(f_p e_q - e_p f_q)}\ldots\ldots\ldots\textbf{(4.4)}$$

$$\boldsymbol{P_{qp}} = V_q^2 |y_{line}(k)| \cos(\theta_k) - V_q V_p |y_{line}(k)| \cos(\delta_{pq} - \theta_k)$$

$$\boldsymbol{P_{qp} = V_p^2\, g_{line}(k) - g_{line}(k)(e_p e_q + f_p f_q) - b_{line}(k)(f_p e_q - e_p f_q)}\ldots\ldots\ldots\ \textbf{(4.5)}$$

Similarly,

$$\boldsymbol{Q_{pq}} = V_p^2 |y_{line}(k)| \sin(\theta_k) - V_p V_q |y_{line}(k)| \sin(\delta_{pq} - \theta_k)$$

$$\boldsymbol{Q_{pq} = -V_p^2\, b_{line}(k) + b_{line}(k)(e_p e_q + f_p f_q) - g_{line}(k)(f_p e_q - e_p f_q)}\ \ldots\ldots\ \textbf{(4.6)}$$

$$\boldsymbol{Q_{qp}} = V_q^2 |y_{line}(k)| \sin(\theta_k) - V_p V_q |y_{line}(k)| \sin(\delta_{pq} - \theta_k)$$

$$\boldsymbol{Q_{qp} = -V_q^2\, b_{line}(k) + b_{line}(k)(e_p e_q + f_p f_q) - g_{line}(k)(f_p e_q - e_p f_q)}\ \ldots\ldots\ldots\ \textbf{(4.7)}$$

For current flow,

$$\boldsymbol{Ipq = (V_p \angle \delta_p - V_q \angle \delta_q)\, y_{line}(k) \angle \theta_k = y_{line}(k) * (V_p \angle (\delta_p + \theta_k) - V_q \angle (\delta_q + \theta_k))} \textbf{=a+jb}$$

a= $\boldsymbol{v_p\, cos(\delta_p + \theta_k) - v_q\, cos(\delta_p + \theta_k)}$; $\boldsymbol{b = v_p\, sin(\delta_p + \theta_k) - v_q\, sin(\delta_p + \theta_k)}$

$$I_{pq} = \sqrt{(V_p^2 + V_q^2 - 2 * V_p V_q\ cos\ (\delta_p - \delta_q))} * y_{line}(k)$$

Therefore,

$$\boldsymbol{(I_{pq})^2 = \left(V_p^2 + V_q^2 - 2 * V_p V_q\ cos\ (\delta_p - \delta_q)\right) * y_{line}^2(k)} \text{..... (4.8)}$$

And $\boldsymbol{y_{line}^2(k) = (g_{line})^2 + (b_{line})^2}$

Elements of Jacobian are as follow:

Active power injection

term1= $\boldsymbol{(e_p e_q + f_p f_q)}$ ***& term2=*** $\boldsymbol{(f_p e_q - e_p f_q)}$

$$\frac{\partial P_p}{\partial \delta_p} = -\sum_{q \neq p}^{n} [G_{pq}(term2) - B_{pq}(term1)].$$

$$\frac{\partial P_p}{\partial \delta_q} = G_{pq}(term2) - B_{pq}(term1).$$

$$\frac{\partial P_p}{\partial V_p} * V_p = 2\ V_p^2 G_{pp} + \sum_{q \neq p}^{n} [B_{pq}(term2) + G_{pq}(term1)]$$

$$\frac{\partial P_p}{\partial V_q} * V_q = B_{pq}(term2) + G_{pq}(term1).$$

Reactive power injection

term1= $\boldsymbol{(e_p e_q + f_p f_q)}$ ***& term2=*** $\boldsymbol{(f_p e_q - e_p f_q)}$

$$\frac{\partial Q_p}{\partial \delta_p} = \sum_{q \neq p}^{n} [B_{pq}(term2) + G_{pq}(term1)]$$

$$\frac{\partial Q_p}{\partial \delta_q} = -B_{pq}(term2) - G_{pq}(term1)$$

$$\frac{\partial Q_p}{\partial V_p} * V_p = -2\ V_p^2 B_{pp} + \sum_{q \neq p}^{n} [G_{pq}(term2) - B_{pq}(term1)]$$

$$\frac{\partial Q_p}{\partial V_q} * V_q = G_{pq}(term2) - B_{pq}(term1)$$

Active power line flow

term1=($e_p e_q + f_p f_q$) & term2=($f_p e_q - e_p f_q$)

$$\frac{\partial P_{pq}}{\partial \delta_p} = g_{line}(k)term2 - b_{line}(k)term1$$

$$\frac{\partial P_{pq}}{\partial \delta_q} = -g_{line}(k)term2 + b_{line}(k)term1$$

$$\frac{\partial P_{pq}}{\partial V_p} * V_p = 2V_p^2 g_{line}(k) - b_{line}term2 - g_{line}(k)term1$$

$$\frac{\partial P_{pq}}{\partial V_q} * V_q = -b_{line}term2 - g_{line}(k)term1$$

$$\frac{\partial P_{qp}}{\partial \delta_p} = g_{line}(k)term2 + b_{line}(k)term1$$

$$\frac{\partial P_{qp}}{\partial \delta_q} = -g_{line}(k)term2 - b_{line}(k)term1$$

$$\frac{\partial P_{qp}}{\partial V_p} * V_p = b_{line}term2 - g_{line}(k)term1$$

$$\frac{\partial P_{qp}}{\partial V_q} * V_q = 2V_q^2 g_{line}(k) + b_{line}term2 - g_{line}(k)term1$$

Reactive power line flow:

term1=($e_p e_q + f_p f_q$) & term2=($f_p e_q - e_p f_q$)

$$\frac{\partial Q_{pq}}{\partial \delta_p} = b_{line}(k)term2 - g_{line}(k)term1$$

$$\frac{\partial Q_{pq}}{\partial \delta_q} = b_{line}(k)term2 + g_{line}(k)term1$$

$$\frac{\partial Q_{pq}}{\partial V_p} * V_p = -2V_p^2 g_{line}(k) - g_{line} term2 + b_{line}(k) term1$$

$$\frac{\partial Q_{pq}}{\partial V_q} * V_q = -g_{line} term2 + b_{line}(k) term1$$

$$\frac{\partial Q_{qp}}{\partial \delta_p} = -b_{line}(k) term2 + g_{line}(k) term1$$

$$\frac{\partial Q_{qp}}{\partial \delta_q} = b_{line}(k) term2 - g_{line}(k) term1$$

$$\frac{\partial Q_{qp}}{\partial V_p} * V_p = g_{line} term2 + b_{line}(k) term1$$

$$\frac{\partial Q_{qp}}{\partial V_q} * V_q = 2V_p^2 b_{line}(k) + g_{line} term2 + b_{line}(k) term1$$

Current flow:

term1=($e_p e_q + f_p f_q$) & term2=($f_p e_q - e_p f_q$)

$$\frac{\partial (I_{pq})^2}{\partial \delta_p} = 2[(g_{line})^2 + (b_{line})^2] term2$$

$$\frac{\partial (I_{pq})^2}{\partial \delta_q} = -2[(g_{line})^2 + (b_{line})^2] term2$$

$$\frac{\partial (I_{pq})^2}{\partial V_p} V_p = 2((g_{line})^2 + (b_{line})^2)({V_p}^2 - term1)$$

$$\frac{\partial (I_{pq})^2}{\partial V_q} V_q = 2((g_{line})^2 + (b_{line})^2)({V_q}^2 - term1)$$

Voltage magnitude:

$$\frac{\partial V_p}{\partial \delta_p} = 0\,, \qquad \frac{\partial V_p}{\partial \delta_q} = 0, \qquad \frac{\partial V_p}{\partial V_p} V_p = 2(V_p)^2\,, \qquad \frac{\partial V_p}{\partial V_q} V_q = 0$$

4.5 WLS- STATE ESTIMATION ALGORITHM FLOWCHART

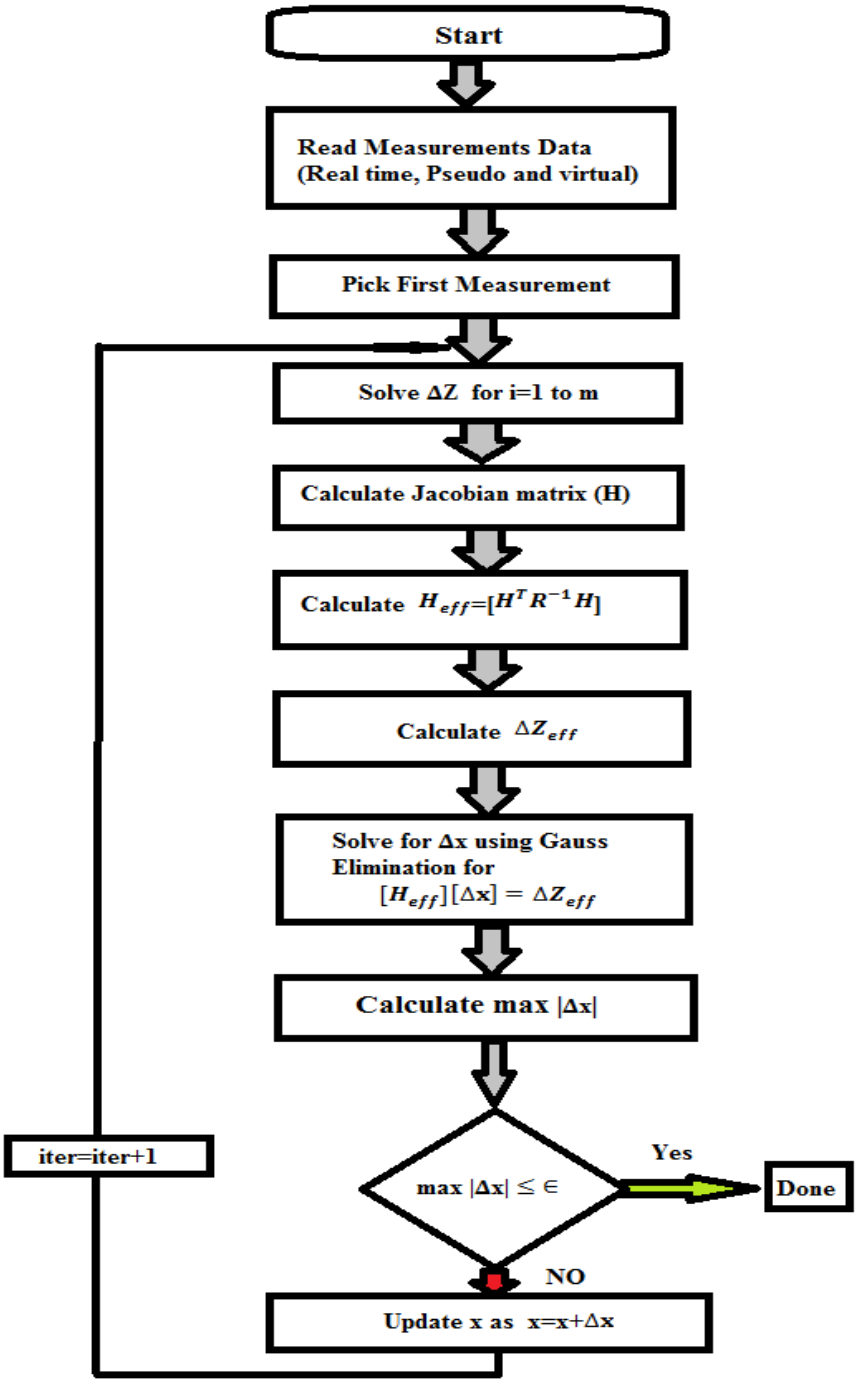

Fig.4.3 Flowchart for WLS- State estimation Algorithm

4.6 CONVENTIONAL BAD DATA DETECTION METHOD OR NORMAL EQUATION (NE) METHOD

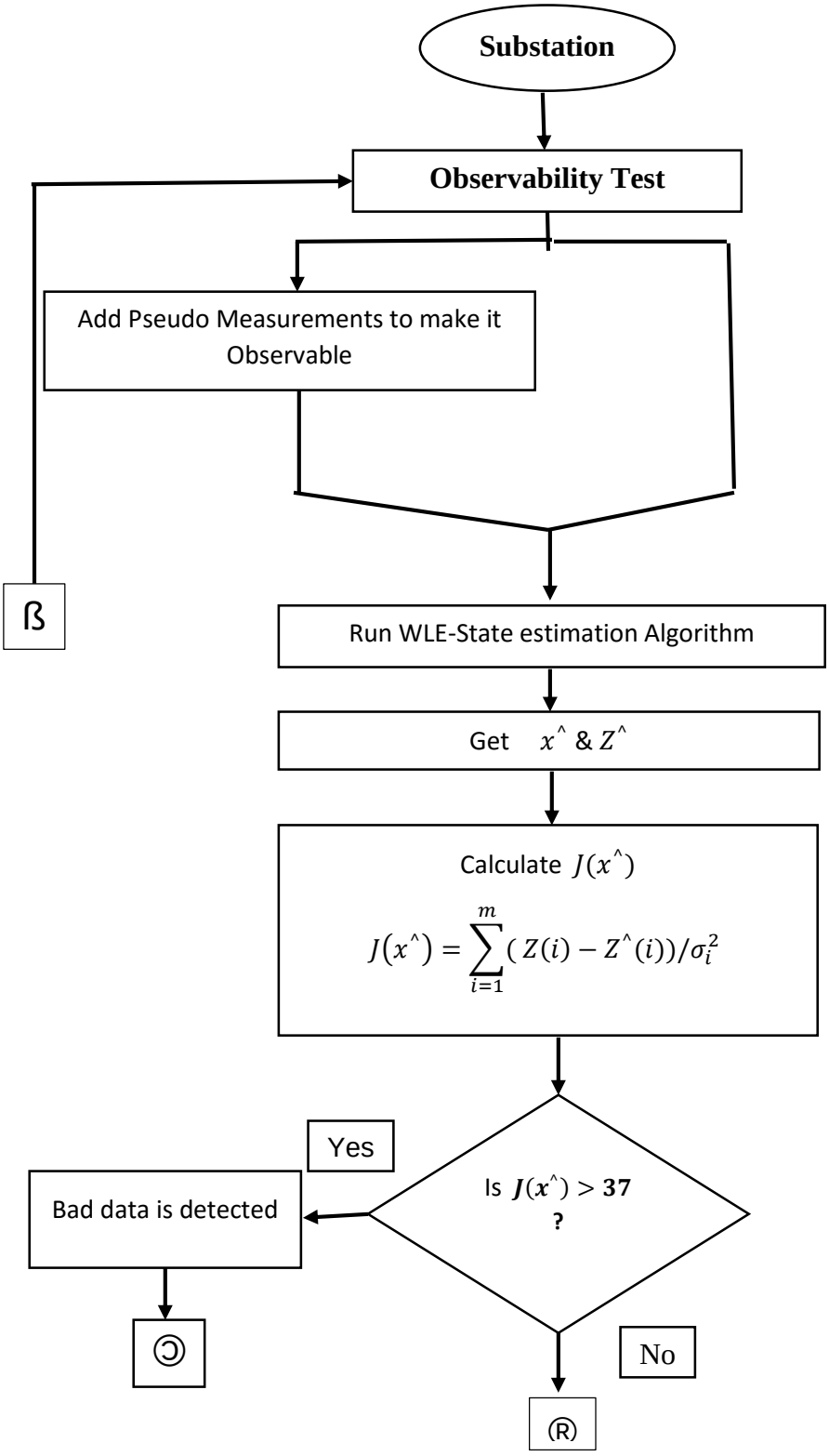

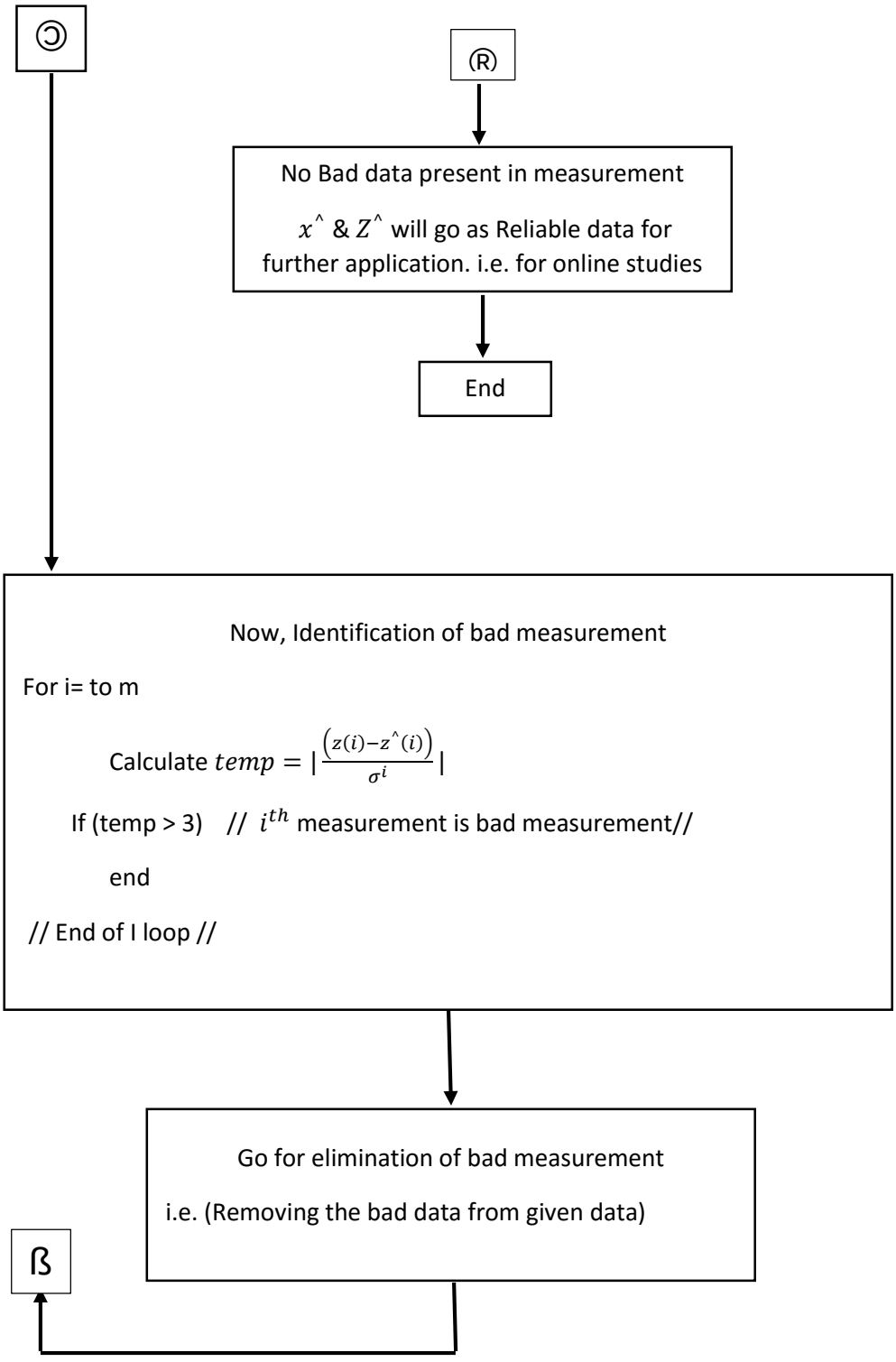

Fig. 4.4 Flowchart of Conventional bad data detection method or Normal Equation (NE) Method

4.7 CASE STUDIES

4.7.1 IEEE 10 bus network

- **The first test system is IEEE 10-Bus radial network**

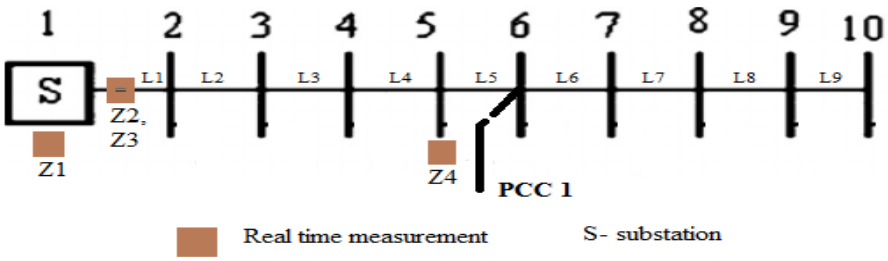

Fig. 4.5 IEEE 10-Bus radial network with real time measurements

Total no of buses (n) =10

Total no of lines (nline) =9

Total number of Number of PCCs= 1

Total number of real time measurements (m) =4

Line, load and measurement data of IEEE 10-Bus System is given *in Appendix A*.

- **Case studies**

Several distinct combinations of power injections at the PCC 1 are taken. Three illustrative cases has selected and are presented. It is assumed that the system operator has no prior information about the power injected at the PCC 1 and thus considers all injections null. The actual power injections at the PCC are as follows.

Case A: Reference case where power is not injected at the PCC 1.

Case B: Power injection of 250 + j100 kVA at PCC 1.

Case C: Power injection of 150 + j300 kVA at PCC 1

These real and reactive power injection at PCC1 are input measurements to the conventional State Estimation method or NE method.

4.7.1.1 CASE RESULTS

Conventional state estimation method, several distinct combinations of power injections at the PCC 1 has taken, and Results of all the cases of IEEE 10-bus radial network are shown in table 4.2

Case	Number of iterations	$J(x)^{\wedge}$	Bad data	Bad measurement
A	3	18.84	NO	-
B	3	275.52	YES	$P_{inj}(PCC\ 1)$,$Q_{inj}(PCC\ 1)$
C	3	370.30	YES	$P_{inj}(PCC\ 1)$,$Q_{inj}(PCC\ 1)$

Table 4.2 Presence of bad data for all cases in IEEE 10 bus network using NE method

Case	*temp* value of bad data measurements	
	$P_{inj}(PCC\ 1)$	$Q_{inj}(PCC\ 1)$
A	2.7015	1.2472
B	15.0039	6.1017
C	10.2432	15.8518

Table 4.3 *temp* value of bad data measurements for all cases in IEEE 10 bus network using NE method

4.7.1.2 Discussions

Three different cases of real and reactive power injections measurements at PCC1 has been considered and using conventional State Estimation method, bad data in the measurement set has been identified, bad data measurements and *temp* value of bad measurements has been shown in table 4.2 and table 4.3. In case A, no bad data is present in measurement set, but in Case B and Case C, real and reactive power injections measurement bad data at PCC1 are present.

4.7.2 IEEE 34-node test feeder

- Another test system is IEEE 34-node test feeder as shown below:

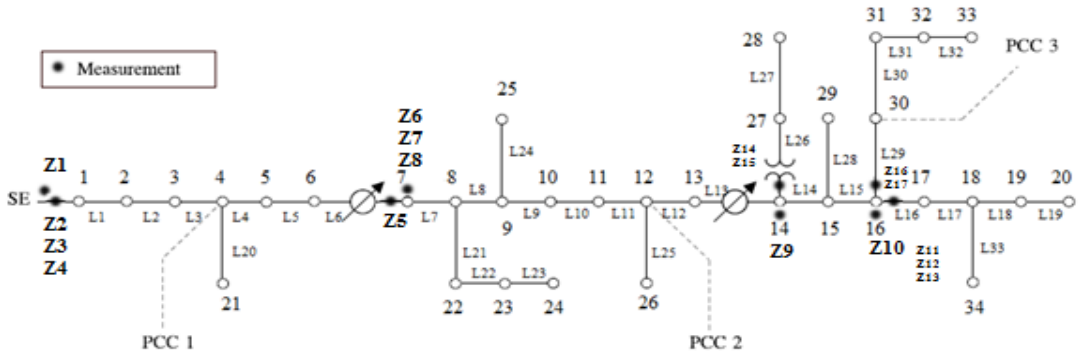

Fig.4.6 IEEE 34-node test feeder with real time measurements.

Total no of buses (n) =34

Total no of lines (nline) =33

Total number of Number of PCCs= 3

Total number of real time measurements (m) =17

Line, load and measurement data of IEEE 34-node test feeder System is given in Appendix B.

- ## Case studies

Several distinct combinations of power injections at the PCCs are taken four illustrative cases has selected and are presented. It is assumed that the system operator has no prior information about the power injected at the PCCs and thus considers all injections null. The actual power injections at the PCCs are as follows.

Case A: Reference case where power is not injected at the PCCs

Case B: Power injection of 250 + j200 kVA at the PCC 2

Case C: Power injection of 100 + j250 kVA at the PCC 2.

Case D: Power injection at PCC 2 and PCC 3 totalizing 350 + j 160 kVA

PCC	Active power injection [kW]	Reactive power injection [kVAr]
2	150	100
3	200	60

Table 4.4 power injections at PCC2 and PCC

These real and reactive power injection at PCCs are input measurements to the conventional State Estimation method or NE method

4.7.2.1 Case results

Conventional state estimation method, several distinct combinations of power injections at PCCs has been taken, Results of all the cases of IEEE 34-node test feeder are shown in table 4.5

Case	Number of iterations	$J(x)^{\wedge}$	Bad data	Bad measurement
A	3	25.24	NO	-
B	3	288.60	YES	$P_{inj}(PCC\ 2)$,$Q_{inj}(PCC\ 2)$
C	3	307.98	YES	$P_{inj}(PCC\ 2)$,$Q_{inj}(PCC\ 2)$
D	3	445.91	YES	$P_{inj}(PCC\ 2)$,$Q_{inj}(PCC\ 2)$, $P_{inj}(PCC\ 3)$,$Q_{inj}(PCC\ 3)$

Table 4.5 presence of bad data for all cases in IEEE 34-node test feeder using NE method

Case	*temp* value of bad data measurements					
	$P_{inj}(PCC\ 1\ )$	$Q_{inj}(PCC\ 1)$	$P_{inj}(PCC\ 2\ )$	$Q_{inj}(PCC\ 2)$	$P_{inj}(PCC\ 3\ )$	$Q_{inj}(PCC\ 3)$
A	0.3282	0.3027	1.254	0.565	1.1526	0.4215
B	0.3282	0.3027	6.152	4.15	1.1526	0.4215
C	0.3282	0.3027	3.85	6.28	1.1526	0.4215
D	0.3282	0.3027	6.021	5.12	10.98	4.038

Table 4.6 *temp* value of bad data measurements for all cases in IEEE 34-node test feeder network using NE method

4.7.2.2 Discussions

Several distinct combinations of power injections at PCCs has been taken, using convectional State Estimation, bad measurement data at PCCs has been identified, As shown in table 4.5. Table 4.6 shows the temp values of bad data measurements. In reference case, no bad data is present but in case B,C and D, real and reactive power injections bad data are present. Therefore, the real and reactive power injection measurements considered in Case B,C and D are not a reliable measurements.

4.8 Merits and Demerits

Merits:

1. Conventional State Estimation filter out the information to provide a more accurate picture of the status of the system.
2. It reduces measurement errors by utilizing the redundancy available in the most measurement systems.
3. Conventional State Estimation allows the system operator to make decisions aimed at maintaining the security of the power system.
4. It has Ability to provide information for unmetered or unmonitored parts of the system.

Demerits:

1. Conventional State Estimation and bad data identification become much worse and virtually intractable when active and reactive injections at more than one PCC are uncertain.

CHAPTER 5

EXTENDED STATE ESTIMATION

5.1 INTRODUCTION

The operation of smart distribution systems is a recognized challenge to be faced by distribution operators in the next few years. The high penetration level of Distributed Generators (DG) will call for new tools for real time monitoring. In this context, Distribution System State Estimation (DSSE) together with the availability of new measurement technologies will play an important role in the Distribution Management System (DMS).

Distribution and transmission systems are very different from each other. The major differences are:

- The number of measurements is *very limited.*
- In order to achieve the observability, the historical load data (that have limited accuracy) is used as Pseudomeasurements
- High R/X ratio
- Radial and weakly meshed operation;
- Unbalanced operation, etc.

The conventional state estimator makes use of a three-phase network modeling where active and reactive power injection levels at PCCs are estimated and checked in real time with the values expected by the system operator. The real and reactive power injection measurements at PCCs may be available in real time. However, direct metering alone is not reliable enough to assist operator decisions. Raw measurements are inevitably contaminated by errors to a certain degree and may occasionally turn into bad data. On the other hand, state estimation intrinsically recognizes measurement inaccuracies and does not rely solely on local information, but also takes into account measurements of other system quantities in order to filter out the measurement errors. Thus, state estimation results are much more reliable than simply using raw measurements

Real time measurements have low value of standard deviation σ, while the Pseudomeasurements are assigned with a higher to highlight the lower confidence given to such quantities.

Other than real time measurements there are two additional measurements:

- Pseudomeasurements (power injections at PCCs)
- Virtual measurements: (zero injections)

The standard deviations (squared) appear in the covariance matrix [R]. In order to emphasize the accuracy of virtual measurements, high weighting factors are used. The assignment of high weights to virtual measurements and low weights to pseudo measurements may *cause ill-conditioned system.*

The following specific sources of ill-conditioning have been described:

1. Very large weighting factors used to enforce virtual measurements;
2. Short and long lines simultaneously present at the same bus;
3. Large proportion of injection measurements.

These sources of ill-conditioning can appear in a stronger way in conventional State estimation method. And the Pseudo measurements are modeled as power injection measurements at PCC. Because of this the conventional state estimation may not give proper estimated value of active and reactive power injections at PCC. Therefore, the conventional state estimation and conventional bad data identification are available for monitoring transmission systems *are not suitable for distribution systems.*

Using a three-phase model and considering possibly unbalanced operating conditions, even the simplest case when only active injection measurements of a single PCC are incorrect leads to a situation of multiple and possibly correlated bad data. Because of limited degree of redundancy available at distribution level, as well as the relatively inaccurate customer load pseudo measurements, the errors would tend to spread among sound correlated measurements. *This so-called smearing effect* tends to increase the number of large normalized residuals, thus complicating conventional bad data identification. Difficulties become much worse and virtually intractable with conventional bad data processing methods when active and reactive injections at more than one PCC are uncertain. Therefore, instead of attempting to apply conventional bad data identification methods, **the equality constraint approach** is used in order to identify the active and reactive injections uncertainties.

An extended state estimation method allows the identification of unexpected power injections at multiple PCCs of distribution network. Exploring the filtering properties of state estimation. We can use it to detect inconsistencies in PCC power injections. The extended state estimation

algorithm applies a sparse tableau formulation in which equality constraints are employed to model power injection assumptions at PCCs. The identification of unexpected power injections is then performed using a methodology based on normalized Lagrange multipliers and geometric tests. The use of Lagrange multipliers to handle virtual measurements.(zero injections)

5.2 Problem formulation

The network state is expressed as the vector x, containing the voltage magnitudes and phase angles at each node in the system. To estimate x, the set of measurements from the network, z, is applied. The values in z can comprise of measurements of power injections or voltage magnitudes at system buses, measurements of active and reactive power and current flows in system branches, pseudo-measurements (i.e. estimates) & virtual measurements (zero power injections) of network quantities, or any combination of the above. This forms a set of over-determined, non-linear equations:

$$\boldsymbol{Z = h(x) + \eta\ , \sigma}$$

Where, **Z=** Measurement vector, $\eta = meter\ error$ assumed to be composed by independent zero mean Gaussian variable, with diagonal covariance matrix

R=diag (σ_1^2, σ_2^2,.....,σ_m^2,) , for i=1 to m

$\boldsymbol{\sigma}$ = Standered deviation

h(x)vector of non linear function relating measurements and state

And state variable vector will be composed by voltage magnitude and phase angle of each node is given by,

Power system state estimation can be formulated as equality constrained optimization problem aiming at minimizing the weighted sum of squared residuals as follows:

$$\begin{aligned} &\textbf{min } \boldsymbol{J(x) = 0.5 * r^T * R^{-1} * r} \\ &\boldsymbol{subject\ to} \quad \boldsymbol{r_m - z_m + h_m(x) = 0} \\ &\qquad\qquad \boldsymbol{h_s(x) = 0\ (with\ respect\ to\ zero\ injections\ )} \\ &\qquad\qquad \boldsymbol{h_o(x) = 0\ (With\ rwspect\ to\ injections\ at\ PCCs)} \end{aligned} \qquad \textbf{(5.1)}$$

Where, *x* is a state vector containing nodal voltage magnitude & angle. *zm* denotes the measurement vector, r_m is the estimated residual vector & $\boldsymbol{h_m(x)}$ stands for the vector of nonlinear functions relating measurements and states.

Model information related to zero-injection nodes and the reference bus (Virtual measurements) are included in a set of structural constraints, denoted by $\boldsymbol{h_s(x) = 0.}$ System features which change according to operating conditions i.e. power injection Pseudo measurements at PCCs can be defined as operational constraints, and are represented by $\boldsymbol{h_o(x) = 0}$.

The extended residual vector is defined as

$$r = \begin{bmatrix} r_m \\ 0 \\ 0 \end{bmatrix}$$

Above extended residual vector shows that the *residual of virtual at zero injections and power injection at PCCs assumption are zero.*

While, error covariance matrix is given by:

$$R = \begin{bmatrix} R_m & 0 & 0 \\ 0 & R_s & 0 \\ 0 & 0 & R_o \end{bmatrix}$$

[R] is the error covariance matrix consist of measurements (**Rm**), structural constraints (**Rs**), and operational constraints (**Ro**). Since structural and operational constraints are deterministic, theoretically both **Rs** and **Ro** are null matrices. In practice, however, both matrices are considered equal to ξ **I**, where ξ is a scaling factor (small positive number) and **I** is an identity matrix of appropriate size. The reason for this is to prevent numerical problems in the course of the state estimation solution process.

5.3 EQUALITY CONSTRAINTS SOLUTION

The problem defined in (5.1) can be solved iteratively by the sparse tableau method or Hachtel's method as below:

This performance index J(x) can be differentiated to obtain the first-order optimal condition:

Taylor expansion provides as approximation for nonlinear vector function h(x):

$h(x + \Delta x) \cong h(x) + H(x)\Delta x$……....(5.2)

The minimization problem in (5.1) can then be written as follows:

$J(\Delta x) = (\Delta z - H(x)\Delta x)^T R^{-1}(\Delta z - H(x)\Delta x)$ ...……..(5.3)

Where, $\Delta Z = Z - h(x)\ and\ H(x) = \frac{\partial h}{\partial x}\ (Jacobian\ matrix)$. The first-order optimal condition is:

$\frac{\partial J(x)}{\partial \Delta x} = -H(x)^T R^{-1}(\Delta z - H(x)\Delta x) = 0$……...(5.4)

$H^T(x)R^{-1}(z - h(x) = 0$ ……..…….(5.5)

Hence linear Least-Squares solution can be expressed as:

$$\Delta \boldsymbol{x} = \left(\boldsymbol{H(x)^T R^{-1} H(x)}\right)^{\boldsymbol{T}} \boldsymbol{H^T R^{-1}} \Delta \boldsymbol{z(x)} \text{……,,,.(5.6)}$$

In order to obtain the constraints optimization, the Lagrangian function is considered

$$\boldsymbol{L(r, \lambda) = j(x) - \lambda_m\left(\, r_m - z_m + h_m(x)\right) - \lambda_s\, h_s(x) - \lambda_o h_o(x)}$$

Where**,**

λm, λs & λo are Lagrange multipliers associated to measurements, structural and operational constraints respectively.

The first order optimality conditions are derived:

$$\boldsymbol{\frac{\partial L}{\partial r_m} = R^{-1} r_m - \lambda_m = 0} \text{ …….....(5.7)}$$

$$\boldsymbol{\frac{\partial L}{\partial x} = -H_m(x)^T \lambda_m - H_s(x)^T \lambda_s - H_o(x)^T \lambda_o = 0} \text{……..….(5.8)}$$

$$\boldsymbol{\frac{\partial L}{\partial \lambda_m} = r_m - z_m + h_m(x) = 0} \text{ …….…... (5.9)}$$

$$\boldsymbol{\frac{\partial L}{\partial \lambda_s} = h_s(x) = 0} \text{……. (5.10)}$$

$$\boldsymbol{\frac{\partial L}{\partial \lambda_o} = h_o(x) = 0} \text{ …… (5.11)}$$

From (5.7), $\boldsymbol{\lambda_m = R^{-1}r}$ **and** $\boldsymbol{r_m = R\lambda_m}$**……(5.12)**

The residual vector $r_m = z_m - h(x)_m$ can be explore using Taylor's expansion series with neglecting higher order terms

$$\boldsymbol{r_m(x + \Delta x) = r_m - H(x)_m \Delta x} \text{ ……(5.13)}$$

By (5.11)

$$\boldsymbol{r_m = R\lambda_m + H(x)_m \Delta x} \text{ ……..… (5.14)}$$

Now, after $\boldsymbol{k^{th}}$ ***iteration the updated vector of residual can be written as***:

$$\boldsymbol{r^{k+1} = z - h(x^k)} \text{……(5.15)}$$

This residual can be expanded using linear terms of Taylor series:

$$\boldsymbol{r^{k+1} = R\lambda^{k+1} = r^k - H(x^k)\Delta x^k} \text{……(5.16)}$$

Where, λ^{k+1} is a linear approximation to r^{k+1} after k^{th} *iteration*

From (5.8) and (5.16) the optimization problem can be solved iteratively by using following linear relation:

$$\begin{bmatrix} \mathbf{0} & \mathbf{H^T} \\ \mathbf{H} & \boldsymbol{R} \end{bmatrix} \begin{bmatrix} \Delta \mathbf{x} \\ \boldsymbol{\lambda} \end{bmatrix} = \begin{bmatrix} \mathbf{0} \\ \mathbf{z - h(x)} \end{bmatrix} \text{……... (5.17)}$$

Starting from an initial state x^0*, the correction state vector* Δx *is obtained by (5.17) & state vector is iteratively updated as* $x^{k+1} = x^k + \Delta x$

Where,

$$\boldsymbol{z} = \begin{bmatrix} \boldsymbol{zm} \\ \mathbf{0} \\ \mathbf{0} \end{bmatrix}, \qquad \boldsymbol{h(x)} = \begin{bmatrix} \boldsymbol{h_m(x)} \\ \boldsymbol{h_s(x)} \\ \boldsymbol{h_o(x)} \end{bmatrix}$$

$$\boldsymbol{\lambda} = \begin{bmatrix} \boldsymbol{\lambda m} \\ \boldsymbol{\lambda s} \\ \boldsymbol{\lambda o} \end{bmatrix}, \qquad \boldsymbol{H(x)} = \begin{bmatrix} \boldsymbol{H_m(x)} \\ \boldsymbol{H_s(x)} \\ \boldsymbol{H_o(x)} \end{bmatrix} \qquad \textbf{(5.18)}$$

In order to compare some solutions for the numerical ill condition problem associated with the SE, following methods are considered:

1. **Conventional State estimation i.e. Normal equation methods (NE)**

Following standard deviations are considered in NE methods

- Real time measurements: 0.03 (3%)
- Pseudo measurements: 0.20 (20%)
- Virtual measurements : 1e6 to 1e12 (High weighs are given to virtual measurements)

Therefore, structure of error covariance matrix in NE method is given by

$$R = \begin{bmatrix} R_m & 0 & 0 \\ 0 & R_v & 0 \\ 0 & 0 & R_p \end{bmatrix}$$

The weights of all real time, pseudo and virtual measurements are considered.

1 Augmented matrix approach (Hatchel's formulation) (AM)

Problem defined in (5.1) and its solution is given by (5.17) is called Augmented matrix approach. *In which both, virtual measurements and pseudo measurements of active and reactive power injection at PCC are modeled as structural and operational constraints respectively*.
In order to compare all the three methods of DSSE (NE and AM), following two performance indices are used:

- Condition number of coefficient matrix.
- Sparsity degree

Condition number: The condition number of the coefficient matrix can be used to measure the ill-conditioning of a problem. The condition number can be calculated as shown in equation (5.19)

$$K(A) = \|A\| \|A^{-1}\| \quad \text{..... (5.19)}$$

Where, || || *represents a given matrix norm. and* [A] is Coefficient matrix

The condition number is equal to unity for identity matrices and tends to infinity for matrices approaching singularity. The more singular the coefficient matrix is, the more ill-conditioned the linear system will be. And numerically more unstable. Therefore, lower values for condition numbers are desirable. The condition number of the Gain matrix in the NE method is the square of the condition number of the Jacobian matrix.

Sparsity degree: For the normal equation with constraints and augmented matrix methods, the dimension of the linear system is increased. In order to evaluate the sparsity of the coefficient matrices, the sparsity degree (SD) is defined in equation (5.20). This index yields the percentage of null elements with respect to the total of elements.

$$\boldsymbol{SD = \frac{NT - NNZ}{NT}} \quad \ldots\ldots\ldots\ldots\ldots\ldots\ldots\ldots\ldots\ldots\ldots\ldots \text{(5.20)}$$

Where, NT is total of elements of coefficient matrix (square of the number of state variables) and NNT is the number of nonzero elements. The sparser a matrix is, the lower the number of elements stored will be. Other parameters are used to compare the methods, such as: the number of iterations and the computational time required by each method.

5.4 Distribution network modeling

The extended state estimation problem formulation involves modeling the relationships between measurement information, structural constraints, and operational constraints, with the state vector. In this paper, such a model is derived from the three-phase network.

Let us consider a general distribution network component connecting nodes *i* and *j*,

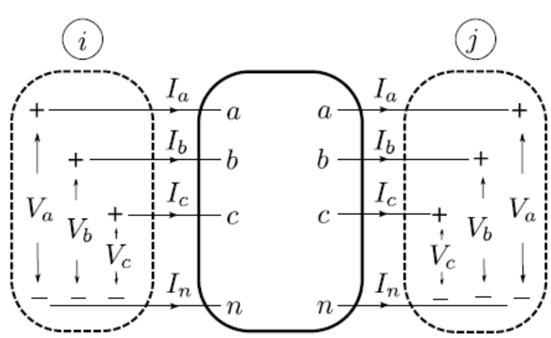

Fig.5.1 General Distribution network component [25]

Single-phase measured quantities can be expressed as functions of the state vector, thus providing the components of vector $h_m(x)$.

- *Function related to Square of current magnitude ($h_I(x)$ in single phase) :*

$$[h_I(x)]_i = [(R\{I_a\})^2]_i + [(I\{I_a\})^2]_i \text{... (Squared Value of Current @ ith Node)}$$

$$[h_I(x)]_j = [(R\{I_a\})^2]_j + [(I\{I_c\})^2]_j \text{... (Squared Value of Current @ jth Node)}$$

Where, I_a *is a branch current*

- *Function related to active (t_{ij}) & reactive (u_{ij}) power flow in single phase:*

$$\left[\boldsymbol{h_{t_{ij}}(x)}\right]_{\boldsymbol{i}} = [\boldsymbol{R}\{\boldsymbol{V_a I_a^*}\}]_{\boldsymbol{i}} \text{..... (Real power flow)}$$

$$\left[\boldsymbol{h_{u_{ij}}(x)}\right]_{\boldsymbol{i}} = [\boldsymbol{R}\{\boldsymbol{V_a I_a^*}\}]_{\boldsymbol{i}} \text{..... (Reactive power flow)}$$

- *Function related to real and reactive power injection in single phase:*

$$[\boldsymbol{h_P(x)}]_{\boldsymbol{i}} = \left(\sum_{\boldsymbol{j}\in\Omega_{\boldsymbol{i}}} \left[\boldsymbol{h_{t_{ij}}(x)}\right]_{\boldsymbol{i}}\right) \text{..... (Real power injection)}$$

$$\left[\boldsymbol{h_Q(x)}\right]_{\boldsymbol{i}} = \left(\sum_{\boldsymbol{j}\in\Omega_{\boldsymbol{i}}} \left[\boldsymbol{h_{u_{ij}}(x)}\right]_{\boldsymbol{i}}\right) \text{..... (Reactive power injection)}$$

Where,

Ω_i is the set of nodes directly connected to node i.

5.4.1 MODELING OF POWER INJECTION ASSUMPTIONS AT PCCS

Using modeling steps describe in section (5.4), power injection at the PCCs are included in the formulation as operational constraint, as below:

$$[\boldsymbol{h_P(x)}]_{\boldsymbol{i}} - \left[\boldsymbol{P_{inj}}\right]_{\boldsymbol{i}} = \begin{bmatrix}\mathbf{0}\\ \mathbf{0}\\ \mathbf{0}\end{bmatrix}, \eta \quad \textbf{.....(5.21)}$$

$$\left[\boldsymbol{h_Q(x)}\right]_i - \left[\boldsymbol{Q_{inj}}\right]_i = \begin{bmatrix}\mathbf{0}\\ \mathbf{0}\\ \mathbf{0}\end{bmatrix} , \eta \qquad \textbf{…….(5.22)}$$

Where, *Pinj is* specified active power injections, while *Qinj* is specified reactive power injections at PCCs as an operational constraints, and $\eta = error$ in Real /reactive power injections, assumed to be composed by independent zero mean Gaussian variable, with diagonal covariance matrix

$$\boldsymbol{R_o}\textbf{=diag }(\boldsymbol{\sigma_1^2}, \boldsymbol{\sigma_2^2}, \textbf{.....}, \boldsymbol{\sigma_{m\_oc}^2}) \textbf{ for i=1 to m\_oc}$$

Where, m_oc is an operational constraints measurements, i.e. real and reactive power injections at PCCs.

The specified power injections in (5.21) and (5.22) can be seen *as guesses to be confirmed* or rejected by available measurements through the state estimation process. However, there may be particular situations in which some knowledge about those injections may be available to the system operator, as a result of load forecast and generation level prediction. The corresponding degree of uncertainty should be evaluated in order to assign *nonzero variances* to such information, leading to *a nonzero **Ro** matrix*. The proposed model is able to accommodate distinct diagonal values in **Ro**, so that different levels of uncertainty can be assigned to individual PCC injections.

5.5 IDENTIFICATION OF UNEXPECTED POWER INJECTIONS AT PCCS

The identification of erroneous assumptions regarding power injections at PCCs utilizes a methodology based on the application of normalized Lagrange multipliers (NLM) as well as collinearity tests (CT). The NLM & CT methodology assumes specified power injections at the PCCs. Those assumptions may be revised by assigning large values to the elements of the covariance matrix **Ro.**

These large values imply large uncertainties around the operational constraints. Thereby nullifying their impact on the state estimation for practical purposes. This technique avoids alterations in the whole set of problem constraints during the identification procedures.

5.5.1 NORMALIZED LAGRANGE MULTIPLIERS (NLM)

The errors in measurements and structural/ operational constraints reflect on the associated Lagrange multiplier values as below:

$$\boldsymbol{\lambda} = \boldsymbol{V} \in \text{..... (5.23)}$$

Where, **V** is the covariance matrix of the Lagrange multiplier vector $\boldsymbol{\lambda}$ and $\in$ is the vector of errors in measurements and structural/operational constraints.

The covariance matrix **V** is given by a submatrix of the inverse of the sparse tableau's matrix described in (5.17).

$$\begin{bmatrix} -\sum & C^T \\ C & V \end{bmatrix} = \begin{bmatrix} 0 & H^T \\ H & R \end{bmatrix}^{-1} \text{..... (5.24)}$$

Therefore, Lagrange multipliers can be normalized as:

$$\boldsymbol{\lambda_i^N} = \frac{\boldsymbol{\lambda_i}}{\sqrt{\boldsymbol{V_{ii}}}} \text{ ..... (5.25)}$$

Where, λi is the *i*th element of $\boldsymbol{\lambda}$, and *Vii* is the *i*th diagonal element of **V**.

Assuming that gross errors on analog measurements and on structural/operational constraints are absent, normalized Lagrange multipliers are zero mean random variables with variances equal to one. Therefore, *large normalized Lagrange multipliers point out the existence of inconsistencies in the mathematical modeling.*

5.5.2 COLLINEARITY TESTS

Collinearity tests are based on the geometric interpretation of $\boldsymbol{\lambda}$, providing straightforward means to conclude about the inconsistency of the assumptions behind the operational constraints selected in *S*. where, set *S*, referred to *as suspect set of constraints which are associated to incorrect PCC power injection assumptions.*

Consider the columns of the covariance matrix **V** are partitioned according to suspect and trusted data, as

$$\boldsymbol{V} = [\boldsymbol{V_S V_T}] \textbf{ ..... (5.26)}$$

V*s* and **V*T*** correspond to the covariance matrices related to suspect and True information, respectively. Assume that measurements out of *S* are perfect as well as constraints out of *S* represent the network model consistently.

Therefore, error vector can be given by,

$$\in = \begin{bmatrix} \in_s \\ \mathbf{0} \end{bmatrix} \quad \text{..... (5.27)}$$

Hence by (5.26) & (5.27) the vector of Lagrange multipliers can be computed as follows:

$$\boldsymbol{\lambda = V_S} \in_s \quad \text{..... (5.28)}$$

The expression (5.28) indicates that the vector of Lagrange multipliers lies onto *C(***V***S)*, which is the space spanned by the columns of the covariance matrix related to suspect information. In general, the degree of pertinence of a vector $\boldsymbol{\lambda}$ to the space provided by the columns of a matrix **V*S*** is given by,

$$\cos(\theta) = \left(\frac{\lambda_S^T V_{SS}^T \lambda}{\lambda^T R \lambda}\right)^{0.5} \quad \text{..... (5.29)}$$

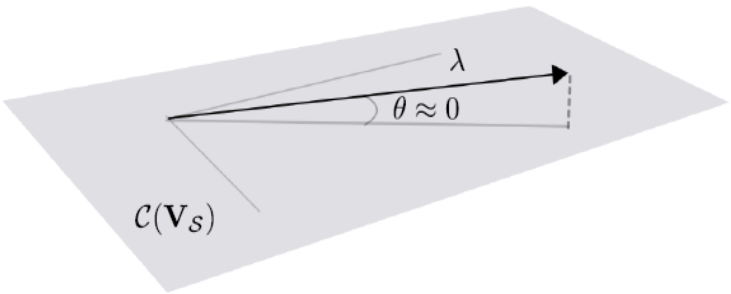

Fig. 5.2 Interpretation of cos θ.

Where,

$$\boldsymbol{\lambda_S = V_S^T R \lambda}$$
$$\boldsymbol{V_{SS} = V_S^T R V_S}$$

There are two cases:

- Case I.

  λ lies perfectly in the space spanned by the columns of VS, so, cos θ=1 ,

  All constraints except those selected in S are consistent.

- Case II.

  $\cos(\theta) \neq 1$ (Measurements and network modeling are not perfect):

  S does not include all inconsistently modeled constraints.

Pertinence tests based on cos θ are referred to in the state estimation as collinearity tests and it is possible to devise an algorithm to identify misleading assumptions regarding power injections at PCCs.

5.6 ALGORITHM FOR COLLINEARITY TEST

Collinearity test is used for identification of unexpected power injections at PCCs.

This algorithm split into two main stages.

Stage 1: Suspect measurements and constraints are included in the suspect set *S*

Stage 2: Information regarding the suspect set are tested in order to verify whether they are indeed erroneous. If not, the corresponding constraint is removed from *S*.

A suspect set *S* is then defined by the constraints related to normalize Lagrange multiplier values larger than a threshold, named λt. *And* λt *is set to 3.*

The algorithm can be summarized as follows.

Step 1: Compute the maximum normalized Lagrange multiplier related to the state estimation solution, as follows:

$$\boldsymbol{\lambda_{max}^{N} = max \left| \lambda_{i}^{N} \right| \quad \forall i.}$$

Step 2: Compare $\boldsymbol{\lambda_{max}^{N}}$ with λt.

a) If $\boldsymbol{\lambda_{max}^{N} \geq \lambda_{t}}$ **,** then there is an error regarding the PCC power injection assumptions include all constraints *i* such that $\boldsymbol{\lambda_{i}^{N}} \geq \lambda t$ in *S*. *Go to step 3.*

b) *If* $\lambda_{\max}^{N} < \lambda_{t}$, then there is no error in PCC power injection assumption. Terminate the algorithm.

Step 3: Compute cos θ for all constraints in the suspect set *S using (5.29).*

a) In case cos $\theta \geq (1 - \in_{cos})$, then all erroneously modeled constraints are included in *S*. Go to step 4.

b) Otherwise, reduced λ_t and update the suspect set S by returning to step2.

Step 4: For each operational constraint *c* associated to a PCC power injection, remove *c* from *S* and update cos θ.

a) If cos $\theta \geq (1 - \in_{cos})$, then *c* is free of error and must be removed from *S*.

b) Otherwise, *c* is kept in *S*.

Step 5: The resulting set $\boldsymbol{\epsilon} = S$ is considered the set of erroneously modeled constraints.

Note : $\in_{cos}$ defines the sensitivity of collinearity test. And $\in_{cos} = 0.02$

5.7 HACHTEL'S AUGMENTED MATRIX METHOD ALGORITHUM

The use of large weights for modeling very accurate virtual measurements leads to ill conditioning of gain matrix [G]. To avoid the use of large weights, virtual measurements and pseudo measurements are model as explicit structural and operational constraints:

Structure of error covariance matrix in AM method is given by

$$R = \begin{bmatrix} R_m & 0 & 0 \\ 0 & R_s & 0 \\ 0 & 0 & R_o \end{bmatrix} \quad \text{..... (5.30)}$$

As discussed in section (5.2), both **Rs** and **Ro** are null matrices. But in practice, however, both matrices are considered equal to ξ **I**, where ξ is a small positive number.

The scaling factor ξ *used to control the numerical stability is set to 1.*

Algorithm Steps for AM methods as follows:

Step1: // Read line and measurement data. (Line data and Measurement data)//

Step2: // Print out all above data and crosscheck it.//

Step3: // Form the sparsity vectors NLCONT, ITAGF, ITAGTO, ADJL, & ADJQ //

// Sparsity vectors for IEEE 10-Bus and IEEE 34-node test feeder has been given is APPENDIX A and APPENDIX B respectively//

Step4: // Form Ybus using sparsity vectors.//

Step 5: // Form weight matrix [W]. //

Step 6: // Set initial guess voltages. //

Step7: // Initialization of iterative process. //

Step8: // Set |delxmax|=0 //

Step 9: // Calculate Zcal vector//

// For i=1 to m //

// calculate Δz as //

```
for i=1 to m
delz(i)=(z(i)-zcal(i));
```

//end of ith loop//

Step10: // Form Jacobian matrix [A] //

// 1st initialized matrix [A]//

```
// for i=1 to m
    for j=1:2*n
        A(i,j)=0;
    End of jth loop
End of ith loop//
```

Step 11:// Form A3 matrix, and [A3] = $\begin{bmatrix} 0 & A^T \\ A & R \end{bmatrix}$ ….. Called sparse tableau's matrix

// Form error covariance matrix [R] //

```
for i=1 to m
    for j=1 to m
        R(i,i)=(sigma(i)*sigma(i));
    End of jth loop
End of ith loop
```

// form zero matrix //

```
for i=1 to 2*n
    for j=1 to 2*n
        zero(i,j)=0;
    end of jth loop
```

end of ith loop

// form column matrices [A1], [A22] //

A1=horzcat(A,R); and

A22=horzcat(zero,A^T);

// form matrix [A3] //

A3=vertcat(A22,A1);

Step12: // Form B3 matrix, and [B3]= $\begin{bmatrix} 0 \\ \Delta Z \end{bmatrix}$//

```
for i=1:2*n
        zero1(i)=0;
end
```

B3=vertcat($zero1^T$,$delZ^T$);

Step13:// Solve $\begin{bmatrix} \mathbf{0} & \mathbf{H^T} \\ \mathbf{H} & \mathbf{R} \end{bmatrix} \begin{bmatrix} \Delta\mathbf{x} \\ \boldsymbol{\lambda} \end{bmatrix} = \begin{bmatrix} \mathbf{0} \\ \mathbf{z} - \mathbf{h}(\mathbf{x}) \end{bmatrix}$ using Gauss elimination method.//

Step 14: // Update delta and v of all the buses.//

Step16: // One iteration is over //

// Update iteration count //

iter=iter+1

if (iter ≥ itermax) .. if Yes, // Go to 90//

if No, //Go to step 9 //

100:// problem converge in 'iter' iteration //

// go for identification of unexpected power injections at PCCs using NLM & CT described in section (5.5), (5.5.1), (5.5.2) and section (5.6) as below: //

101:// The covariance matrix **V** is given by a submatrix of the inverse of the sparse tableau's matrix described in step 11.//

$$\begin{bmatrix} -\sum & C^T \\ C & V \end{bmatrix} = \begin{bmatrix} 0 & H^T \\ H & R \end{bmatrix}^{-1}$$

102:// Lagrange multipliers can be normalized as:

$$\boldsymbol{\lambda_i^N = \frac{\lambda_i}{\sqrt{V_{ii}}}}$$

// large normalized Lagrange multipliers point out the existence of inconsistencies in the mathematical modeling. //

103://Compute the maximum normalized Lagrange multiplier related to the state estimation solution, as follows:

$$\boldsymbol{\lambda_{max}^N = max \left| \lambda_i^N \right| \quad \forall i.}$$

104:// Compare $\boldsymbol{\lambda_{max}^N}$ with λt. *And* λt *is set to 3.*

c) If $\boldsymbol{\lambda_{max}^N \geq \lambda_t}$ **,** then there is an error regarding the PCC power injection assumptions *include all constraints i* such that $\boldsymbol{\lambda_i^N} \geq \lambda t$ in *S*.

Go to 105://.

d) *If* $\lambda_{\max}^{N} < \lambda_t$, then there is no error in PCC power injection assumption. Terminate the algorithm.

105:// Compute cos θ for all constraints in the suspect set *S, where,* suspect set *S* is the constraints related to normalize Lagrange multiplier values larger than a threshold λt.//

// $\cos(\theta)=\left(\frac{\lambda_S^T V_{SS}^T \lambda}{\lambda^T R \lambda}\right)^{0.5}$ and $\lambda_S = V_S^T R \lambda$, $V_{SS} = V_S^T R V_S$ //

// V_S *is covarience matrix related to suspect information* //

// Form matrix [L2]= $V_S^T R$ //

// Form matrix [Vss]=$L2V_S$ //

// Form matrix [λ_s]= $L2\lambda$ //

// calculate $\cos(\theta)$, *and given by* $\cos(\theta)=\left(\frac{\lambda_S^T V_{SS}^T \lambda}{\lambda^T R \lambda}\right)^{0.5}$ //

// In case cos $\theta \geq (1 - \epsilon_{cos})$, then all erroneously modeled constraints are included in *S*. Go to 106.//

//Otherwise, reduced λ_t and update the suspect set S by returning to 104.//

106:// For each operational constraint *c* associated to a PCC power injection, remove *c* from *S* and update cos θ.

//If cos $\theta \geq (1 - \in_{cos})$, then operational constraint *c* is free of error and must be removed from *S*.//

// otherwise, *c* is kept in *S*//

// Note : $\in_{cos}$ defines the sensitivity of collinearity test. And $\in_{cos}$*=0.02//*

// Stop //

90:// Problem not converge in itermax iteration. //

5.8 Case Studies

5.8.1 IEEE 10 bus network

- **The first test system is IEEE 10-Bus radial network**

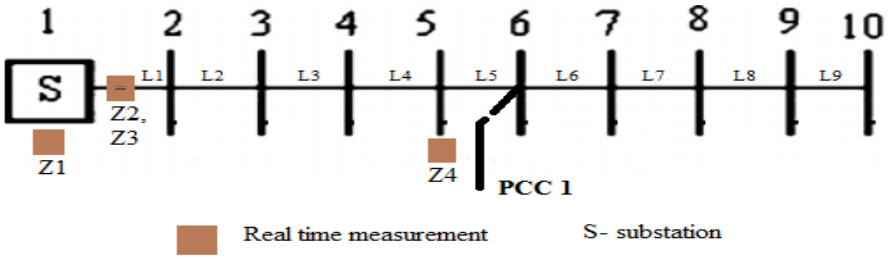

Fig. 5.3 IEEE 10-Bus radial network with single PCC

Total no of buses (n) =10

Total no of lines (nline) =9

Total number of Number of PCCs= 1

Total number of real time measurements (m) =4

Line, load and measurement data of IEEE 10-Bus System are given *in Appendix A*

- **Case studies**

Several distinct combinations of power injections at the PCC 1 are taken. Three illustrative cases has selected and are presented. It is assumed that the system operator has no prior information about the power injected at the PCC 1 and thus considers all injections null. The actual power injections at the PCC are as follows.

Case A: Reference case where power is not injected at the PCC 1.

Case B: Power injection of 250 + j100 kVA at PCC 1.

Case C: Power injection of 150 + j300 kVA at PCC 1

These real and reactive power injection at PCC1 are input measurements to the conventional State Estimation method or NE method.

5.8.1.1 Case Results

In this section the results obtain by using two methods under analysis are presented:

- Normal equation method (conventional state estimation method)(NE)
- Hachtel's augmented matrix method.(AM)

In order to compare all the methods of DSSE (NE and AM), following two performance indices are used:

- Condition number of coefficient matrix.
- Sparsity degree

A convergence tolerance is set to 1e-3. And $\lambda_t = 3$.

Measurement type	**Number of measurements**	**Standard deviation (σ) For Normal Equation(NE) method**	**Standard deviation (σ) For Augmented matrix (AM)method**
Real time	4	0.03 (3%) or 0.000159	0.03 (3%) or 0.000159
Virtual	16	1e5	1
Pseudo	7	0.20 (20%)	1

Table 5.1 Information about Standard deviation (σ) For real time, virtual and pseudo measurements for IEEE 10-Bus network.

In order to evaluate the performance of the methodologies, the weighting factors associated with the virtual measurements has varied. The condition numbers of the coefficient matrix are as follow:

Methods	Weighting factor (virtual measurements)			
	1e5	1e6	1e8	1e12
NE	1.0170e+07	4.145e+07	1.4145e+08	4.0621e+10
AM	3.9555e+04			

Table 5.2 Condition number of Coefficient Matrix for 10-bus network

Observations: Result of Table 5.2 shows that, the AM method is more numerically stable compare to NE method. The condition number of NE method is increases with the weighting factors of virtual measurements.

Method	Number of elements	Nonzero elements	Sparsity degree (%)
NE	$(20)^2$	154	61.5
AM	$(47)^2$	295	86.64

Table 5.3 Sparsity degree for 10-bus radial network

Observation: Table 5.3 shows the sparsity degree of each method. And AM method is not particularly expensive, due to their higher sparsity degree compare to NE method.

Hachtel's Augmented matrix method (AM): Several distinct combinations of power injections at the PCC 1 are tested by using AM methods and normalized Lagrangian multipliers are as follow: *And tolerance for the collinearity test is $\in_{cos}$ is defined as 0.02 i.e, if cos(θ) value of power injection constraints is greater than 0.98, remove that real or reactive power constraints from suspect set S.*

Case	Active power constraint at PCC1		Reactive power constraint at PCC1	
	$\lvert\lambda_i^N\rvert$	$\{\lvert\lambda_i^N\rvert \geq \lambda_t\}$?	$\lvert\lambda_i^N\rvert$	$\{\lvert\lambda_i^N\rvert \geq \lambda_t\}$?
A	0.0730	NO	0.1299	NO
B	5.9951	YES	0.6035	NO
C	2.4303	NO	3.5801	YES

Table 5.4 Normalized Lagrangian Multiplier for all cases of IEEE 10-Bus network.

Case	Active power injection		Reactive power injection	
	Cos (θ)	Permanently removed from S?	Cos (θ)	Permanently removed from S?
B	0.9289	NO	0.9654	NO
C	0.9158	NO	0.9586	NO

Table 5.5 Collinearity test results for case B and Case C of IEEE 10-bus network.

Condition number of coefficient matrix is sensitive to method used. The number of iteration and The average executive time for both methods of DSSE are as shown in table 5.6

Method	Iterations	Executive time (sec.)
NE	3	0.2228
AM	3	0.2958

Table 5.6 Number of iteration and executive time (sec.) for IEEE 10-bus network.

Observation: Although the condition numbers of coefficient matrix has sensitive to method used, the numbers of iterations is the same and the average executive times are close, as shown in Table 5.6

5.8.1.2 OBSERVATIONS AND DISCUSSIONS

- As shown in Table 5.4, the normalized Lagrangian multipliers ($\boldsymbol{\lambda_i^N}$) values related to operational constraints (Active and reactive power injections at PCC 1) of all the cases are compared with threshold value ($\boldsymbol{\lambda_t}$). From table 5.4, one can notice that, In case A, $\boldsymbol{\lambda_i^N}$ is less than threshold $\boldsymbol{\lambda_t}$, **this results indicates that, there are no any errors regarding the power injection assumption at PCC 1**. Indeed, this case represents the reference condition for which power injections at PCC1 are zero.
- In case B, power injection amounts to 250+j100 kVA at PCC 1. The normalized Lagrange multipliers associated to active and reactive power injections at the PCC 1 for case B are shown in Table 5.4. Unlike the case A, the normalized Lagrange multipliers related to PCC 1 are larger than the specified threshold. The maximum normalized Lagrange multiplier value for this case is 5.9951, then collinearity test has been performed, and table 5.5, result correctly indicates that there are erroneous modeling assumptions regarding the active and reactive power injections at PCC 1.
- Similarly, in case B, power injected at PCC1 with low power factor. Power injection amount to 150+j300 kVA. The normalized Lagrange multipliers associated to active and reactive power injections at the PCC 1 for case C are also shown in Table 5.4 The maximum normalized Lagrange multiplier value for this case is 3.5801, then collinearity test has been performed, and table 5.5.

- The algorithm identifies only the erroneous modeling assumptions related to indicates that there are erroneous modeling assumptions regarding the active and reactive power injections at PCC 1.

5.8.2 IEEE 34-node test feeder

Another test system is IEEE 34-node test feeder as shown below:

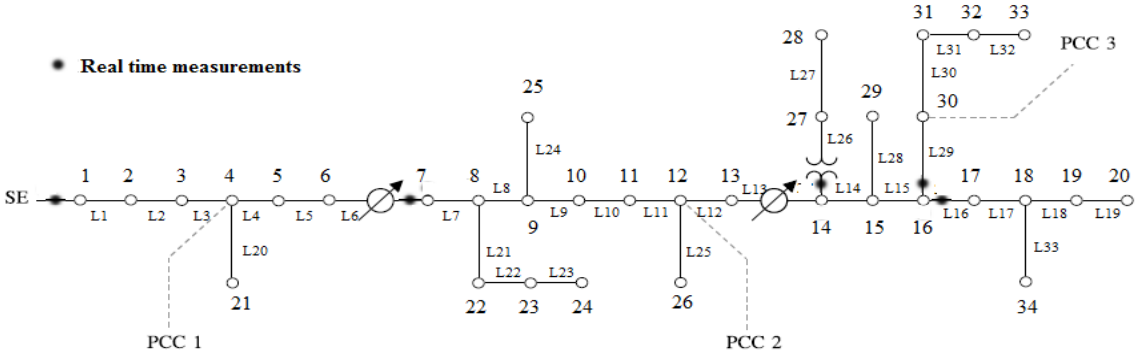

Fig.5.4 IEEE 34-node test feeder with three PCCs

Total no of buses (n) =34

Total no of lines (nline) =33

Total number of Number of PCCs= 3

Total number of real time measurements (m) =17

Line, load and measurement data of IEEE 34-node test feeder System is given in Appendix B.

- **Case studies**

Several distinct combinations of power injections at the PCCs are taken four illustrative cases has selected and are presented. It is assumed that the system operator has no prior information about the power injected at the PCCs and thus considers all injections null. The actual power injections at the PCCs are as follows.

Case A: Reference case where power is not injected at the PCCs

Case B: Power injection of 250 + j200 kVA at the PCC 2

Case C: Power injection of 100 + j250 kVA at the PCC 2.

Case D: Power injection at PCC 2 and PCC 3 totalizing 350 + j 160 kVA

PCC	Active power injection [kW]	Reactive power injection [kVAr]
2	150	100
3	200	60

These real and reactive power injection at PCCs are input measurements to the conventional State Estimation method or NE method

Measurement type	**Number of measurements**	**Standard deviation (σ) For Normal Equation(NE) method**	**Standard deviation (σ) For Augmented matrix (AM)method**
Real time	17	0.03 (3%) or 0.000159	0.03 (3%) or 0.000159
Virtual	45	1e5	1
Pseudo	32	0.20 (20%)	1

Table 5.7 Information about Standard deviation (σ) For real time, virtual and pseudo measurements for IEEE 34-Node test feeder network.

5.8.2.1 Case Results

In order to evaluate the performance of the methodologies, the weighting factors associated with the virtual measurements has varied. The condition numbers of the coefficient matrix are as follow:

Methods	Weighting factor (virtual measurements)			
	1e5	1e6	1e8	1e12
NE	1.9579e+09	2.455e+09	3.215e+012	3.2721e+14
AM	3.3026e+06			

Table 5.8 Condition number of Coefficient Matrix for IEEE 34-node test feeder

Observation: Result of Table 5.8 shows that, the AM method is more numerically stable compare to NE method. The condition number of NE method is increases with the weighting factors of virtual measurements.

Table 5.9 shows the sparsity degree of each method. And AM method is not particularly expansive, due to their higher sparsity degree compare to NE method.

Method	Number of elements	Nonzero elements	Sparsity degree (%)
NE	$(68)^2$	1648	64.35
AM	$(162)^2$	1026	96.09

Table 5.9 Sparsity degree for IEEE 34-node test feeder

Observation: Table 5.9 shows the sparsity degree of each method. And AM method is not particularly expensive, due to their higher sparsity degree compare to NE method.

Hachtel's Augmented matrix method (AM): Several distinct combinations of power injections at the PCCs are tested by using AM methods and normalized Lagrangian multipliers are as follow:

And tolerance for the collinearity test is $\in_{cos}$ is defined as 0.02 i.e, if cos(θ) value of power injection constraints is greater than 0.98, remove that real or reactive power constraints from suspect set S.

At PCC 1:

Case	**Active power constraint at PCC1**		**Reactive power constraint at PCC1**	
	$\lvert\lambda_i^N\rvert$	$\{\lvert\lambda_i^N\rvert \geq \lambda_t\}$?	$\lvert\lambda_i^N\rvert$	$\{\lvert\lambda_i^N\rvert \geq \lambda_t\}$?
A	0.0930	NO	0.099	NO
B	0.145	NO	0.0921	NO
C	0.215	NO	1.1241	NO

At PCC 2:

Case	**Active power constraint at PCC2**		**Reactive power constraint at PCC2**	
	$\lvert\lambda_i^N\rvert$	$\{\lvert\lambda_i^N\rvert \geq \lambda_t\}$?	$\lvert\lambda_i^N\rvert$	$\{\lvert\lambda_i^N\rvert \geq \lambda_t\}$?
A	0.0830	NO	0.339	NO
B	5.5951	YES	3.728	YES
C	2.958	NO	3.4715	NO

At PCC 3:

Case	Active power constraint at PCC3		Reactive power constraint at PCC3	
	$\lvert\lambda_i^N\rvert$	$\{\lvert\lambda_i^N\rvert \geq \lambda_t\}$?	$\lvert\lambda_i^N\rvert$	$\{\lvert\lambda_i^N\rvert \geq \lambda_t\}$?
A	0.04130	NO	0.1521	NO
B	1.25	NO	0.9854	NO
C	0.2514	NO	2.2501	NO

At PCC 2 and PCC 3:

Case	Active power constraint at PCC2		Reactive power constraint at PCC2		Active power constraint at PCC3		Reactive power constraint at PCC3	
	$\lvert\lambda_i^N\rvert$	$\{\lvert\lambda_i^N\rvert \geq \lambda_t\}$?	$\lvert\lambda_i^N\rvert$	$\{\lvert\lambda_i^N\rvert \geq \lambda_t\}$?	$\lvert\lambda_i^N\rvert$	$\{\lvert\lambda_i^N\rvert \geq \lambda_t\}$?	$\lvert\lambda_i^N\rvert$	$\{\lvert\lambda_i^N\rvert \geq \lambda_t\}$?
D	**4.9745**	**YES**	**2.984**	**NO**	**3.523**	**YES**	**2.6584**	**NO**

Table 5.10 Normalized Lagrangian Multiplier for all cases of IEEE 34-node test feeder at PCCs

Case B Collinearity test result is as shown in table 5.11

PCC	Active power injection		Reactive power injection	
	Cos (θ)	Permanently removed from S?	Cos (θ)	Permanently removed from S?
2	0.9489	NO	0.9524	NO

Table 5.11 Case B collinearity test results for IEEE 34-node test feeder.

Case C Collinearity test result is as shown in table 5.12

PCC	Active power injection		Reactive power injection	
	Cos (θ)	Permanently removed from S?	Cos (θ)	Permanently removed from S?
2	0.9819	YES	0.9318	NO

Table 5.12 Collinearity test results for case C for IEEE 34-node test feeder

Case D Collinearity test result is as shown in table 5.13

PCC	Active power injection		Reactive power injection	
	Cos (θ)	Permanently removed from S?	Cos (θ)	Permanently removed from S?
2	0.9514	NO	0.9748	NO
3	**0.9798**	**NO**	**0.9758**	**NO**

Table 5.13 Collinearity test results for case D for IEEE 34-node test feeder.

The average executive time of both the methods are as shown in table 5.14

Method	Iterations	Executive time (sec.)
NE	3	0.2698
AM	3	0.3458

Table 5.14 Number of iteration and executive time (sec.) for IEEE 34-node test feeder.

Observation: Although the condition numbers of coefficient matrix has sensitive to method used, the numbers of iterations is the same and the average executive times are close, as shown in Table 5.14

5.8.2.2 OBSERVATION AND DISCUSSIONS:

- Hachtel's Augmented matrix method (AM) has been implemented on IEEE 34-node test feeder, and normalized Lagrangian multipliers ($\boldsymbol{\lambda_i^N}$) values related to operational constraints (Active and reactive power injections at PCCs) of all four cases are compared with threshold value ($\boldsymbol{\lambda_t}$) As shown in table 5.10
- Case A is reference condition for which power injections at PCCs are zero.
- Case B, power injection amount to 250+j200 kVA at PCC 2, in this case the maximum Normalized Lagrangian Multiplier value is 5.5951. as shown in Table 5.10 (at PCC 2).
- Similarly, in case C, power is injected at PCC 2 with a low power factor of 0.7808. The maximum Normalized Lagrangian Multiplier value is 3.4715. as shown in Table 5.10 (at PCC 2).

- In case D, totalizing 350+j160 kVA is injected at PCC 2 and PCC 3, normalized Lagrangian multipliers ($\boldsymbol{\lambda_i^N}$) values related to operational constraints (Active and reactive power injections at PCC 2 and PCC 3) are compared with threshold value ($\boldsymbol{\lambda_t}$) As shown in Table 5.10 (at PCC 2 and PCC 3).

- In case A, i.e. Reference condition, the normalized Lagrangian Multipliers of an operational constraints do not exceeds the threshold value, this results indicate that there is not errors regarding the power injections assumptions at the PCCs.
- In case B, normalized Lagrangian Multipliers of an operational constraints has crossed the threshold value, hence, collinearity test on real and reactive power injections at PCC 2 has conducted. Table 5.11 shows collinearity test result and it indicates that there are erroneous modeling assumptions regarding the active and reactive power injections at PCC 2.
- Similarly, case C collinearity test results is shown in Table 5.12
- In case D, the λ_i^N value of active and reactive power operation constraints at PCC 2 and PCC 3 are shown**, and $\boldsymbol{\lambda_i^N}$ values are greater than** threshold $\boldsymbol{\lambda_t}$, the collinearity test is then performed on real and reactive power injections of PCC 2 and PCC 3 as shown in table 5.13. Cos (θ) value for Active and reactive power injections are shown in Table 5.13. According to step 4 of collinearity test algorithm, the constraints in the suspect set must be individually removed from *S* to evaluate their effect on Cos (θ) ss shown in Table 5.13. And it indicates that, the assumptions regarding the power injection at PCC 2 and PCC 3 are incorrect.

CONCLUSIONS

Due to the ongoing interconnection of DGs in distribution network, PCCs are expected to have large power injection variabilities and uncertainties in comparison with regular load connection points. State estimation methods must be adapted and enhanced to support the real-time monitoring of power injections at PCCs. An extended state estimation method which allows the identification of unexpected power injections at PCCs in distribution grids. The developed state estimator *relies* on a three-phase network model whose power injection levels at PCCs are validated in real time.

Because *of limited numbers of real time measurements* (4 real time measurements) in IEEE 10-Bus radial system and (17 real time measurements) in IEEE 34-node test feeder network initially this systems ware unobservable. And measurements redundancy was very low. In order to make systems observable, network topology observability test were conducted on those system and large number of virtual and pseudo measurements have been added in both the systems.

The performance of the backward/forward sweep method of radial networks has been presented. The backward and forward propagation iterative equation carries the distribution power flow. By using backward propagation the power of each branch has been calculated. The voltage magnitudes at each node are calculated in forward propagation. The results for IEEE
10-Bus and IEEE 34-node test feeder systems have been tabulated.

The identification of unexpected power injections has performed using a methodology based on normalized Lagrange multipliers and geometric tests. Proposed algorithm has been conducted on the IEEE 10-Bus node and IEEE 34-node test feeder illustrate the applicability of the developed approach. Results highlight that the proposed methodology consistently yields the proper identification of unexpected power injections at PCCs. The combined application of normalized Lagrange multiplier tests and collinearity tests have shown to be effective and sufficiently accurate to the problem.

This thesis presented different DSSE methods and comparisons of those methods:

- Normal equation method (NE) or Conventional State estimation method
- Hachtel's Augmented method (AM)

Above Methods have been employed on the IEEE 10-Bus network and IIEEE 34-node test feeder. Ill-conditioning in the coefficient matrix in NE method for state estimation creates numerical stability problem for large system, as showed in results. The comparison study has

been conducted and evaluated the impact of virtual measurement weighting factors on convergence behavior of distribution state estimation methods.

The combined application of normalized Lagrange multiplier tests and collinearity tests has shown to be effective results compare to Normal equation method. Regarding to numerical stability, as we got results, the NE method was found to be prone to convergence problem depending on the weighting factors assigned to the virtual measurements.

Finally, the AM method presented the best sparsity degree. In general the AM method is in not expensive to solve with respect to the effort required by NE method. Compare to NE method, AM method is more numerically stable and can be used for large system and it is possible to conclude that this method can present a satisfactory performance in practical applications.

FUTURE RESEARCH AREAS FOR DSSE

- Concerning future studies, the analysis of other large systems will be evaluated as well as other solution techniques for ill conditioning of system, such as orthogonal transformation methods and hybrid method for DSSE.
- State estimation for distribution system using other than voltage and voltage angle as state variables, such as Branch current.
- A key feature of future DSSEs will be the *flexibility* to incorporate multiple types of input data, e.g. estimators capable of integrating both analogue and digital inputs (e.g. power/voltage measurements and switch/breaker statuses and also measurement data from a range of diverse sources, e.g. SCADA, PMU, smart metering, DG units.
- *Application of Advanced Metering Infrastructure Data:* The introduction of smart meters means that an unprecedented amount of detailed historical data on user loads is becoming available. This data can be used to better understand and model the behavior of distribution network loads, allowing to improve load estimation techniques, and ultimately, DSSE accuracy. This smart meter can be used estimate flows, voltages, and losses in the low voltage distribution network.
- *Computational Intelligence Methods in DSSE:* Computational intelligence methods have been proposed for a range of power systems and smart grids applications. Machine learning techniques can be used for DSSE. A neural network approach is *used to create pseudo-measurements of load point power injections* for use in the DSSE algorithm. A machine learning approach is used to develop load estimates for DSSE. This approach will improves the measurements redundancy and leading to improvement of the performance of the DSSE.
- Almost all of the SE methods have an open-loop information flow, further research is *required on the implementation of "closed-loop" DSSE methods*. A closed-loop DSSE allows the predictive database used to estimate loads (and DG outputs) to be continuously updated and improved based on feedback from the SE

REFERANCES

[1] A. Monticelli, *State Estimation in Electric Power Systems: A Generalized Approach* (Kluwer International Series in Engineering and Computer Science). Boston, MA, USA: Kluwer Academic, 1999.

[2] A. Abur and A. G. Expósito, *Power System State Estimation: Theory and Implementation*. New York, NY, USA: Marcel Dekker, 2004.

[3] C. J. Mozina, "Interconnect protection of dispersed generators," in *Proc. IEEE PES Transm. Distrib. Conf. Expo.*, vol. 2. Atlanta, GA, USA,Oct. 2001, pp. 709–723.

[4] J. A. Michline Rupa, S. Ganesh," Power Flow Analysis for Radial Distribution System Using Backward/Forward Sweep Method", World Academy of Science, Engineering and Technology International Journal of Electrical, Computer, Energetic, Electronic and Communication Engineering Vol:8, No:10, 2014

[5] Mesut E. Baran," Challenges in State Estimation on Distribution Systems", Department of ECE, North Carolina State University Raleigh NC 27695,

[6] T P Vishnu, Vidya Viswan, Vipin A M," Power System State Estimation and Bad Data Analysis Using Weighted Least Square Method", 2015 IEEE International Conference on Power, Instrumentation, Control and Computing (PICC)

[7] Wesley peres, edimar j. oliveira, joão a. p. filho, josé l. r. pereira,guilherme o. alves." branch current based state estimation: equality-constrained wls and augmentedmatrix approaches", Anais do XX Congresso Brasileiro de Automática Belo Horizonte, MG, 20 a 24 de Setembro de 2014

[8] Barry Hayes and Milan Prodanovi´c," State Estimation Techniques for Electric Power Distribution Systems", 2014 UKSim-AMSS 8th European Modelling Symposium

[9] Anggoro Primadianto PLN Indonesia, Wei Ting Lin, Chan Nan Lu," Performance Comparison of Distribution System state Estimation" 2016 IEEE Innovative Smart Grid Technologies - Asia (ISGT-Asia) Melbourne, Australia, Nov 28 - Dec 1, 2016.

[10] M. E. Baran and A. W. Kelley, "State estimation for real-time monitoring of distribution systems," *IEEE Trans. Power Syst.*, vol. 9, no. 3, pp. 1601–1609, Aug. 1994.

[11] catalina gómez-quiles, *student member, ieee*, hugoa.gil, *member, ieee*, antonio de la villa jaén, and antonio gómez-expósito*, fellow, ieee,"* Equality-constrained bilinear state estimation*",* ieee transactions on power systems, vol. 28, no. 2, may 2013.

[12] A. Souza, E. M. Lourenço, and A. Simões Costa, "Real-time monitoring of distributed generation through state estimation and geometrically based tests," in *Proc. Bulk Power Syst. Dyn. Control*, Rio de Janeiro, Brazil, Aug. 2010, pp. 1–8.

[13] A. Simões Costa and M. C. dos Santos, "Real-time monitoring of distributed generation based on state estimation and hypothesis testing,"in *Proc. IEEE Power Tech. Conf.*, Lausanne,Switzerland, Jul. 2007,pp. 538–543.

[14] W. H. Kersting, *Distribution System Modeling and Analysis* (The Electrical Engineering Series), 2nd ed. Boca Raton, FL, USA: CRC Press, Jul. 2011.

[15] E. M. Lourenco, A. Simões Costa, and K. A. Clements, "Bayesian-based hypothesis testing for topology error identification in generalized state estimation," *IEEE Trans. Power Syst.*, vol. 19, no. 2, pp. 1206–1215,
May 2004.

[16] M. E. Baran and A. W. Kelley, "A branch current based state estimation method for distribution systems," *IEEE Transaction on Power Systems,* vol. 10, no. 1, pp. 483-491, 1995.

[17] C. N. Lu, J. H. Teng and W. H. E. Liu, "Distribution system state estimation," *IEEE Transactions on Power Systems,* vol. 10, no. 1, pp.229-240, 1995.

[18] Felix f. wu, wen-hsiung e. liu, lars holten, anders gjelsvik, sverre am," Observability analysis and bad data processing for state estimation using hachtel's augmented matrix method", ieee transactions on power systems, vol. 3, no. 2, may 1988.

[19] E. M. Lourenço, A. J. A. Costa, K. A. Clements, and R. A. Cernev,"A topology error identification method directly based on collinearity tests," *IEEE Trans. Power Syst.*, vol. 4, no. 21, pp. 1920–1929, Nov. 2006.

[20] Souza, A. *"*Monitoring of Distributed Generation in Distribution Systems By Collinearity Geometric Tests*"*. 2008. Master Dissertation, Graduate Program in Electrical Engineering, Federal University of Santa Catarina, Brazil (in Portuguese).

[21] M.E. Baran, "Challenges in State Estimation on Distribution Systems", Proc. of the IEEE PES Summer Meeting, Vancouver, Canada, 2001, pp. 429—433.

[22] M. Carneiro dos Santos, "Real-Time Monitoring of Distributed Generation in Distribution Systems", Master's Thesis, Electrical Engineering Graduate Program, Universidade Federal de Santa Catarina, Brazil, (in Portuguese), 2006.

[23] A.K Mishra, D. Bhujel,"Load flow algorithm fo radial Distribution system with Distributed Generators', IEEE ICSET 2012, Nepal

[24] Abdullah Mahmoudi, Seyed Hossein Hosseinian," Direct solution of Distribution System Load Flow Using Forward/Backward Sweep",Electrical Engineering Department, Amirkabir University of Technology, Tehran, Iran

[25] Young-Hyun Moon, Byoung-Kon Choi Byoung-Hoon Cho, Se-Ho Kim, Bok-Nam Ha, Jung-Ho Lee," Fast and Reliable Distribution System Load Flow Algorithm Based on the Ybus Formulation", KEPRI, 103-16, Munji-dong Yusung-ku 120-749 Korea Cheju Nat'l Univ., Cheju Korea Taejon 305-380, Korea

[26] Jako kilter," Monitoring of Electrical Distribution Network Operation", Tallinn university of Technology, Ehitajate tee 5, Tallinn, Estonia, june 2009

[27] Kevin A. Clements, Antonio Simks Costa, Worcester Polytechnic Institute Worcester, MA 01609," Topology Error Identification Using Normalized Lagrange Multipliers", IEEE Transactions on Power Systems, Vol. 13, No. *2,* May 1998

[28] Bob Uluski,"Distribution_Management_Systems", Electric Power Research Institute, CRN Summit Cleveland Ohio July 20, 2011

[29] Angel Fernández Sarabia," Impact of distributed generation on distribution system", Department of Energy Technology, Science and Medicine, Aalborg University, Aalborg, Denmark, June 2011

[30] K. A. Clements and P. W. Davis, "Multiple bad data detectability and identifiability: A geometric approach," *IEEE Trans. Power Del.*, vol. 1, no. 3, pp. 355–360, Jul. 1986.

[31] Allen J. Wood, Power Technology, Inc. and Rensslaer Polytechnic Institute, Bruce F. wollenberg, Univesity of Minnesota" Power Generation, Operation and control", Second edition

APPENDIX A

NE AND AM STATE ESTIMATION INPUT DATA

IEEE 10-BUS NETWORK:

```
KVA_base=100;
KV_base=23
npcc=1; %%% No of PCC in System


10                      % Number of buses
9                       % Number of lines
100                     % Maximum iteration
0.0001                  % Epsilon

%%% LINE DATA %%%

Lp(k) lq(k)  r(k)    x(k)    ycp(k)  ycq(k)  tap(k)
(Ohm)  (Ohm)

1       2     0.1233  0.4127   0       0        1
2       3     0.014   0.6051   0       0        1
3       4     0.7463  1.205    0       0        1
4       5     0.6984  0.6084   0       0        1
5       6     1.9831  1.7276   0       0        1
6       7     0.9053  0.7886   0       0        1
7       8     2.055   1.164    0       0        1
8       9     4.7953  2.716    0       0        1
9       10    5.3434  3.0264   0       0        1

0 0 0 0 0 0 0 0 0 0      % Shunt admittance data

%%% LOAD DATA %%%

Bus NO.     Pload(i)   Qload(i)
(kW)        (kVAr)
1            0           0
2            1840        460
3            980         340
4            1790        446
5            1598        1840
6            1610        600
7            780         110
8            1150        60
9            980         130
10           1640        200
```

```
% Measurements data

m=27 %% Total number of Measurements
m_oc=2  %% Total number of Operational constraints
```

Measurements/ Z(i)	Zcode (i)	Zlocation(i)	Sigma(i)
Real Time measurements			
1	5	1	0.00159
0.55	3	1	0.03
0.219	3	1	0.03
0.9541	5	5	0.00159
Virtual Measurements			
0	1	2	0.00001
0	2	2	0.00001
0	1	3	0.00001
0	2	3	0.00001
0	1	4	0.00001
0	2	4	0.00001
0	1	5	0.00001
0	2	5	0.00001
0	1	7	0.00001
0	2	7	0.00001
0	1	8	0.00001
0	2	8	0.00001
0	1	9	0.00001
0	2	9	0.00001
0	1	10	0.00001
0	2	10	0.00001
Pseudo Measurements			
0.24256	6	-2	0.20
0.20109	3	5	0.20
0.27475	3	8	0.20
0.1972	6	-9	0.20
0.36	6	-3	0.20
0.01245	**1**	**6**	**0.20**
0.0112	**2**	**6**	**0.20**

```
Z(i)     Zcode(i)     Zloc(i)          sigma(i)

0.01245  1             6                0.20       % Pinj @ PCC 1 for case A
0.0112   2             6                0.2        % Qinj @ PCC 1 for Case A

2.51245  1             6                0.20       % Pinj @ PCC 1 for case B
1.0112   2             6                0.2        % Qinj @ PCC 1 for Base B

1.51245  1             6                0.2        % Pinj @ PCC 1 for Case C
3.0112   2             6                0.2        % Qinj @ PCC 1 for Case C
```

APPEMDIX B

NE AND AM STATE ESTIMATION INPUT DATA

IEEE 34-NODE TEST FEEDER NETWORK:

```
34          % Number of buses
33          % Number of lines
100         % Maximum number of iteration
0.0001      % Epsilon

% LINE DATA (Actual value) %
```

LP(k)	LQ(k)	r(k)	x(k)	ycp(k)	ycq(k)	tap(k)
1	2	0.1233	0.4127	0	0	1
2	3	0.014	0.6051	0	0	1
3	4	0.7463	1.205	0	0	1
4	5	0.6984	0.6084	0	0	1
5	6	1.9831	1.7276	0	0	1
6	7	0.9053	0.7886	0	0	1
7	8	2.055	1.164	0	0	1
8	9	4.7953	2.716	0	0	1
9	10	5.3434	3.0264	0	0	1
10	11	0.1133	0.4127	0	0	1
11	12	0.014	0.6051	0	0	1
12	13	0.7563	1.205	0	0	1
13	14	0.6984	0.6084	0	0	1
14	15	1.9831	1.7276	0	0	1
15	16	0.9153	0.7886	0	0	1
16	17	2.055	1.164	0	0	1
17	18	4.7853	2.716	0	0	1
18	19	5.3434	3.0264	0	0	1
19	20	0.1333	0.4127	0	0	1
4	21	0.014	0.6051	0	0	1
8	22	0.7463	1.205	0	0	1
22	23	0.6884	0.6084	0	0	1
23	24	1.9831	1.7276	0	0	1
9	25	0.9453	0.7886	0	0	1
12	26	2.055	1.164	0	0	1
14	27	4.7953	2.716	0	0	1
27	28	5.3434	3.0264	0	0	1
15	29	5.09434	3.0264	0	0	1
16	30	4.7953	2.71	0	0	1
30	31	4.7953	2.716	0	0	1
31	32	1.9831	1.7276	0	0	1
32	33	0.7563	1.205	0	0	1
18	34	0.014	0.6051	0	0	1

```
% Shunt Admittance data
```

```
0 0 0 0 0 0 0 0 0 0 0 0 0 0 0 0 0 0 0 0 0 0 0 0 0 0 0 0 0 0 0 120 0 150

% LOAD DATA (Actual value)%

Bus No.     Pload(i)    Qload(i)
1           0            0
2           1840         460
3           980          340
4           1790         446
5           1598         1840
6           1610         600
7           780          110
8           1150         60
9           980          130
10          1640         200
11          1540         360
12          780          240
13          1490         346
14          1198         840
15          1110         300
16          899          90
17          1050         60
18          780          130
19          1240         100
20          1340         260
21          980          340
22          1190         246
23          1098         1240
24          1210         400
25          780          110
26          1050         60
27          980          230
28          1140         120
29          1240         460
30          910          340
31          1250         160
32          900          130
33          1140         202
34          1240         160
```

% Measurement data

m=94 Total No. of Measurements

m_oc=6 Total number of Operational constraints

Measurements/ Z(i)	Zcode (i)	Zlocation(i)	Sigma(i)
Real Time measurements			
0.9998	5	1	0.00159
0.120	3	1	0.03
0.2150	4	1	0.03
0.2928	3	6	0.03
0.09108	4	6	0.03
0.9925	5	7	0.00159
0.5283	6	-6	0.03
0.9897	5	14	0.00159

0.9784	5	16	0.00159
0.15093	3	16	0.03
0.07910	4	16	0.03
0.1183	6	-16	0.03
0.101093	3	26	0.003
0.0183	6	-26	0.03
0.1079	3	29	0.03
0.12572	6	-29	0.03
0.6910	4	29	0.03
Virtual measurements			
0	1	2	0.00001
0	2	2	0.00001
0	1	3	0.00001
0	2	3	0.00001
0	1	5	0.00001
0	2	5	0.00001
0	1	8	0.00001
0	2	8	0.00001
0	1	9	0.00001
0	2	9	0.00001
0	1	10	0.00001
0	2	10	0.00001
0	1	11	0.00001
0	2	11	0.00001
0	1	13	0.00001
0	2	13	0.00001
0	1	15	0.00001
0	2	15	0.00001
0	1	17	0.00001
0	2	17	0.00001
0	1	18	0.00001
0	2	18	0.00001
0	1	19	0.00001
0	2	19	0.00001
0	1	20	0.00001
0	2	20	0.00001
0	1	21	0.00001
0	2	21	0.00001
0	1	22	0.00001
0	2	22	0.00001
0	1	23	0.00001
0	2	23	0.00001
0	1	24	0.00001
0	2	24	0.00001
0	1	25	0.00001

0	2	25	0.00001
0	1	27	0.00001
0	2	27	0.00001
0	1	28	0.00001
0	2	28	0.00001
0	1	31	0.00001
0	2	31	0.00001
0	1	32	0.00001
0	1	33	0.00001
0	2	33	0.00001
Pseudo Measurements			
0.7472	3	2	0.20
1.02578	4	2	0.20
0.2028	3	3	0.20
0.0959	4	3	0.20
0.215	6	-3	0.20
0.20109	3	5	0.20
0.2557	4	5	0.20
0.2622	6	-5	0.20
0.1117	4	8	0.20
0.1679	3	9	0.20
0.1214	4	9	0.20
0.1997	6	-9	0.20
0.001109	3	15	0.20
0.10	4	15	0.20
0.1526	6	-15	0.20
0.1214	3	18	0.20
0.107	4	18	0.20
0.126	6	-18	0.20
1.19	4	22	0.20
0.30856	6	-22	0.20
0.42015	4	24	0.20
0.8308	6	-24	0.20
0.09475	4	6	0.20
0.5247	6	-6	0.20
0.5195	4	32	0.20
0.015	**1**	**4**	**0.20**
0.01125	**2**	**4**	**0.20**
0.850	**1**	**12**	**0.20**
0.0256	**2**	**12**	**0.20**
0.094	**1**	**30**	**0.20**
0.1012	**2**	**30**	**0.20**

% Measurement data for all four cases %

PCC	Meas. value	Case A		Case B		Case C		Case D	
		Pinj	Qinj	Pinj	Qinj	Pinj	Qinj	Pinj	Qinj
1	Z(i)	0.015	0.01125	0.015	0.01125	0.015	0.001125	0.015	0.001125
2	Z(i)	0.850	0.0256	**3.350**	**2.0256**	**1.850**	**2.5256**	**2.350**	**1.0256**
3	Z(i)	0.094	0.1012	0.094	0.1012	0.094	0.1012	**2.094**	**0.7012**